

# **Relative Permeability Upscaling for Heterogeneous Reservoir Models**

Mohamed Ali Gomaa Fouda

Submitted for the degree of Doctor of Philosophy

Heriot-Watt University

School of Energy, Geoscience, Infrastructure and Society

February 2016

The copyright in this thesis is owned by the author. Any quotation from the thesis or use of any of the information contained in it must acknowledge this thesis as the source of the quotation or information.

# ABSTRACT

Detailed geological models usually contain multi-million grid cells, which makes the running of reservoir simulation difficult and time consuming. Therefore, reducing the number of grid cells, and in turn averaging reservoir properties within them, is desirable in order to make running simulations more feasible. Averaging reservoir properties within the coarse cells is usually referred to as upscaling, which can be achieved using different methods.

Many upscaling techniques have been introduced in the literature. However, developing a practical and robust upscaling method has been a research topic for a long time. In this thesis, some of the upscaling methods, their application and limitations are presented. Special attention is given to two phase upscaling methods as they are within the scope of this project. Afterwards, a new two phase upscaling method, called Transmissibility Weighted Relative permeabilities (TWR), is proposed to upscale relative permeability curves in heterogeneous reservoirs. Also, a new method to generate well pseudos is introduced as a means of adjusting well results.

The TWR method and the well pseudos were tested using synthetic 2D and 3D water flood models for different conditions in order to check the method's performance. The results showed that the upscaled relative permeability curves (pseudo functions) succeeded in compensating for sub-grid heterogeneity and numerical dispersion so that the coarse models reproduced the fine models results.

In order to make the use of the pseudo functions feasible in practice, a new method to group them, based on curve fitting of Chierici (1984) functional models, was introduced. Calculations of the TWR pseudos and the well pseudos were performed by writing C++ codes to do so. The grouping of the pseudos was accomplished using a non-linear regression solver.

To my family, my wife and my daughter.

## ACKNOWLEDGMENT

Foremost, I would like to express my sincere gratitude and thanks to the God for giving me the willpower and health to complete this work.

I would like to express my deepest thanks to Dr. Gillian E. Pickup for her support, motivation and for being source of inspiration and suggestions, which helped me a lot to complete this PhD study. I would like also to thank Dr. Gillian for being always available to discuss and share her knowledge with me although I was studying off campus.

In addition, I would like to take this opportunity to express my gratitude to MND a.s. - Czech Republic, represented by Ing. Zbyněk Parma, the general manager, for sponsoring me during my study, and special thanks goes to RNDr. Jana Hamršmídová, the director of geology department, for her support, help and advices. Also, I would like to thank Ing. Richard Bittner, CSc., the head of reservoir engineering department, for sharing his knowledge with me and for his continuous help. My sincere thanks also goes to my colleagues who helped and supported me.

Finally, I would like to thank my family: my mother and my father for their support and for being with me by their hearts even they are far away, my wife for her patience and support during the years of my study and for her love and encouragement during the hard times, and my lovely daughter for being the source of hope and happiness in my life.

**ACADEMIC REGISTRY**  
**Research Thesis Submission**



Name:	Mohamed Ali Gomaa Fouda		
School/PGI:	EGIS / Institute of Petroleum Engineering		
Version: <i>(i.e. First, Resubmission, Final)</i>	Final	Degree Sought (Award and Subject area)	PhD Petroleum Engineering

**Declaration**

In accordance with the appropriate regulations I hereby submit my thesis and I declare that:

- 1) the thesis embodies the results of my own work and has been composed by myself
- 2) where appropriate, I have made acknowledgement of the work of others and have made reference to work carried out in collaboration with other persons
- 3) the thesis is the correct version of the thesis for submission and is the same version as any electronic versions submitted\*.
- 4) my thesis for the award referred to, deposited in the Heriot-Watt University Library, should be made available for loan or photocopying and be available via the Institutional Repository, subject to such conditions as the Librarian may require
- 5) I understand that as a student of the University I am required to abide by the Regulations of the University and to conform to its discipline.

\* Please note that it is the responsibility of the candidate to ensure that the correct version of the thesis is submitted.

Signature of Candidate:	<i>M. Gomaa</i>	Date:	<i>27/04/2016</i>
-------------------------	-----------------	-------	-------------------

**Submission**

Submitted By <i>(name in capitals)</i> :	
Signature of Individual Submitting:	
Date Submitted:	

**For Completion in the Student Service Centre (SSC)**

Received in the SSC by <i>(name in capitals)</i> :	
Method of Submission <i>(Handed in to SSC; posted through internal/external mail)</i> :	
E-thesis Submitted <i>(mandatory for final theses)</i>	
Signature:	Date:

Please note this form should bound into the submitted thesis.

Updated February 2008, November 2008, February 2009, January 2011

# TABLE OF CONTENTS

<b>Chapter 1 Introduction.....</b>	<b>1</b>
1.1. Background and motivation .....	2
1.2. Objectives of the thesis.....	6
1.3. Outline of the thesis.....	7
<b>Chapter 2 Literature Review .....</b>	<b>8</b>
2.1. Introduction .....	9
2.2. Reservoir models upscaling.....	9
2.3. Analytical methods.....	13
2.4. Single phase upscaling .....	15
2.4.1. Background .....	15
2.4.2. Single phase flow equations.....	16
2.4.3. Single phase flow techniques.....	17
2.5. Near well upscaling .....	22
2.6. Two phase upscaling .....	27
2.6.1. Background .....	27
2.6.2. Two phase flow equations.....	30
2.6.3. Pseudo functions calculation methods.....	31
2.6.4. Impact of upgridding on pseudo functions results improvement.....	54
2.6.5. Flow regimes and selection of the proper pseudoization method.....	55
2.6.6. Well pseudo functions .....	57
2.6.7. Directional pseudo functions .....	58
2.6.8. Comparison between pseudo generation methods .....	59
2.6.9. Review of pseudo functions generation methods.....	60
2.6.10. The use of pseudo functions generated from a specific case to another .....	63
2.6.11. Grouping the pseudo functions.....	63
2.6.12. Summary and conclusions .....	65

<b>Chapter 3 Transmissibility Weighted Relative Permeability (TWR) .....</b>	<b>66</b>
3.1. Introduction .....	67
3.2. The TWR and the well pseudos methods .....	68
3.2.1. Upscaling the absolute permeability .....	70
3.2.2. Upscaling relative permeability curves using the TWR method .....	70
3.2.3. Upscaling well blocks relative permeability curves (the well pseudos) .....	73
3.2.4. Calculation of the coarse grid well connection factor .....	76
3.2.5. New method to group the pseudo functions .....	77
3.3. Summary and conclusions .....	80
<b>Chapter 4 Testing of the TWR method and the well pseudos .....</b>	<b>81</b>
4.1. Introduction .....	82
4.2. Testing of the TWR method using 2D cross-sectional model.....	83
4.2.1. Model description.....	83
4.2.2. Fine and coarse water flood simulation using rock curves .....	86
4.2.3. Coarse water flood simulation using Stone's (1991) pseudo functions .....	90
4.2.4. Coarse water flood simulation using the TWR pseudo functions.....	95
4.2.5. Coarse water flood simulation using the TWR and well pseudos .....	98
4.3. Additional testing of the TWR method and the well pseudos using 2D model .	103
4.3.1. Upward permeability coarsening .....	107
4.3.2. Upward permeability fining .....	110
4.3.3. Thief zone in the middle of the model.....	113
4.4. Testing of the TWR and the well pseudos methods using 3D model .....	122
4.5. Summary and conclusions .....	129
<b>Chapter 5 Application of the TWR method to the SPE 10 model 2 .....</b>	<b>130</b>
5.1. Introduction .....	131
5.2. Model description.....	131
5.3. The top 4 layers of the Tarbert formation .....	133

5.4. The layer 59 (the upper Ness formation).....	141
5.5. Summary and conclusions .....	146
<b>Chapter 6 Conclusions and Future Guidelines .....</b>	<b>147</b>
6.1. Summary and conclusions .....	148
6.2. Future guidelines .....	151
<b>References .....</b>	<b>152</b>



## LISTS OF TABLES

<b>Table 2-1:</b> Types of analytic averaging methods .....	14
<b>Table 2-2:</b> Comparison between some of pseudo functions generation methods.....	59
<b>Table 4-1:</b> Test models used for initial testing of the TWR pseudos .....	84
<b>Table 4-2:</b> Reservoir properties used in the fine model .....	84
<b>Table 4-3:</b> Fluid properties and initial conditions used in the fine and coarse models...	84
<b>Table 4-4:</b> Permeability distributions for the cases with thief zone in the middle, permeability coarsening upwards and permeability fining upwards .....	105
<b>Table 4-5:</b> Test models used for additional testing of the TWR pseudos .....	106
<b>Table 4-6:</b> Fluid properties and initial conditions used in the fine and coarse models.	106
<b>Table 4-7:</b> Reservoir properties used in the fine 2D models .....	106
<b>Table 4-8:</b> Test fine and coarse 3D models .....	122
<b>Table 4-9:</b> Fluid properties and initial conditions used in fine and coarse models .....	123
<b>Table 4-10:</b> Reservoir properties used in the fine 3D model.....	123
<b>Table 5-1:</b> Fluid and rock properties associated to the SPE 10 model 2.....	132
<b>Table 5-2:</b> Wells configuration in the test models .....	133
<b>Table 5-3:</b> Fine and coarse models of the top 4 layers of the Tarbert formation.....	133
<b>Table 5-4:</b> Fine and coarse models of the layer 59 (the Upper Ness formation) .....	141

## LISTS OF FIGURES

<b>Figure 2-1:</b> Parallel flow (left) and series flow (right), adapted from Salazar and Villa (2007).....	13
<b>Figure 2-2:</b> Coarse cell with no-flow boundary conditions .....	19
<b>Figure 2-3:</b> Schematic shows local-global coupling, from Chen et al. (2003) .....	22
<b>Figure 2-4:</b> Equivalent transmissibility - near well upscaling, from Ding (1995) .....	24
<b>Figure 2-5:</b> Fine and coarse grid system – near well upscaling, adapted from Durlofsky et al. (2000) .....	26
<b>Figure 2-6:</b> Stratified model used to calculate Hearn pseudo functions. This figure is adapted from Hearn, C. L. (1971).....	34
<b>Figure 2-7:</b> Multi-step pseudo functions, adapted from Kossack, et al. (1990).....	46
<b>Figure 2-8:</b> Regional upscaling method, from Coll et al. (2001).....	55
<b>Figure 2-9:</b> Comparison between results of using pseudo functions to upscale 2D horizontal model to 1D, adapted from Darman et al., 2001. ....	61
<b>Figure 2-10:</b> Comparison between results of using pseudo functions to upscale 2D dipping model to 1D, adapted from Darman et al., 2001.....	62
<b>Figure 3-1:</b> Workflow of the new two phase upscaling methods .....	69
<b>Figure 3-2:</b> Upscaling of relative permeability at the downstream edge of coarse blocks (x-z cross-section) .....	70
<b>Figure 3-3:</b> Upscaling of relative permeability at the well connections using well connection factor weighting .....	74
<b>Figure 3-4:</b> Snapshot of a Excel spreadsheet to perform Chierici (1984) functions fitting to the TWR pseudos .....	79
<b>Figure 4-1:</b> Fine and coarse synthetic 2D cross-sectional models .....	85
<b>Figure 4-2:</b> Relative permeability curves used in the fine model, calculated using Corey (1954) method .....	85
<b>Figure 4-3:</b> Permeability distributions in the 2D cross-sectional fine model using Sequential Gaussian Simulation (PETREL, Schlumberger).....	86

<b>Figure 4-4:</b> Upscaled permeability in the x direction in the coarse model using geometric averaging method .....	86
<b>Figure 4-5:</b> Comparison between water saturation profiles of the fine and coarse models (both with rock curves) at initial conditions, after 1 year of water flooding, at the water breakthrough time and at the end of the water flood. ....	88
<b>Figure 4-6:</b> Comparison between cumulative oil production in case of fine and coarse models (both with rock curves).....	89
<b>Figure 4-7:</b> Comparison between results of the fine and coarse models (both with rock curves) in terms of field water production rate .....	89
<b>Figure 4-8:</b> Comparison between results of the fine and coarse models (both with rock curves) in terms of injector bottom hole pressure.....	90
<b>Figure 4-9:</b> Comparison between water saturation profiles of coarse model with rock curves and coarse model with Stone (1991) pseudo functions at initial conditions, after 1 year of water flooding, at the water breakthrough time and at the end of the water flood .....	92
<b>Figure 4-10:</b> Comparison between fine and coarse models (with rock curves) and coarse model (with Stone's (1991) pseudo functions) in terms of field water production rate.....	94
<b>Figure 4-11:</b> Comparison between the fine and coarse models (with rock curves) and the coarse models (with Stone's (1991) pseudo functions) in terms of injector bottom hole pressure.....	94
<b>Figure 4-12:</b> TWR pseudo functions generated for the 2D cross sectional model .....	95
<b>Figure 4-13:</b> Comparison between water saturation profiles of coarse model with Stone (1991) pseudo functions and coarse model with TWR pseudos at the initial conditions, after 1 year of water flooding, at the water breakthrough time and at the end of the water flood. ....	97
<b>Figure 4-14:</b> Comparison between the fine model (with rock curves), coarse model (with Stone's (1991) pseudos) and coarse model (with TWR pseudo) in terms of field water production rate.....	98
<b>Figure 4-15:</b> Comparison between the fine model (with rock curves), coarse model (with Stone's (1991) pseudos) and coarse model (with TWR pseudo) in terms of injector bottom hole pressure .....	98
<b>Figure 4-16:</b> Well pseudos assigned to the producer and injector well blocks.....	99

<b>Figure 4-17:</b> Comparison between water saturation profiles of coarse model with TWR pseudos and coarse model with both TWR pseudos and well pseudos at the initial conditions, after 1 year of water flooding, at the water breakthrough time and at the end of the water flood .....	100
<b>Figure 4-18:</b> Comparison between fine model (with rock curves), coarse model (with TWR pseudos) and coarse model (with TWR pseudos + well pseudos) in terms of field water production rate.....	101
<b>Figure 4-19:</b> Comparison between fine model (with rock curves), coarse model (with TWR pseudos) and coarse model (TWR pseudos + well pseudos) in terms of field oil production cumulative.....	102
<b>Figure 4-20:</b> Comparison between fine model (with rock curve), coarse model (with TWR pseudos) and coarse model (with TWR pseudos + well pseudos) in terms of injector bottom hole pressure. ....	102
<b>Figure 4-21:</b> Fine and coarse 2D cross sectional synthetic models .....	104
<b>Figure 4-22:</b> Permeability distributions (in the x direction) in fine and coarse models with thief zone in the middle.....	107
<b>Figure 4-23:</b> Comparison between water saturation profiles of fine model (with rock curves), coarse model (with rock curves) and coarse model (with TWR pseudos in the x direction + well pseudos) after 1 year of water flooding .....	108
<b>Figure 4-24:</b> Comparison between the fine model (with rock curves), coarse model (with rock curves) and the coarse model (with TWR pseudos in the x direction + well pseudos) in terms of field water production rate.....	109
<b>Figure 4-25:</b> Comparison between the fine model (with rock curves), coarse model (with rock curves) and coarse model (with TWR pseudos in the x direction + well pseudos) in terms of injector bottom hole pressure .....	109
<b>Figure 4-26:</b> Permeability distributions (the x direction) in the fine and coarse models used to simulate the case with permeability fining upwards.....	110
<b>Figure 4-27:</b> Comparison between water saturation profiles of fine model (with rock curves), coarse model (with rock curves) and coarse model (with TWR pseudos in the x direction) after 1 year of water flooding .....	111
<b>Figure 4-28:</b> comparison between fine model (with rock curves), coarse model (with rock curves) and coarse model (with TWR pseudos in the x direction + well pseudos) in terms of field water production rate. ....	112

<b>Figure 4-29:</b> comparison between the fine model (with rock curves), coarse model (with rock curves) and coarse model (with TWR pseudos in the x direction +well pseudos) in terms of injector bottom hole pressure .....	112
<b>Figure 4-30:</b> Permeability distributions (in the x direction) of fine and coarse models with thief zone in the middle. Permeability was upscaled using flow-based method (no-flow boundary conditions) .....	113
<b>Figure 4-31:</b> TWR pseudo functions generated for the model with thief zone.....	115
<b>Figure 4-32:</b> Comparison between water saturation profiles of fine model (with rock curves), coarse model (with rock curves), coarse model (with TWR pseudos in the x direction + well pseudos) and coarse model (with TWR pseudos in the x and z directions + well pseudos) after 1 year of water flooding.....	115
<b>Figure 4-33:</b> Comparison between fine and coarse models (rock curve), coarse model (TWR pseudos in the x direction +well pseudos) and coarse model (TWR pseudos in the x and z directions +well pseudos) in terms of field water production rate .....	116
<b>Figure 4-34:</b> Comparison between fine and coarse models (rock curve), coarse model (TWR pseudos in the x direction + well pseudos) and coarse model (TWR pseudos in the x and z directions + well pseudos) in terms of injector bottom hole pressure. ....	117
<b>Figure 4-35:</b> Grouping of oil pseudos in the x direction.....	118
<b>Figure 4-36:</b> Grouping of water pseudos in the x direction .....	118
<b>Figure 4-37:</b> Grouping of oil pseudos in the y direction.....	119
<b>Figure 4-38:</b> Grouping of water pseudos in the y direction .....	119
<b>Figure 4-39:</b> TWR pseudos regions in both the x and z directions.....	120
<b>Figure 4-40:</b> Comparison between results of the TWR pseudos (with and without grouping) in terms of field water production rate. ....	121
<b>Figure 4-41:</b> Comparison between results of the TWR pseudos (with and without grouping) in terms of injector bottom hole pressure.....	121
<b>Figure 4-42:</b> Permeability distributions (in the x direction) of the fine and coarse 3D models. Permeability of the coarse model was upscaled using flow based method with no flow boundary conditions.....	124
<b>Figure 4-43:</b> comparison between results of the fine model (with rock curves), the coarse model (with rock curves) and the coarse model (with TWR pseudos in the x and y directions) in terms of field water production rate.....	125
<b>Figure 4-44:</b> comparison between results of the fine model (with rock curves), the coarse model (with rock curves) and the coarse model (with TWR pseudos in the x and y directions) in terms of injector bottom hole pressure .....	126

<b>Figure4-45:</b> Grouping of oil and water pseudos in the positive and negative x directions .....	127
<b>Figure 4-46:</b> Grouping of oil and water pseudos in the positive and negative y directions .....	127
<b>Figure 4-47:</b> Comparison between results of the TWR pseudos (with and without grouping) in terms of field water production rate .....	128
<b>Figure 4-48:</b> Comparison between results of the TWR pseudos (with and without grouping) in terms of injector bottom hole pressure .....	128
<b>Figure 5-1:</b> The permeability distribution of the SPE 10 model 2 (Christie and Blunt, 2001) .....	131
<b>Figure 5-2:</b> Relative permeability curves (rock curves) of the SPE 10 model 2 .....	132
<b>Figure 5-3:</b> The permeability distributions (in the x direction) of the fine and coarse models, representing the top 4 layers of the Tarbert formation .....	134
<b>Figure 5-4:</b> TWR pseudos generated for the coarse model in the positive x and y directions .....	135
<b>Figure 5-5:</b> TWR pseudos grouping in the positive x and y directions. ....	136
<b>Figure 5-6:</b> TWR pseudos regions in the positive x and y directions (a) and the transmissibility in the x and y directions (b) .....	137
<b>Figure 5-7:</b> Comparison between the water saturation profile after 6 months of the fine model (layer no.4) with rock curves (b) and the coarse model with TWR pseudos (a). .....	139
<b>Figure 5-8:</b> Comparison between the fine model (with rock curves) and the coarse model (with TWR pseudos + well pseudos) in terms of field water production rate ...	139
<b>Figure 5-9:</b> Comparison between the fine model and the coarse model results in terms of injector bottom hole pressure.....	140
<b>Figure 5-10:</b> Comparison between the fine model and the coarse model results in terms of water production rate of the producers. ....	140
<b>Figure 5-11:</b> The permeability distributions (in the x direction) of the fine model representing the layer 59 .....	141
<b>Figure 5-12:</b> TWR pseudos grouping in the y direction .....	142
<b>Figure 5-13:</b> TWR pseudos regions in the x directions (a), transmissibility in the x directions (b), TWR pseudos regions in the y directions (c), and transmissibility in the y directions (d). ....	143

<b>Figure 5-14:</b> Comparison between the water saturation profile of the coarse and fine models after 6 months of water injection.....	144
<b>Figure 5-15:</b> Comparison between the coarse and fine models in terms of oil production rate.....	144
<b>Figure 5-16:</b> Comparison between the coarse and fine models in terms of cumulative oil production. ....	145
<b>Figure 5-17:</b> Comparison between the coarse and fine models in terms of injector bottom hole pressure. ....	145

## NOMENCLATURE

$A$	coarse cell face area perpendicular to flow direction
$\bar{D}$	centre depth of the coarse block
$\bar{f}_w$	average fractional flow for water phase
$\bar{f}_o$	average fractional flow for oil phase
$g$	gravity coefficient
$h$	reservoir thickness
$H$	the difference between depths of coarse and fine cell centres
$I_w$	fine scale well index
$k$	reservoir permeability
$\bar{K}_z$	average vertical permeability
$k^*$	average reservoir permeability
$k_a$	arithmetic average of reservoir permeability
$k_h$	harmonic average of reservoir permeability
$k_g$	geometric average of reservoir permeability
$k_\omega$	power average of reservoir permeability
$kh$	permeability thickness product
$k_r$	relative permeability
$\bar{k}_r$	pseudo relative permeability of phase p
$\bar{k}_{rw}$	pseudo water relative permeability
$\bar{k}_{ro}$	pseudo oil relative permeability
$k_{ro}^*$	normalised oil relative permeability
$k_{rw}^*$	normalised water relative permeability
$L$	coarse cell length
$\tilde{m}$	well (source/sink) term
$N_g$	gravity number
$N_c$	capillary number
$\nabla p$	pressure gradient
$\Delta P$	pressure drop
$P$	pressure
$P_{wb}$	well bottom-hole pressure
$P_f$	fine well block pressure



$P_C$	coarse well block pressure
$P_c$	capillary pressure
$\bar{P}_o$	average pressure in the oil phase
$\bar{P}_w$	average pressure in the water phase
$\bar{P}_{c,ow}$	pseudo capillary pressure
$\bar{p}_p$	pseudo pressure
Q	total flow rate on the coarse cell face
q	well flow rate
$r_w$	wellbore radius
$r_o$	equivalent pressure radius
$S_w$	water saturation
$\bar{S}_p$	average phase saturation
$\bar{S}_w$	average water saturation
$S_{or}$	residual oil saturation
$S_{wc}$	connate water saturation
t	layer thickness
T	transmissibility between fine cells
$\bar{T}$	sum of transmissibilities at the interface between two coarse cells
$T_{avg}$	average transmissibility
u	Darcy velocity
V	cell volume
$V_p$	pore volume
WI	coarse scale well index
$\Delta x$	gridblock dimensions in the x directions
$\Delta y$	gridblock dimensions in the y directions
$\Delta z$	gridblock thickness

#### **SUBSCRIPTS:**

$i, j$	denotes coarse blocks i and j
o	oil
p	phase
w	water

x the x direction  
y the y direction  
z the z direction

**GREEK:**

$\Delta$  an operator which indicates a difference  
 $\nabla$  gradient vector  
 $\rho$  fluid density  
 $\mu$  fluid viscosity  
 $\bar{\mu}$  average viscosity  
 $\phi$  rock porosity  
 $\Phi$  potential  
 $\sigma$  standard deviation  
 $\alpha$  dip angle  
 $\omega$  power coefficient  
 $\lambda_t$  total mobility  
 $\bar{\lambda}_t$  average total mobility  
 $\lambda_{ro}^o$  endpoint mobility of oil phase

**INDICES:**

$i$  index of layer  $i$   
 $i, j, k$  indices for fine scale cells in the x, y and z directions  
 $I, J, K$  indices for coarse-scale cells in the x, y and z directions  
 $n$  number of layers  
 $nc$  no. of fine grid blocks at the centre column of a coarse grid block for which the pseudo pressure will be calculated  
 $I_l$  first fine cell in the x direction within a coarse cell  
 $I_c$  last cell in the x direction within a coarse cell  
 $J_l$  first fine cell in the y direction within a coarse cell  
 $J_c$  last cell in the y direction within a coarse cell  
 $K_l$  first fine cell in the column of cells at the interface between two coarse blocks  
 $K_c$  last fine cell in the column of cells at the interface between two coarse blocks

# **Chapter 1 : Introduction**

## **1.1 Background and motivation**

Heterogeneous reservoirs are characterized by variation in reservoir properties in all directions and at different length scales within the reservoir. Reservoirs can be described to have high, medium or low levels of heterogeneity according to multiple criteria such as the magnitude of petrophysical properties variation, the distance within which the reservoir properties vary as well as depositional and post-depositional environments. Generally, reservoir heterogeneities can be divided into small-scale and large-scale heterogeneities. The small-scale heterogeneities include, for example, variations in pore size and pore-throat diameter, grains sorting and lamination. The large-scale heterogeneities may include stratification, presence of channels and variation in reservoir properties. Contrary to homogenous reservoirs, it is difficult to describe the heterogeneous reservoirs by, for example, collecting data obtained from drilling a well in a certain location in the reservoir. This is because reservoir properties (e.g. porosity and permeability) might be completely different in different parts of the reservoir. In practice, reservoir properties are described by collecting the available well data (e.g. well logs and core plugs) assigned to specific well locations, and then using geostatistical methods to populate the properties throughout the reservoir. Several realisations might be considered in order to assess the underlying uncertainties such as uncertainty in estimates of hydrocarbon in-place and uncertainty in identifying possible reservoir boundaries.

Reservoir heterogeneity has a great impact on the fluid flow behaviour and in turn on the productivity of the reservoir. Important information such as water breakthrough time, pressure and oil recovery is dependent on reservoir heterogeneity. Therefore, it is crucial to study and understand how the heterogeneity influences the reservoir performance in order to maximize the recovery. This is usually investigated by building reservoir models, which are in turn used to run fluid flow simulations to assess any uncertainties.

Reservoir models have been used for decades to study the subsurface flow in porous media in order to predict and increase the recovery. When building reservoir models, the frequently applied approach is to build first a geological model, which represents the initial description of the reservoir heterogeneity. The geological models usually consist of tens or even hundreds of millions of grid blocks. Although, the geological models are referred to as very fine, the fine cells are still much larger than

the small-scale heterogeneity, especially in the areal direction. Therefore, it becomes necessary to average the small-scale reservoir properties in order to make them suitable for use in the geological model. However, the geological models after averaging the properties within them are still very detailed and are not feasible for running reservoir simulations. This is due to the high computation time costs and possible rise of convergence problems, especially when it is required to run multiple fine-scale simulations in order to assess various geological and development scenarios. Therefore, building more coarse and practical models (usually referred to as simulation models) becomes important. In the simulation model, the number of fine grid cells is reduced by merging the fine cells into larger. Afterwards, the reservoir properties are averaged within the coarse domain. The process of coarsening the fine grid is usually referred to as upgridding, while averaging reservoir properties within the coarse cells is referred to as upscaling.

From the discussion above, two stages of upscaling are usually considered when building reservoir models. The first stage is upscaling from small-scale heterogeneity to geological model, in which the small-scale properties are averaged within the fine geological model cells. The second stage is upscaling from geological model to simulation model, in which the fine grid is coarsened (i.e. upgridded), and then the reservoir properties are averaged within the coarse cells, forming a simulation model. Only the second stage of upscaling (i.e. from geological model to simulation model) will be of interest to this thesis. It is assumed that upscaling from small-scale heterogeneity to geological model has been achieved successfully in all case studies. Thus, the fine model will represent the “correct” solution to which results of the coarse model are supposed to be compared, when possible.

The target of upscaling is to replace the very fine and detailed models with coarse models, including much less data. These coarse models are more feasible for running simulations than the fine models. However, upscaling does not aim to speed up reservoir simulations at the cost of simulation results. On the contrary, upscaling techniques aim to build coarse models that preserve the most important flow characteristics of fine models and capture the sub-grid heterogeneity.

There are many upscaling methods that have been introduced in the literature. Some of these methods are analytical and others are numerical. The analytical methods (also called averaging methods) such as arithmetic, harmonic and geometric methods

are simple and can be applied successfully to properties such as porosity and water saturation. However, applying these averaging methods to permeability requires idealized conditions that may not be present in heterogeneous reservoirs. Numerical methods are performed by running reservoir fine-scale simulation to solve pressure equations. These methods can be divided, according to the fluid phases flowing in the reservoir, into single phase and two phase upscaling methods. The single phase upscaling methods aim to upscale absolute permeability (or transmissibility) by solving pressure equations. Single phase numerical upscaling methods such as Durlofsky (1991), Christie et al. (2000) and Zhang et al. (2005) ought to provide better results than the analytical methods. However, results of the single phase upscaling methods are greatly dependent on selection of the appropriate boundary conditions (Christie and Blunt, 2001), which may cause large errors when applied to two phase problems. Alternatively, the two phase upscaling methods are used when single phase upscaling methods are not enough to compensate for fluid dynamic behaviour and fine scale heterogeneity.

The two phase upscaling methods are used to upscale relative permeability curves, which are also referred to as pseudo functions. There are many two phase upscaling methods introduced in the literature that can be used to upscale relative permeability curves. These methods can be divided according to the calculation procedure into: methods that apply Darcy's two phase law (e.g. Kyte and Berry, 1975 and PVW method), methods using average total mobility (e.g. Stone, 1991), methods using streamtubes (e.g. Hewett and Yamada, 1995) and methods using history matching (e.g. Tan, 1995). Also, there are many approaches followed when upscaling relative permeability curves such as the full fine grid simulation approach (referred to as FFG), in which the fine grid results are used to generate the pseudo functions. However, this approach is impractical when applied to large models. Another approach is the renormalization approach, in which the grid block sizes are increased until the simulation model is obtained (e.g. King and Muggeridge, 1993). Also, the Representative Elementary Volume (REV) approach is used to run a fine scale simulation for only small selected parts of the reservoirs. One more recent approach was introduced by Durlofsky and Chen (2008), and is called ensemble level upscaling.

Upscaling of relative permeability curves was originally proposed in order to compensate for vertical effects in 2D areal models (e.g. Hearn et al., 1971). Later, they

were used in 3D coarse models to compensate for the heterogeneity details in complex reservoirs (e.g. the Kyte and Berry, 1975). When building a simulation model representing a heterogeneous reservoir, a significant loss of heterogeneous features could occur, if the fine-grid relative permeabilities (also referred to as rock curves) are used to run coarse scale simulations. Instead, relative permeability curves should be upscaled to adjust the results of the coarse model after being upscaled using single phase upscaling methods. The upscaled relative permeabilities can be used to control numerical and physical dispersion in the coarse grid models. They can be also used to capture the heterogeneity in the fine scale model so that the fluid flow behaviour in the coarse model could be preserved. However, there are many issues related to generation and application of the upscaled relative permeability curves, which makes them less attractive compared to single phase methods.

Many reviews, such as Darman et al. (1999), have been made to compare some of the two phase upscaling methods indicating the methods' weaknesses and strengths. Also, critical reviews pointing out to the difficulties when applying the pseudo functions were presented in the literature such as Barker and Thibeau (1997). All of this has motivated the work presented in this thesis in order to propose a new method to upscale relative permeability curves in heterogeneous reservoirs. The method introduced here can be used to upscale relative permeability curves in 2D and 3D models with avoiding one of the issues that arise when upscaling, which is pressure averaging. Also, another issue was considered when applying the proposed method, which is the impracticality associated with the use of one pseudo function per each coarse cell. This was solved by applying a method to group similar pseudos together and use a representative pseudo curve for a selected region in the reservoir.

The method presented in this thesis is referred to as transmissibility weighted relative permeabilities (or TWR), which can be classified as a dynamic two phase upscaling method. However, running fine-scale simulation can only be considered for a sector model and not for full fine model. Afterwards, the generated TWR pseudos are grouped and a representative of each group can be used for the corresponding region in the model. The applied grouping method used in this thesis starts with curve fitting of functional models of Chierici (1984) to the TWR curves. The calculated Chierici (1984) parameters are then plotted to check possible clusters of pseudos.

Two more subjects when applying pseudo functions for coarse scale simulations were considered in this work. The first is the use of well pseudos, especially for the wells placed at the edge of the model in cells that are usually assigned rock curves. A new method to generate the well pseudos using the well connection factor weighting is provided. The second subject is the application of directional pseudo functions. The TWR pseudos were generated in all the positive and negative x, y and z directions.

Calculations of the TWR method were performed by writing C++ codes to generate pseudo functions and well pseudos for 2D models. Afterwards, the codes were extended to generate pseudos for 3D models. Finally, the codes were again extended to generate directional pseudos in the positive and negative directions.

## **1.2 Objectives of the thesis**

The aim of this thesis is to propose a two phase upscaling method to upscale relative permeability curves in heterogeneous reservoirs. The method avoids pressure averaging because it may result in the following (Barker and Thibeau, 1997):

1. Negative pseudos, if the flow direction is opposite to the direction in which average pressure gradient was calculated, and
2. Infinite pseudos, if the average pressure gradient is zero while flow between the cells, for which this average gradient was calculated, is nonzero.

Also, generation of directional pseudos were considered when applying the proposed method in order to control the flow in different directions, as suggested for example by Azoug and Tiab (2003) and Darman et al. (2003). In addition, this thesis introduces a method to group the generated pseudo functions, which should make use of the pseudos more feasible in practice.

In order to achieve these objectives, the following was considered:

- Carrying out a thorough literature review in order to gain knowledge about the existing upscaling methods, their application and limitations.
- Developing the proposed two-phase upscaling method.
- Writing C++ programs to perform calculations of the proposed method.
- Testing the proposed methods using 2D and 3D models and analysing the results.



- Application of the proposed methods to the heterogeneous SPE 10 model 2 (Christie and Blunt, 2001).

### **1.3 Outline of the thesis**

This thesis is organized as follows:

Chapter 1 provides a brief background to the concept of upscaling for reservoir models, in addition to description of types of the upscaling methods that are introduced in the literature. Also, introduction to the objectives of the thesis, including the development of a new method to upscale relative permeability curves, is provided.

Chapter 2 introduces a detailed literature review about many of the upscaling methods. This includes analytical methods, single phase upscaling methods, near well upscaling, and two phase upscaling methods. Special attention was given to the two phase upscaling methods, which is the scope of this thesis. Also, the background to grouping of upscaled relative permeabilities (pseudo functions) is provided.

Chapter 3 introduces a description to the proposed two phase upscaling method (TWR) including the workflow of the method and the equations applied. Also, introduction to a new method to generate well pseudos was provided. Finally, a method to group the pseudo functions based on curve fitting is proposed.

Chapter 4 describes the tests carried out to check the performance of the proposed TWR method and the well pseudos when applied to 2D and 3D models, followed by analysis and discussion of the results. Also, the grouping of pseudos method was tested in order to make handling of the generated pseudos more feasible in practice.

Chapter 5 describes application of the TWR method, well pseudos and grouping to the SPE 10<sup>th</sup> Comparative Solution study model 2 (Christie and Blunt, 2001), where the TWR and well pseudos were generated for a coarse model, corresponding to the top four layers of the Tarbert formation.

Chapter 6 provides summary and conclusions learnt from this work.

Appendices provide details of the C++ codes that were written in order to upscale the relative permeability curves for 2D and 3D models using the proposed TWR and the well pseudo methods.

## **Chapter 2 : Literature Review**

## 2.1. Introduction

In this chapter, a general literature review on upscaling for reservoir simulation will be provided. The purpose of carrying out this review was to gain deeper understanding of the existing upscaling techniques, their advantages, limitations and challenges included. This has formed the basis for developing a new method to upscale relative permeability curves (introduced in Chapter3), which is the target of this project. The aim of this review is not to assess all the upscaling methods, rather to understand the main aspects in the area of upscaling through introducing few methods as representatives. This chapter is organized as follows: first, a general overview of upscaling is provided, followed by a review of the traditional analytical (averaging) methods, single phase upscaling methods and near well upscaling methods. Finally, many of two phase upscaling methods, which are of concern to this thesis, are discussed. Although some of the upgridding methods (e.g. Durlofsky et al. 1996 and Stern and Dawson 1999) were also reviewed, they were not discussed here because they are out of the scope of this thesis.

## 2.2. Reservoir models upscaling

Geological reservoir models are usually built using tens or even hundreds of millions of grid blocks, each of them represents part of the reservoir, and is characterized by specific reservoir parameters such as porosity and permeability. These reservoir parameters are usually populated over the entire grid using geostatistics (e.g. stochastic methods). Description of the spatial distribution is dependent on the information collected during drilling of wells in specific locations in the field. It is very time consuming and difficult, if not impossible in some cases, to run reservoir flow simulations using this very large number of grid blocks with a lot of information included. This is especially true, if these simulations have to be run many times to assess, for example, the underlying geologic uncertainty or history match the model. Therefore, it is necessary to reduce the number of grid cells and average the data included within them so that they can be processed in a more practical manner. Reducing the number of grid cells can be managed by coarsening the fine-grid models through merging the fine cells into coarser ones (this is referred to as upgridding). Consequently, it becomes important to estimate the equivalent values of reservoir properties that should be assigned to that coarser domain. This process of coarsening the grid and averaging the reservoir properties within them is referred to as upscaling.

Upscaling of reservoir properties has been practiced for decades to build reservoir models that are feasible for running simulations. The practical reservoir models that include a reasonable number of grid cells to run simulations (e.g. in the order of  $10^5$ - $10^6$  cells) are usually referred to as simulation models, while the reservoir models that include detailed properties and a huge number of grid cells are generally referred to as geological models. It should be noted that upscaling does not aim to speed up reservoir simulations on the cost of simulation results. On the contrary, the idea is to build coarse models that preserve the most important flow characteristics of fine models and capture the sub-grid heterogeneity. In other words, the goal of upscaling is to replace the very detailed description of rock properties with equivalent properties of a coarser scale (Christie, 1996 and 2001). This means that the coarse models should be practical but reliable and be able to reproduce the fine model results.

From the above, it might sound achievable when speaking about upscaling of reservoir properties such as porosity and water saturation, which can be easily averaged in a straight forward process. For example, porosity can be averaged within the coarse domain using arithmetic averaging coupled with suitable weighting (usually volume weighting). The same procedure may also apply for water saturation averaging (using pore volume weighting). However, the upscaling problems arise when it comes to upscaling reservoir permeability. This is because permeability is not additive, so that it cannot be adequately upscaled in reservoirs with high levels of heterogeneity using, for example, arithmetic averaging methods (Renard and Marsily, 1997).

Many upscaling techniques have been already introduced in the literature to upscale permeability (or transmissibility) such as analytical methods, single phase flow upscaling methods and two phase upscaling methods. The analytical methods (e.g. arithmetic and geometric averaging) do not require running fine flow simulations and are simple to apply. This makes these methods attractive and feasible for use. However, application of analytical methods requires some idealized conditions so that the results may not be satisfactory when applied for complex reservoirs. The single phase upscaling methods require running flow simulations and ought to give better results than the analytical methods. Single phase upscaling techniques aim to upscale absolute permeability (or transmissibility) by solving pressure equation that is a combination of Darcy's single phase flow equation and mass conservation. The challenge of using these methods relies on the boundary conditions applied. Upscaling

results, especially in complex reservoirs, are greatly dependent on selection of the appropriate boundary conditions (Christie and Blunt, 2001).

Single phase upscaling methods were classified by Durlofsky (2003), according to the way boundary conditions are set, to: local, extended-local, global, and quasi global (also called local-global). In the local methods, a region of fine cells is selected and the parameters of the corresponding coarse block are calculated. The same approach is followed in the extended-local methods but an additional region (border) around the target region is considered. The global methods consider running full fine scale simulation then calculate the coarse scale parameters. Finally, the quasi global methods consider running global coarse scale simulation to estimate the boundary conditions that can be used to calculate the equivalent parameters using extended-local methods.

Additional techniques of upscaling include approaches to upscale regions near wells (called near-well upscaling methods) are also discussed in this chapter. These methods were proposed because upscaling parameters in the region where wells are placed is different from upscaling using the local or extended local methods mentioned above. The difference lies in the assumption that flow near wells is neither linear nor slowly varying (Durlofsky, 1999). The flow in the vicinity of wells is rather radial and is affected by high pressure gradient (Ding, 1995). Therefore, applying upscaling methods without taking this assumption into account would have great impact on the upscaling results. Instead, coupling the upscaling methods with near well upscaling can improve the results significantly. Some of the near well upscaling methods are introduced in this chapter such as Ding (1995) and Durlofsky et al. (2000).

Two phase upscaling methods aim to upscale relative permeability and capillary pressure curves in order to improve results of the coarse models, after being upscaled using single-phase methods. The upscaled relative permeability curves are usually referred to as pseudo functions. Like the single phase upscaling methods, pressure equations can be solved to obtain the upscaled parameters, but this time using Darcy's two phase flow equation. However, there are two phase upscaling methods that do not use Darcy's flow equation to calculate the pseudo functions. For example, Stone (1991) used total mobility and fractional flow to upscale relative permeability curves.

When using two phase upscaling methods, applying well pseudos (i.e. upscaled relative permeability in the well connections) may play the same role of improving upscaling results similar to that of near-well upscaling methods, used in conjunction with single phase upscaling methods. Well pseudos (e.g. Emanuel and Cook, 1974) are used to adjust the well results and preserve the well location in the coarse grid. Also, the well pseudos were found to be more effective than the use of LGR (Azoug and Tiab, 2003). Understanding the impact of well pseudos helped to propose a new approach for generation of well pseudos, as discussed in Chapter 3.

Deciding which upscaling method to use depends on what circumstances they will be applied. Analytical methods can be successfully applied to upscale properties such as porosity but will require conditions like a homogeneous and isotropic reservoir in order to be used for upscaling permeability adequately. Single phase upscaling methods are more practical than two phase methods but less accurate when applied for reservoirs with high heterogeneity levels. On the other hand, the two phase upscaling methods may provide better results than single phase methods for two phase problems but they are less feasible when applied to large field models, due to the high computation time cost required. Also, selection of the best two phase method to apply depends for example on balance of forces. According to Durlofsky (2003), selection of a suitable upscaling method can be decided according to: the question for which the model was built to answer, the method of production (primary, secondary, etc.), and the heterogeneity level that can be assigned to the coarse model.

Generally, without regard to the upscaling method used, the upscaling process can be considered successful when the coarse model gives results as close as the fine model results, or in other words, the fine model can be replaced by the coarse model. This is of course assuming that the fine model represents the “correct” answer of the problem investigated. Comparisons between the coarse and fine models are usually done case by case. However, comparisons can be also done at the ensemble level (e.g. P90, P50 and P10) such as in Durlofsky and Chen (2008).

The upscaling techniques considered when carrying out this literature review will be discussed in more detail in the following sections.

### 2.3. Analytical methods

Analytical or averaging methods include for example arithmetic, harmonic, geometric, and power averaging methods. These methods are usually used to upscale properties such as porosity and water saturation together with applying volume weighting (e.g. pore volume weighting). Successful application of the analytical methods to average permeability requires idealized circumstances which are not usually available in real fields. For example, permeability can be adequately upscaled using the arithmetic methods only when fluid flows parallel to uniform layers, while the harmonic average can be used when fluid flows across the layers, see Figure 2-1. However, the reservoir layers are not usually homogeneous and isotropic. Therefore, though practical, using these methods to average permeability may lead to inaccurate results for two-phase flow.

In order to upscale permeability in a system with correlated, random permeability and no specific flow direction, the geometric permeability average can be applied (Matheron, 1967). Also, a general form of the analytic approaches is expressed by the power averaging method (Journal and Deutch, 1986). The power coefficient  $\omega$  ranges between -1 and 1. In general, if  $\omega = 1$ , the result will be the same as arithmetic average and if  $\omega = -1$ , the result will be similar to harmonic average. In other words, the arithmetic and harmonic averages form the higher and lower bounds for permeability, respectively. Equations applied to average permeability using the analytical methods are shown in Table 2-1.

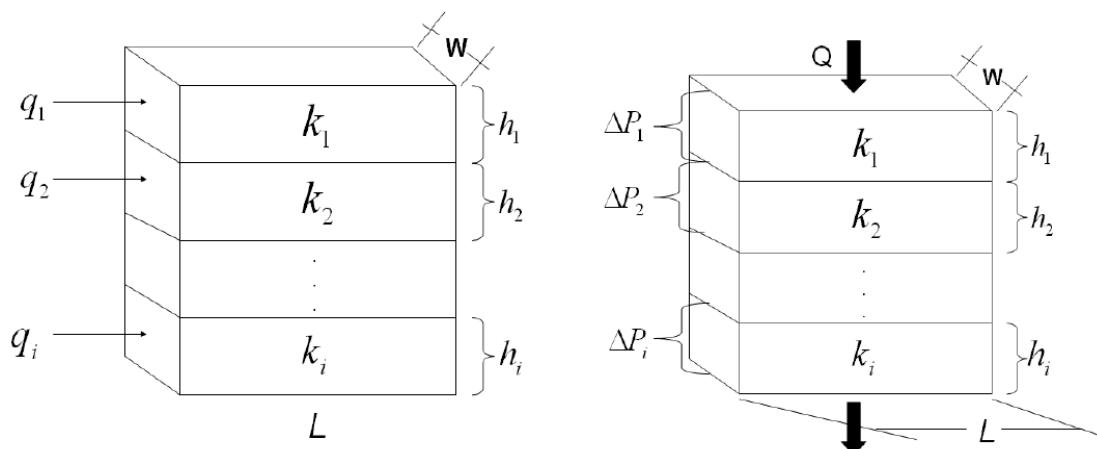


**Figure 2-1:** Parallel flow (left) and series flow (right), adapted from Salazar and Villa (2007)

There are additional analytical approaches that can be applied to average permeability. For example, the method by Kasap and Lake (1989) can be used to calculate tensor average permeability in anisotropic layers. Also, permeability can be averaged by using the renormalization method, developed by King (1988). Nevertheless, in order to obtain better upscaling results in general, the numerical flow based methods (single and two phase upscaling methods) are usually applied.

Method of averaging	Expressions to average permeability ( $k^*$ )
Arithmetic	$k^* = k_a = \frac{\sum_{i=1}^n t_i k_i}{\sum_{i=1}^n t_i}$ <p><math>t_i</math> is thickness of layer i,  <math>k_i</math> is the permeability of layer i, and  n is number of layers.</p>
Harmonic	$k^* = k_h = \frac{\sum_{i=1}^n t_i}{\sum_{i=1}^n (t_i/k_i)}$ <p><math>t_i</math> is thickness of layer i,  <math>k_i</math> is the permeability of layer i, and  n is number of layers.</p>
Geometric	$k_g = \exp\left(\frac{\sum_{i=1}^n \ln(k_i)}{n}\right)$ <p> <math>k^* = k_g(1 - \sigma_Y^2/2)</math> in 1D  <math>k^* = k_g</math> in 2D  <math>k^* = k_g(1 + \sigma_Y^2/6)</math> in 3D  <math>\sigma</math> is standard deviation and <math>Y = \ln(k)</math> </p>
Power Law	$k^* = k_\omega = \left[\frac{\sum_{i=1}^n k_i^\omega}{n}\right]^{1/\omega}$ <p><math>\omega</math> is the power coefficient</p>

**Table 2-1:** Types of analytic averaging methods



## 2.4. Single phase upscaling

### 2.4.1. Background

Single phase upscaling methods are widely used because they are in most cases practical and require fewer computations, in comparison to two phase upscaling methods. Single phase upscaling methods assume that the flow is linear and in a steady-state and, as its name indicates, assumes a single phase to flow in the system. However, this type of upscaling method can be also applied for two or even multiphase flow problems. Accuracy of results will vary depending on many parameters, such as heterogeneity level and boundary conditions selected to solve the pressure equations. The aim of single phase upscaling is to upscale absolute permeability or transmissibility in order to preserve the sub-grid heterogeneity and in turn to reproduce the results of a fine grid model using coarse grid model.

The direct methods used for single phase upscaling are called pressure solver methods. Calculations in these methods are performed by selecting boundary conditions then calculating the equivalent value of permeability. The upscaled permeability can be then used in coarse scale simulations to provide similar flow rate as the fine model (Christie, 1996). There are several types of boundary conditions that can be used to calculate the equivalent permeability. A comparison between types of boundary conditions for its accuracy when used for upscaling was carried out by Pickup et al. (1992). The no-flow boundary conditions assume that there is no flow on two sides of the domain and that pressure is fixed on the other two sides. This type of boundary conditions is the most commonly applied and it is generally suitable for models with very little cross flow between layers that are almost horizontal. Also, it was found in the SPE 10th Comparative Solution study (Christie and Blunt, 2001) that the no flow boundary condition provided the most accurate results for the studied case, as a single phase upscaling approach. Another type of boundary conditions is the periodic boundary conditions. This type of boundary conditions allows flow through the edges and assumes equal pressure drop periodically and it can be used to calculate permeability tensors (e.g. Durlofsky, 1991). The linear flow boundary conditions combine two of the assumptions provided by periodic and no-flow boundary conditions. The first is that it allows flow through the edges and the second is that pressure is fixed at each side. The difference is that pressure in this type of boundary conditions is interpolated linearly from one side to the other. Effective flux boundary conditions

(EFBCs) were applied by Wallstrom et al. (2002a). These boundary conditions are characterized by suppression of flux into high permeability cells in the sub-grid simulation. The EFBCs were also applied to two phase upscaling (Wallstrom et al., 2002b). Another approach was applied by Zhang et al. (2005) and called well drive upscaling (WDU). The WDU method uses well drive boundary conditions, to simulate the actual flows in the reservoir, using high pressures at the injector wells, low pressures at the producers and no-flow through the edges.

The main challenge when applying single phase upscaling methods is the selection of the appropriate boundary conditions. Generally, upscaling results are greatly affected by the way the boundary conditions were set (Christie and Blunt, 2001). Many attempts have been done in order to reduce the effect of boundary conditions when upscaling. For example, using flow jackets or skin (e.g. Gomez-Hernandez and Journel, 1990) was applied by considering extra cells (border) around the edges defining the coarse domain, for which equivalent parameters will be computed. It was found that the flow jackets provide better results than when using local single phase methods alone. In a comparison carried out by Kazemi et al. (2012) between many upscaling methods applied to a heterogeneous carbonate model, it was found that the well drive upscaling (WDU) gave the best results when compared to the conventional pressure solvers with no-flow boundary condition, linear boundary condition and flow jackets.

#### 2.4.2. Single phase flow equations

The equations governing single phase flow are obtained by coupling Darcy's single phase flow equation and the mass conservation equation (Durlafsky, 2003):

Darcy's single flow equation (in absence of gravity) is given by:

$$\mathbf{u} = - \frac{1}{\mu} \mathbf{k} \cdot \nabla p \quad (2.1)$$

where,

$\mathbf{u}$  is the Darcy velocity,

$\mathbf{k}$  is reservoir permeability,

$\mu$  is fluid viscosity, and

$\nabla p$  is pressure drop between two adjacent blocks.

Mass conservation equation is given by:

$$\frac{\partial}{\partial t}(\rho\phi) + \nabla \cdot (\rho u) + \tilde{m} = 0 \quad (2.2)$$

where,

$\rho$  is fluid density,

$\phi$  is rock porosity,

$u$  is the Darcy velocity, and

$\tilde{m}$  is the well (source/sink) term.

By combining equations (2.1) and (2.2) we get:

$$\frac{\partial}{\partial t}(\rho\phi) - \nabla \cdot \left( \frac{\rho}{\mu} k \cdot \nabla p \right) + \tilde{m} = 0 \quad (2.3)$$

Assuming that the system is homogeneous and the fluid and rock are incompressible, would mean that  $\rho$  does not vary in space or time and, if the system is in steady-state,  $\partial\phi / \partial t = 0$ . Therefore, equation (2.3) can be simplified to single phase pressure equation as:

$$\nabla \cdot \left( \frac{1}{\mu} k \cdot \nabla p \right) = \tilde{q} \quad (2.4)$$

where,

$\tilde{q}$  is the volumetric source term and  $\tilde{q} = \tilde{m}/\rho$ .

In order to account for the gravity term the pressure in equation (2.4) can be replaced by potential. Also, the equations above assume a 1D system, but they can be extended to 2D and 3D.

### 2.4.3. Single phase flow techniques

There are many reviews in the literature that give complete overview of the single phase upscaling techniques such as Wen and Gomez-Hernandez (1996), Durlofsky (2003), and Farmer (2002). Some reviews also provide advice on what circumstances these techniques can be applied such as Renard and Marsily (1997). In this thesis only few of single upscaling techniques will be reviewed.

- Local upscaling techniques:

In this type of upscaling a region of fine cells is selected, and the parameters of the corresponding coarse block are calculated. These methods calculate the equivalent permeability using local boundary conditions. However, if the assumed boundary condition is not appropriate with regard to reservoir heterogeneity, the error in upscaling could be large. For example, in case of using no-flow boundary conditions to calculate vertical effective permeability of a coarse cell with size similar to shale barriers, with zero permeability, the effective permeability will be zero. This would yield errors in simulation, in case that the fluid can flow vertically through the model. Although some authors suggested using flow jackets to improve the upscaling results (e.g. Gomez-Hernandez and Journel, 1990), it is still obvious that the upscaled permeability is dependent on boundary conditions. It was recommended by King (1997) to vary the boundary conditions when calculating the effective permeability using local methods. Afterwards, answers for different boundary conditions should be compared. If the answers are different then more care should be taken to study the upscaled region.

The simplest procedure to upscale permeability within a coarse grid block using the local methods was first introduced in literature by Warren and Price (1961) and can be described as follows:

1. Assume that no-flow boundary conditions are applied to the coarse grid block (i.e. no flow on four sides of the coarse cell and constant pressure on the other two sides), see Figure 2-2.
2. Solve the pressure equation to obtain pressures in each fine grid block included within the coarse block.
3. Use Darcy's single phase flow equation to calculate the flow rates in the fine cells.
4. Sum up the flow rates on the face of the coarse grid cell.
5. Calculate the effective permeability using the following equation:

$$k_{eff} = \frac{Q \mu L}{A \Delta P} \quad (2.5)$$

where,

Q is the total flow rate on the coarse cell face,

$\mu$  is the flowing phase viscosity,

A is the coarse cell face area perpendicular to flow direction,

$\Delta P$  is the pressure drop, and

$L$  is the coarse cell length.

Calculations above should be repeated to calculate effective permeability for different directions of flow.

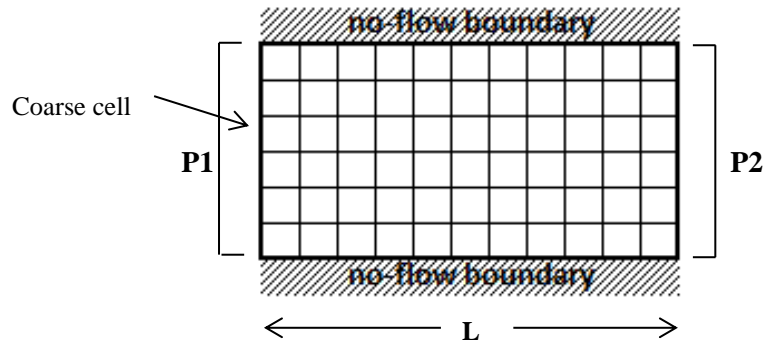


**Figure 2-2:** Coarse cell with no-flow boundary conditions

Different approaches with different boundary conditions were also introduced in the literature to upscale the permeability using local methods. For example Durlofsky (1991) used local periodic boundary conditions to upscale permeability tensors for heterogeneous reservoirs. The equivalent permeability was obtained by averaging the fine scale velocity field. Also, Christie et al. (2000) presented a method to upscale permeability using effective medium boundary conditions (EMBCs). This method was then applied by Wallstrom et al., 2002a) and the boundary conditions name has been changed to effective flux boundary conditions (EFBCs), not to be mixed with the effective medium theory (EMT) proposed by Kirkpatrick (1973). The Wallstrom et al. (2002a) method procedure starts with applying no-flow boundary conditions in order to calculate the effective permeability. After that, the EFBCs are applied with that effective permeability in the background to calculate the effective permeability for the coarse block. The EFBCs provide improvement to coarse scale simulation by suppressing flux through the high permeability streaks. However, the results of this method are not good enough in heterogeneous models.

Another single phase approach presented in the literature is direct upscaling of transmissibility, instead of permeability (e.g. White and Horn, 1987). However, if there is a vertical discontinuity at, for example, the coarse cell centre, the upscaled transmissibility will erroneously cause fluid to flow to the adjacent coarse cell when there is no or little flow. Same as with the shale barrier example mentioned previously, skin or flow jackets can improve the transmissibility upscaling results. This is done by using an additional region around the target region in order to decrease the errors arising

from using improper local boundary conditions. The local method is then called extended local (e.g. Christie and Clifford, 1998 and Gomez-Hernandez and Journel, 1990).

- Extended local methods

These methods follow similar approach as in the local procedure but with an additional border (referred to as skin or flow jacket) around the region of interest. This approach can improve upscaling results especially in complex reservoirs. Techniques proposed by Gomez-Hernandez and Journel, (1990) and Christie and Clifford (1998) suggested the use of flow jackets to improve the upscaling results. This was also demonstrated by Efendiev (1999). In the case of oriented permeability fields, the use of extended local methods seem to have greater improvement in the permeability upscaling results than traditional local upscaling methods, Wen and Durlofsky (2000).

Generally, the results of local and extended local upscaling techniques are mainly dependent on selection of the appropriate boundary conditions, which is not known in advance (Durlofsky, 2003).

- Global upscaling techniques

In these methods the full model fine scale simulation is run and the coarse scale parameters are calculated. The main advantage of the global methods is that the local boundary conditions are avoided so that the dependency of the upscaled permeability (or transmissibility) on boundary conditions is less. However, there are some related problems with the application of global approaches such as isolated flow bodies. Stone et al. (2007) discussed the problem of isolated sand bodies when applying the global methods. The problem in brief is that when solving the pressure equations globally, the pressure in the isolated sand bodies (e.g. sand surrounded with shale of zero permeability) will be constant, which means that there is no flow. Therefore, upscaling permeability for these regions becomes impossible. This may not be a problem in case of sand bodies without wells producing from them, because these regions will not have impact on the results. The problem arises when a sand body includes a well producing from it. In this case, it is important to upscale the permeability within that sand body. The solution provided in Stone et al. (2007) is to select a separate domain for the sand body of interest, apply suitable boundary conditions and solve pressure equations for it.

Additional challenges in application of global methods to real field models were discussed in Wu et al. (2007).

There are many examples for using the global upscaling techniques to upscale permeability or transmissibility. For example, Holden and Nielsen (1998) used the global approach of single phase upscaling to upscale permeability. The aim was to provide coarse scale pressure and velocity fields that are very close to those of the fine scale model. Also, Nielsen and Tveito (1998) provided a method that uses iteration on velocity for example to compute the optimal permeability for the coarse model using results of the fine model. Another global upscaling method is Well Drive Upscaling (WDU), proposed by Zhang et al. (2005). In this method transmissibility is upscaled using natural well drive conditions, while applying global pressure solution. The method is coupled with the near well upscaling approach proposed by Ding (1995) to calculate well indices. Additionally, when multiple relative permeability curves are used in the fine model, the WDU method provides a transmissibility weighted approach to calculate the coarse scale relative permeability. This is done instead of using the majority vote approach, which uses the relative permeability curve of the most common rock types within a coarse cell to be the representative for that coarse cell.

- Quasi global (local-global) methods

The target of the local-global methods is to obtain the global flow effects without running a global fine scale simulation. Instead, a global coarse scale simulation is run to estimate the boundary conditions that can be applied for extended local calculation of upscaled transmissibility, see Figure 2-3. Examples for the local-global methods are Chen et al. (2003), who proposed a coupled local global method, and Durlofsky and Chen (2006), who proposed an adaptive local global method. Another example of local-global methods is Chen et al. (2009).

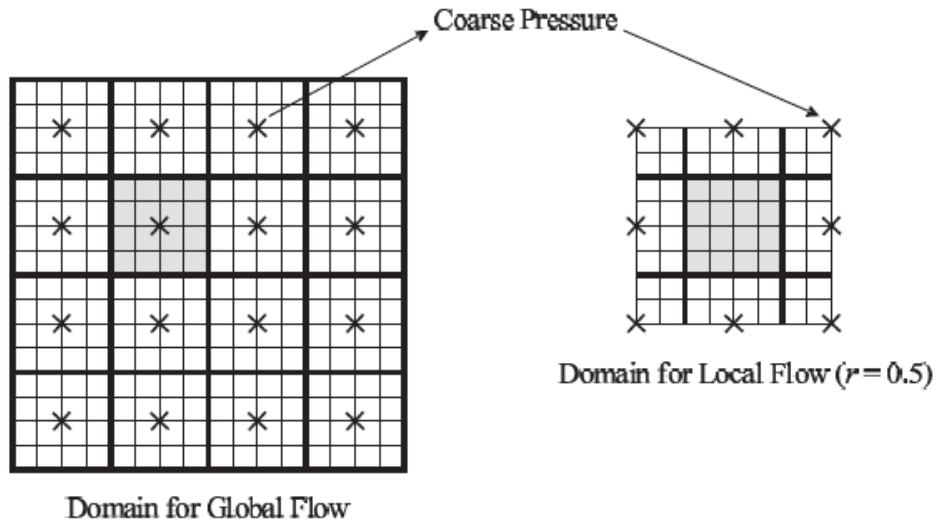


**Figure 2-3:** Schematic shows local-global coupling, from Chen et al. (2003)

### 2.5. Near well upscaling

Upscaling in the region where a well is placed is different from the local or extended local upscaling methods in the assumption that flow near the well is neither “linear” nor “slowly varying” (Durlofsky, 1999). The flow in the vicinity of wells is rather “radial” and is affected by high pressure gradient (Ding, 1995). Therefore, many of the upscaling techniques may not give good results if the heterogeneity in the well nearby is significant, which requires a specific treatment to be upscaled. Using near well upscaling can provide a significant improvement to the upscaling results.

Many approaches have been published on the near well upscaling subject. For example, Ding (1995) developed a method to determine well block transmissibility in addition to well index. Also, Soeriawinata et al. (1997) introduced a method for calculation of effective permeability in the well blocks (i.e. well connections) using a combination of arithmetic and harmonic means based on radial flow. Muggeridge et al. (2002) introduced a reduced computational domain of Ding’s (1995) method. Later, Ding (2003) provided near well upscaling on coarse corner point grid. Durlofsky et al. (2000) provided improvements to the approach by Ding (1995). The methods by Ding (1995) and Durlofsky et al. (2000) will be reviewed in more detail below.



- Near well upscaling (Ding, 1995)

In this approach two patterns of flow are considered, radial flow pattern (representing high pressure gradient) near the wells and linear flow pattern (representing high pressure gradient) away from the wells. Upscaling of the region where the flow is assumed to be linear is performed using no-flow boundary conditions, while the upscaling procedure in the vicinity of the well (i.e. the radial flow region) is described as follows:

- Choose a well(s) near which upscaling will be performed.
- Select a region around the well in the fine model.
- Set a boundary condition for the fine near well region and run fine-scale steady state simulation.
- On the coarse model, define the coarse region corresponding to the selected near well region on the fine model. See Figure 2-4.
- Calculate equivalent flow rate on the interface of the coarse grid region, equivalent pressure in the coarse grid region, and equivalent well flow rate, in addition to bottom-hole pressure.
- Calculate well index and transmissibility near the well using the following equations (2.6) and (2.7) :

$$T_{ij} = \frac{Q_{ij}}{P_j - P_i} \quad (2.6)$$

where,

$T_{ij}$  is the equivalent transmissibility between two coarse blocks i and j,

$Q_{ij}$  is the equivalent flux on the interface between the coarse blocks i and j, and

$P_j - P_i$  is the pressure difference between the blocks i and j.

$$WI_i = \frac{q_i}{P_i - P_{wbi}} \quad (2.7)$$

where,

$WI_i$  is the well index on a coarse well block i,

$q_i$  is the well flow rate,

$P_i$  is the equivalent well connection pressure, and

$P_{wbi}$  is the well bottom hole pressure of well placed in block i.

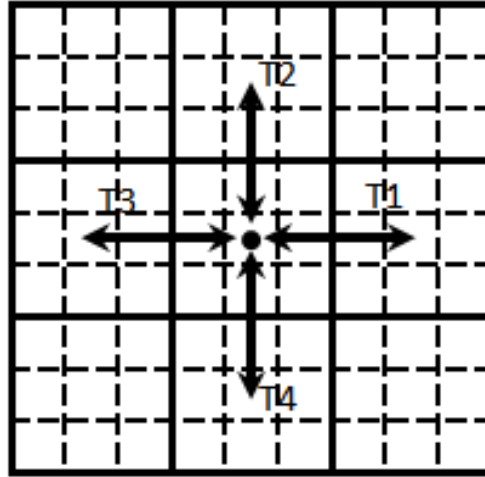


**Figure 2-4:** Equivalent transmissibility - near well upscaling, from Ding (1995)

- Scale-up in the near well region (Durlafsky, 1999)

This approach is consistent with Ding's (1995) approach in running fine grid simulation and calculating well block transmissibilities. However, this approach solves specific local flow problems and considers a 3D system, while the work by Ding (1995) considered only 2D. Also, enhancements to the general approach were provided.

The procedure of Durlafsky et al. (2000) is described as follows:

- Solve the single phase pressure equation (i.e. Darcy single phase flow equation combined with conservation of mass) using no-flow boundary conditions.
- Average the pressure over the regions corresponding to coarse grid blocks, see Figure 2-5, using bulk volume weighting.
- Calculate total flow rates at the downstream edge of coarse cells.
- Calculate upscaled well block transmissibilities using the average pressure and the total flow rate from steps b) and c) respectively.
- Calculate flow rate out of the well into each layer using Peaceman's well model (1978, 1983) as follows:

$$q = I_w (P_{wb} - P_f) \quad (2.8)$$

where,

$P_f$  is the fine well block pressure,

$P_{wb}$  is the well bottom hole pressure, and

$I_w$  is the fine scale well index.

The well index  $I_w$  is given by:

$$I_w = \left( \frac{2\pi k_g \Delta z}{\ln(r_o/r_w)} \right)_{i,j} \quad (2.9)$$

where,

$k_g$  is the geometric mean of  $k_x$  and  $k_y$ ,

$\Delta z$  is the grid block thickness,

$r_w$  is the wellbore radius, and

$r_o$  is the equivalent pressure radius.

The equivalent pressure radius  $r_o$  is given by:

$$r_o = 0.28 \frac{[(k_y/k_x)^{1/2} (\Delta x)^2 + (k_x/k_y)^{1/2} (\Delta y)^2]^{1/2}}{(k_y/k_x)^{1/4} + (k_x/k_y)^{1/4}} \quad (2.10)$$

where,

$k_x$  and  $k_y$  are permeability in the x and y directions respectively, and

$\Delta x$  and  $\Delta y$  are the gridblock dimensions in the x and y directions.

f) Sum the flow rates calculated in step e.

g) Calculate the coarse scale well index, from the equation:

$$WI = q_o(P_{wb} - P_i) \quad (2.11)$$

where,

$WI$  is the coarse scale well index,

$q_o$  is the total flow rate out of the well,

$P_{wb}$  is the wellbore pressure, and

$P_i$  is the coarse well block pressure.

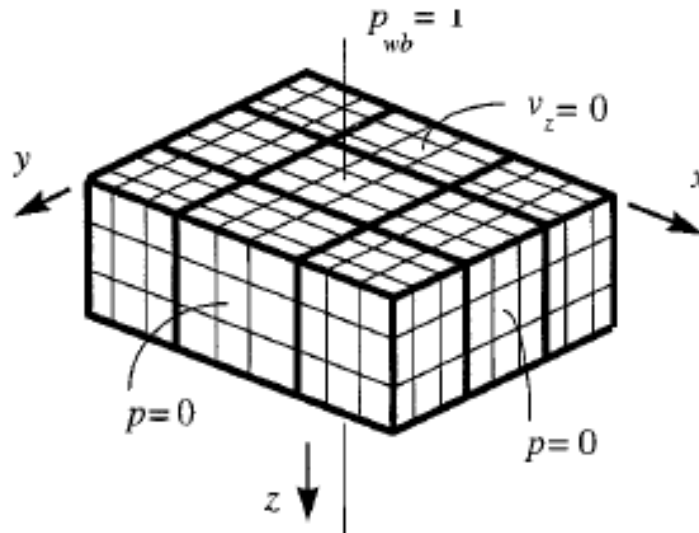


**Figure 2-5:** Fine and coarse grid system – near well upscaling, from Durlofsky et al. (2000)

Limitations of the Durlofsky et al (2000) method:

1. It does not include the entire well length so that it is valid only for vertical wells. Further extension of the method was provided by Mascarenhas (1999) to be valid for horizontal wells. This was achieved by extending the local solution region radially and including the entire well length.
2. The method might not be very accurate in the early transient period.
3. As with Ding (1995), the method does not upscale multiphase flow (i.e. does not upscale relative permeability) so that, when used for multiphase flow problems, they might be adequate only for moderate degree of coarsening Durlofsky et al. (2000).

Upscaling relative permeability in well blocks was considered, for example, by Emanuel and Cook (1974). In Chapter 3, a method is proposed to upscale relative permeability curves in well connections using well connection factor weighting. The aim of these well pseudos is to adjust well results in the coarse model by maintaining the well position in the coarse connections.

## 2.6. Two phase upscaling

### 2.6.1. Background

Using fine-grid relative permeability curves (also called rock curves) for running coarse scale simulations may lead to remarkable loss of heterogeneity. This in turn affects the fluid flow behaviour in the coarse model and may give poor results. The two phase upscaling approach is a means of upscaling relative permeability and capillary pressure curves in order to capture the impact of sub-grid heterogeneity, compensate for numerical dispersion that arises from the gridding, and capture the fluid behaviour. Generally, the two phase upscaling methods are used when single phase upscaling methods are not enough to compensate for fluid dynamic behaviour and fine scale heterogeneity.

Using two phase upscaling methods should enable the coarse model to reproduce the important results of the fine-grid model, such as water breakthrough time, cumulative production, average field pressure, etc. The two phase upscaling methods (e.g. Kyte and Berry, 1975 and pore volume weighted (PVW)) proved to be successful in some cases at providing better results than the results of single-phase upscaling methods. However, due to the extensive calculations required and impracticality when applied for real field cases, the two phase upscaling methods are not as popular as the single phase methods.

The upscaled relative permeability and capillary pressure curves are usually referred to as pseudo relative permeability and pseudo capillary pressure curves or simply as *pseudo functions*. The word “pseudo” is used to differentiate between the curves used for fine grid simulation (i.e. the rock curves) and the upscaled curves used for coarse grid simulation (i.e. the pseudo functions). The latter are determined by two phase or multi-phase upscaling methods, the former are measured in laboratory or calculated using equations such as Corey (1954) or Chierici (1984). Also, the word “pseudo” is used because the pseudo functions can compensate for the numerical dispersion and can account for small scale heterogeneity.

Pseudo functions were originally generated to compensate for vertical effects in 2D areal model (e.g. Hearn et al., 1971). Afterwards, they were used in 3D coarse models to compensate for the heterogeneity details in complex reservoirs (e.g. pore volume weighted method). Pseudo functions act as a supplement to enhance results of

the coarse models after being upscaled using single-phase methods. Beside the use of pseudo functions to upscale from a geological model to a simulation model, the pseudo functions have also been used to upscale from lamina-scale to geological model (e.g. Pickup et al. 2000).

Many methods and approaches to estimate the pseudo functions have been presented in the literature. Pseudo functions can be divided, according to the way they were generated, into analytical (also called static), dynamic, streamline and history matching pseudo functions. The analytical pseudos are those obtained by straightforward calculations without need for running fine grid simulations. For example Coats et al. (1967 and 1971) introduced the vertical fluid equilibrium approach in which it is assumed that fluids segregate in the vertical direction by static equilibrium between gravity and capillary pressure. Also, Hearn et al. (1971) proposed a method to generate pseudo functions in order to approximate viscous flow in a stratified reservoir with an areal model, where gravity and capillary pressure forces are very small or negligible (i.e. flow is viscous-dominated). However, the use of the methods mentioned above is very limited due to the assumptions applied, which might be unreliable for real field cases.

The dynamic pseudo functions, as their name indicates, require dynamic fine grid simulations to be run, and then the results are used to generate pseudos for the coarse models. The dynamic estimation of pseudo functions was first introduced by Jacks et al. (1973) who developed a method to calculate dynamic pseudo relative permeabilities from results of simulation runs of vertical cross section models. Also, KYTE and BERRY (1975) introduced a widely used method that depends on calculation of pressure potential between coarse cells to calculate dynamic pseudo functions. These pseudo functions can be used to compensate for vertical variation in pressure, saturation and reservoir properties when reducing the dimensions of a 3D reservoir model to a 2D areal model. In order to improve the KYTE and BERRY (1975) method, the pore volume weighted (PVW) method was developed, in which pressure is averaged using pore volume. Stone (1991) proposed a method that is based on averaging total mobility rather than pressure and use of fractional flow to calculate the pseudos. Alternatively, Smith (1991) used a steady-state pseudoization method (capillary dominated method) to generate pseudos. Also, Pickup and Sorbie (1996) applied the steady-state assumptions. Darman et al. (1999) introduced transmissibility-weighted (TW) method to calculate

pseudo functions in cases with a large gravity impact such as immiscible gas-oil displacement.

Multiple approaches to improve the results of two phase upscaling methods were also developed. For example, Tan (1995) generated pseudo functions by using history matching by non-linear regression. Also, the streamtubes approach (e.g. Hewett and Yamada, 1995) was applied. Another approach was introduced by King and Muggeridge (1993), which applied renormalization in order to replace the direct upscaling process of a fine model to a coarse model by a series of upscaling steps.

More recent approaches of two phase upscaling were introduced. For example, Durlofsky and Chen (2008) proposed an ensemble-level method in order to generate pseudo functions using combined numerical and statistical procedures for models with geological uncertainty. Also, a method focusing on upscaling for EOR processes was introduced by Muggeridge and Hongtong (2014) with the aim of generating pseudo functions to compensate for numerical dispersion in coarse models.

Generally, selection of the appropriate two phase upscaling method depends on the balance of viscous, capillary and gravity forces. For example, it cannot be expected that methods ignoring the gravity term to work best for dipping reservoirs. Therefore, in order to predict the balance of forces, dimensionless gravity and capillary numbers are calculated. The dimensionless gravity number is obtained by dividing gravity forces by viscous forces. Likewise, the dimensionless capillary number is calculated by dividing capillary forces by viscous forces. However, there are many definitions of the capillary and gravity numbers in the literature (e.g. Shook et al. 1992, and Zhou and Fayers, 1993).

Some of the above mentioned two phase upscaling methods and approaches will be briefly reviewed in this chapter.

**2.6.2. Two phase flow equations**

Similar to the single phase flow equations, the two phase flow equations are obtained by combining Darcy's equation and Mass conservation (Durlflosky, 2003).

Darcy's two-phase flow equation (in absence of gravity) is given by:

$$u_p = - \frac{k_{rp}}{\mu_p} k \cdot \nabla p_p \quad (2.12)$$

where,

$u_p$  is the Darcy velocity and the subscript  $p$  denotes the phase (e.g. water or oil),

$k$  is reservoir permeability,

$k_{rp}$  is the relative permeability to the phase  $p$ ,

$\mu_p$  is viscosity of the phase  $p$ , and

$\nabla p$  is pressure gradient between two adjacent blocks.

Mass conservation equation is given by:

$$\frac{\partial}{\partial t} (\phi \rho_p S_p) + \nabla \cdot (\rho_p u_p) + \tilde{m}_p = 0 \quad (2.13)$$

where,

$\rho_p$  is the phase  $p$  density,

$\phi$  is rock porosity,

$S_p$  is the phase  $p$  saturation,

$u_p$  is the Darcy velocity of the phase  $p$ , and

$\tilde{m}_p$  is the well (source/sink) term for the phase  $p$ .

By combining equations (2.12) and (2.13) we get:

$$\frac{\partial}{\partial t} (\phi \rho_p S_p) - \nabla \cdot \left( \frac{\rho_p k_{rp}}{\mu_p} k \cdot \nabla p_p \right) + \tilde{m}_p = 0 \quad (2.14)$$

The equations above assume 1D system and can be extended to be used for 2D and 3D systems. Also gravity and capillary pressure terms can be added.



### 2.6.3. Pseudo functions calculation methods

There are several methods used to generate pseudo functions to be used for upscaling. These methods can be divided according to the calculation procedure as follows:

- A. Pseudo functions generated by upscaling Darcy's law: such as Jacks et al. (1973) and Kyte and Berry (1975).
- B. Pseudo functions generated by averaging total mobility: such as Stone's method (1991).
- C. Pseudo functions generated by using streamtubes: such as Hewett and Yamada (1995).
- D. Pseudo functions generated by history matching: such as Tan (1995).

Also, pseudo functions can be classified based on flow regimes for which they were generated (Soedarmo et al., 1994), as follows:

1. Pseudo functions generated for viscous dominated flow, such as the Hearn et al. (1971) method.
2. Pseudos generated for gravity dominated flows, such as Coats et al. (1967 and 1971) methods.
3. Dynamic pseudos generated for general use with all flow regimes, such as the Kyte and Berry (1975) method.

According to Guzman et al. (1999), the main approaches followed when upscaling using pseudo functions are:

The first approach depends on running the fine grid flow simulation for a model (also called Full Fine Grid simulations and denoted as FFG). Afterwards, the fine grid results are used to calculate pseudo functions. These pseudo functions are then used to run the coarse grid simulation and compare its results with the fine grid results in order to check the effectiveness of pseudo functions.

The second approach is based on running fine grid flow simulation only for small selected parts of the reservoir volume, called Representative Elementary Volume

(REV), then use of the results to calculate the pseudos, which will be later used to adjust the coarse grid model. The main difficulty when applying the REV approach is to ensure the use of appropriate boundary condition (Thibeau et al., 1995).

The third approach uses a small successive renormalization approach in which the grid block sizes are increased until the simulation model is obtained. This procedure can speed up the upscaling process because boundary conditions (e.g. constant pressure) are applied for the grid blocks allowing independent solutions.

There are more recent approaches introduced in the literature, such as the ensemble-level method by Durlofsky and Chen (2008), where comparison between the results of coarse and fine models is made at the ensemble level (e.g. P90, P50 and P10), rather than case by case.

In the following sections a brief description of the main two phase upscaling techniques and approaches used to generate pseudo functions will be presented.

### 2.6.3.1 Vertical equilibrium method (Coats et al., 1967 and 1971)

The vertical equilibrium pseudo functions were introduced by Coats et al. (1967 and 1971) to be used for cases with gravity-capillary equilibrium and almost no impact of viscous forces assuming instantaneous segregation of the fluid phases in the vertical dimension. These limitations make this method valid only for reservoirs with very low flow rates. Also, the method can be applied only for fairly homogeneous reservoirs with good vertical communication. The procedure of this method can be described as follows:

1. Pseudo relative permeabilities are calculated using absolute permeability weighting as follows:

$$\bar{k}_{rw} = \frac{\int_0^h k_{xy}(z) k_{rw}(z) dz}{\int_0^h k_{xy}(z) dz} \quad (2.15)$$

where,

$\bar{k}_{rw}$  is the pseudo water relative permeability,

$k_{xy}$  is the absolute permeability for flow parallel to the x-y plane,

$k_{rw}$  is the water relative permeability,

h is the reservoir thickness, and

dz is layer thickness.

2. The corresponding saturation value for the calculated pseudo in step 1 is calculated using porosity weighting and is given by:

$$\bar{S}_w = \frac{\int_0^h \phi(z) S_w(z) dz}{\int_0^h \phi(z) dz} \quad (2.16)$$

where,

$\phi$  is the porosity,

$h$  is the reservoir thickness,

$dz$  is layer thickness, and

$\bar{S}_w$  is the average water saturation.

An interesting observation was provided by Darman et al. (1999) while comparing results of their new pseudos generation method TW (described later in this chapter) to those calculated by vertical equilibrium (VE) pseudo functions for an immiscible gas-oil displacement system. Darman et al. (1999) found that even though the gravity number was high, indicating gravity dominated flow, the VE method did not reproduce the fine grid results. By increasing the number of layers in the fine model, the coarse grid using the VE method was giving better and better results compared to the fine-scaled model. They attributed the reason for this to the dimension of the fine grid model they used (25 ft), which they considered that was not fine enough to provide an accurate solution for gravity segregation so that it could be suitable for application of the vertical equilibrium method.

Some modifications for the VE method have been introduced in order to extend its use in stratified reservoirs, for example Zapata and Lake (1981) introduced VE method to be used for cases with viscous dominated flow regimes. Also, Ingsoy et al. (1995) developed a new VE method to be used for reservoirs with significant gravity segregation.

### **2.6.3.2 Hearn method (1971)**

This method was introduced by Hearn in 1971 in order to approximate viscous flow in a stratified reservoir with an areal model. Hearn (1971) assumed that viscous forces dominate vertical fluid distribution in a reservoir with small vertical communication between its layers (i.e. stratified reservoir), and that mobility ratio is unit so that the displacing fluid proceeds as piston like. The stratified model (see Figure 2-6) was used as assumption to count for permeability variation in the vertical direction,

which will be represented by pseudo functions. The author recommended when applying his method to use layers with the same thickness as the core samples and to arrange them in order of decreasing water breakthrough.

Equations used to calculate the Hearn pseudos are described as follows:

Average water saturation after breakthrough of layer (n) is given by

$$\bar{S}_w = \frac{\sum_{i=1}^n t_i \phi_i (1 - S_{ori}) + \sum_{i=n+1}^N t_i \phi_i S_{wci}}{\sum_{i=1}^N t_i \phi_i} \quad (2.17)$$

where,

$t_i$  is thickness of layer  $i$ ,

$\phi_i$  is porosity of layer  $i$ ,

$N$  is total number of layers,

$S_{roi}$  is residual oil saturation in layer  $i$ , and

$S_{wci}$  is connate water saturation in layer  $i$ .

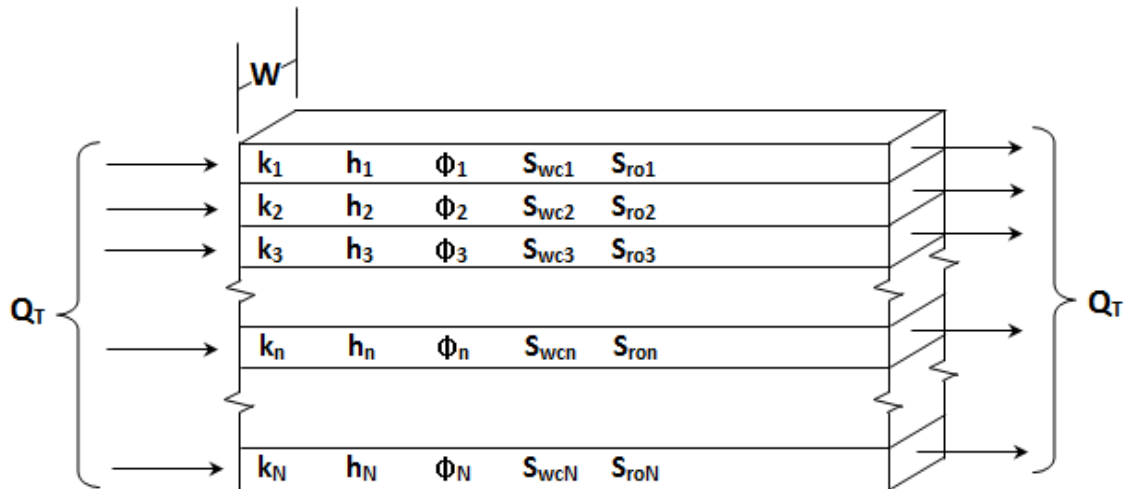


**Figure 2-6:** Stratified model used to calculate Hearn pseudo functions. This figure is adapted from Hearn, C. L. (1971).

After breakthrough of the last layer (N)

$$S_{wN} = \frac{\sum_{i=1}^N t_i \phi_i (1 - S_{ori})}{\sum_{i=1}^N t_i \phi_i} \quad (2.18)$$

After breakthrough in layer (n), the upscaled relative permeabilities are:

$$\bar{k}_{wn} = \frac{k_{rw} \sum_{i=1}^n k_i t_i}{\sum_{i=1}^N k_i t_i} \quad (2.19)$$

$$\bar{k}_{on} = \frac{k_{ro} \sum_{i=n+1}^N k_i t_i}{\sum_{i=1}^N k_i t_i} \quad (2.20)$$

where,

$\bar{k}_{wn}$  and  $\bar{k}_{on}$  are pseudo water and oil relative permeabilities of layer n respectively,

$k_{rw}$  and  $k_{ro}$  are water and oil relative permeabilities respectively,

N is total number of layers,

$k_i$  is absolute permeability of layer i, and

$t_i$  is thickness of layer i.

Generally, the Hearn (1971) method is more applicable for water-oil displacement problems than gas-oil due to the assumptions used (i.e. viscous dominated flow).

In 1982, Simon and Koederitz introduced a procedure to extend Hearn's method in order to account for the effects of phase production in a non-unit mobility ratio displacement in stratified reservoirs. The method estimates a vertical saturation distribution at the shock front of each layer, and then estimates the corresponding pseudo relative permeability value. Calculation of the saturation distribution in this method was kept at the shock front only because it was found that pseudo relative permeabilities generated behind the shock front tends to have abrupt change of slope, which needs to be smoothed before use in simulator. Simon and Koederitz (1982) concluded that their procedure is considered as improvement to Hearn's method.

### **2.6.3.3. Jacks et al. method (1973)**

This method was introduced by Jacks, Smith and Mattax (1973) in order to calculate dynamic pseudo relative permeabilities from results of simulation runs of vertical cross section model. The Jacks et al. (1973) method is considered as alternative to Coats et al. (1967 and 1971) and Hearn (1971) in terms of accounting for the effects of wide range of flow rates. According to Jacks et al. (1973), his method differs from that by Coats (1967 and 1971) and Hearn (1971) in the approach of calculating vertical saturation distribution. In Jacks et al. (1973) method, the saturation values are calculated

by running a fine grid simulation of fluid displacement in cross-sectional (x-z) model, then dynamic relative permeabilities are generated for each column of blocks in the cross-section model for each time step. Dynamic pseudo functions created by the Jacks et al. (1973) method can be used together with pseudo capillary pressure created by the vertical equilibrium method to adjust a 2D areal model to give results as close as results of a 3D model.

The Jacks et al. (1973) method assumes that the phase potential difference between fine cells is equal to average potential difference between coarse cells. The pseudo relative permeability is calculated by using transmissibility weighting for each column of cells as follows:

$$\bar{k}_{rp} = \frac{\sum_k (T k_{rp})_k}{\bar{T}} \quad (2.21)$$

where,

$\bar{k}_{rp}$  is the pseudo relative permeability of phase p,

$k_{rp}$  is the relative permeability of phase p,

T is the transmissibility between fine cells,

k is subscript denotes column of cells for which the pseudo will be calculated, and

$\bar{T}$  is the transmissibility of each column of cells (k) and it is given by:

$$\bar{T} = \sum_k T_k \quad (2.22)$$

In Jacks et al. (1973) method, each column of cells will act as single cell in the coarse model. This means reduction of a 3D problem to 2D problem.

Pseudos generated by the Jacks et al. (1973) method are only dependent on saturation distribution, which is why they are considered partially dynamic pseudos (Cao and Aziz, 1999). Jacks et al. (1973) pointed out that the reliability of pseudo functions can be checked by using them to reproduce the pressure distribution and average saturation of a cross-section model using a one dimensional areal model simulation.

### 2.6.3.4 Kyte and Berry method (1975)

This method was introduced by Kyte and Berry in 1975 in order to calculate dynamic pseudo functions that can be used to convert a 3D reservoir model to a 2D areal model. These pseudo functions should compensate for vertical variation in pressure, saturation and reservoir properties. Also, Kyte and Berry (1975) used pseudo functions to compare results of reducing a 2D cross-sectional model to a 1D areal model. This was achieved by accounting for block lengths difference between the two models via pseudo relative permeabilities, and by accounting for different flow potentials in different layers of the 2D cross-sectional model via pseudo capillary pressure curves. The results demonstrated that the proposed pseudo functions gave very good results.

In the Kyte and Berry (1975) method, the pressure is averaged only at the centre of coarse grid blocks, and then the potential difference is calculated. The averaged pressure (also called pseudo pressure) is calculated by the following equation:

$$\bar{p}_p = \frac{\sum_j [k_{rp} kh (p_p + \rho_p g H)]_{nc}}{\sum_j (k_{rp} kh)_{nc}} \quad (2.23)$$

where,

$\bar{p}_p$  is the pseudo pressure,

$k_{rp}$  is relative permeability of phase p,

$kh$  is the permeability thickness product,

$\rho_p$  is density of phase p,

$nc$  is the no. of fine grid blocks at the centre column of a coarse grid block for which the pseudo pressure will be calculated, and

$H$  is the difference between depths of coarse and fine cell centres respectively.

The pseudo relative permeability of phase p is calculated from:

$$\bar{k}_{rp} = \frac{-\bar{\mu}_p \sum_k (q_p)_k}{T_{avg} (\Delta \bar{p}_p - \bar{\rho}_p g \Delta \bar{D})} \quad (2.24)$$

where,

$\bar{k}_{rp}$  is the pseudo relative permeability of phase p,

$\bar{\mu}_p$  is average viscosity of phase p,

$q_p$  is flow rate of phase p,

$g$  is the gravity coefficient,

$\bar{D}$  is the centre depth of the coarse block,

$T_{avg}$  is the average transmissibility and is calculated by applying harmonic averaging of the product of upscaled permeability and coarse cells geometry, and

$\Delta\bar{p}_p$  is the potential difference.

The corresponding average water saturation is given by:

$$\bar{S}_w = \frac{\sum_{i=I_1}^{I_2} \sum_{K=K_1}^{K_2} (V_p S_w)_{ik}}{\sum_{i=I_1}^{I_2} \sum_{K=K_1}^{K_2} (V_p)_{ik}} \quad (2.25)$$

where,

$V_p$  is the pore volume,

$S_w$  is the water saturation, and

$i$  and  $k$  are numbered horizontal and vertical locations of fine cells.

The pseudo capillary pressure is calculated as following:

$$\bar{P}_{c,ow} = \bar{P}_o - \bar{P}_w \quad (2.26)$$

where,

$\bar{P}_o$  and  $\bar{P}_w$  are the average pressure in the oil and water phases respectively.

The comparison between pseudo function generation methods, carried out by Darman, et al. (2001), showed that pseudo functions generated by Kyte and Berry (1975) give the worst results for a horizontal cross-sectional model. This is because in the horizontal model the gravity and capillary pressure terms can be neglected, causing fluids potential to be equal (i.e.  $\Delta\Phi_g = \Delta\Phi_o$ ). This approximation is not applicable for the Kyte and Berry (1975) method, because in their method the phase relative permeability is used as weighting factor for fluid potential difference, which means unequal fluid potentials (i.e.  $\Delta\Phi_g \neq \Delta\Phi_o$ ), Darman et al. (1999).



With the aim to improve the Kyte and Berry (1975) method, a flux weighted potentials (FWP) approach was used to calculate the average phase potential by using a fine grid solution and Darcy's flux as weighting factor. Even though, the FWP method showed better results over the Kyte and Berry (1975) in some cases, the FWP could still yield nonzero pseudo capillary pressures when no capillary pressure curves was used (Guzman et al., 1999).

The average phase potential is calculated by:

$$\bar{\Phi}_p = \frac{\sum_{K_c} (q_p \Phi_p)_k}{\sum_{K_c} (q_p)_k} \quad (2.27)$$

where,

$\Phi_p$  is the phase potential,

$q_p$  is the Darcy flux of phase p, and

c is a subscript denoting that the summation is made over the column of fine grid blocks that correspond to coarse grid mesh point.

The pseudo relative permeability is calculated by:

$$\bar{k}_{rp} = - \frac{\bar{\mu}_p \bar{q}_p}{T \Delta \bar{\Phi}_p} \quad (2.28)$$

The pseudo capillary pressure is calculated by:

$$\bar{P}_{c,ow} = \bar{\Phi}_o - \bar{\Phi}_w - g \Delta \bar{\rho}_{ow} \Delta \bar{D} \quad (2.29)$$

The pore volume weighted (PVW) method (Intera information technologies, 1994) is another approach that is used to improve the results of the Kyte and Berry (1975). In the PVW method, the same steps as in the Kyte and Berry (1975) are followed except that the pseudo pressure is calculated using pore volume weighting. According to Barker and Thibeau (1997), the pore volume weighted method can be more usable than the Kyte and Berry method because the PVW method calculates zero pseudo capillary pressure in cases where capillary pressure in the fine grid is zero, while Kyte and Berry may calculate values for pseudo capillary pressures where they do not exist.

The pseudo pressure using the PVW method is given by:

$$\bar{P}_p = \frac{\sum_J [V\Phi (P_p + \rho_p gH)]_J}{\sum_J (V\Phi)_J} \quad (2.30)$$

where,

V is the cell volume, and

$\Phi$  is the porosity.

The pseudo capillary pressure is calculated by:

$$\bar{P}_{c,ow} = \bar{P}_o - \bar{P}_w \quad (2.31)$$

Another advantage of the pore volume weighted method is that it should generate monotonic pseudo capillary pressure curves due to using pore volume weighting to average the pressure. In the case of non-monotonic curves, it is necessary to smooth those curves first before using in a simulator, Azoug and Tiab (2003).

According to Barker and Thibeau, in their critical review of pseudo functions methods (1997), the following problems may occur when applying the Kyte and Berry in practice:

1. Negative pseudo functions might be generated when the flow direction is opposite to the direction in which average pressure gradient was calculated.
2. Infinite pseudos might be generated in cases where the average pressure gradient is zero while flow between the cells for which this average gradient was calculated is nonzero.
3. Multi-valued pseudo relative permeabilities might be generated in cases where the same value of average saturation is repeated for a certain coarse cell.
4. Calculation of pseudo capillary pressures for a fine grid with no capillary pressure. This is due to different average pressure definition in different directions in a multidimensional problem.

**2.6.3.5 Stone's method.**

This method was introduced by Stone in 1991. The method does not require averaging potential difference between grid blocks as in the Kyte and Berry (1975), instead it is based on averaging total mobility and uses fractional flow instead of Darcy's equations to calculate the pseudos. The method can be described using the following equations:

The average fractional flow for water phase is calculated using total flow weighting and is given by:

$$\bar{f}_w = \frac{\sum_k(Qf_w)_k}{\sum_k(Q)_k} \quad (2.32)$$

Similarly, the average oil fractional flow is given by:

$$\bar{f}_o = \frac{\sum_k(Qf_o)_k}{\sum_k(Q)_k} \quad (2.33)$$

where,

$Q$  is the total flow rate at the downstream edge of a coarse cell,  $f_w$  and  $f_o$  are water and oil fractional flows respectively, and  $k$  is a subscript denoting column of cells for which the pseudos will be calculated.

The average total mobility is calculated using transmissibility weighting and is given by:

$$\bar{\lambda}_t = \frac{\sum_k(T\lambda_t)_k}{\sum_k(T)_k} \quad (2.34)$$

where,

$\lambda_t$  is the total mobility in fine cells at the interface between adjacent coarse cells, and  $T$  is the transmissibility between fine cells along the interface between coarse cells.

In order to derive an equation to calculate the pseudo relative permeability, using the above calculated average fractional flow and average total mobility, the procedure below was followed:

Neglecting gravity and capillary forces, the fractional flow equation is given by:

$$f_w = \frac{1}{1 + \frac{k_{ro}}{\mu_o} \frac{\mu_w}{k_{rw}}} \quad (2.35)$$

where,

$k_{ro}$  and  $k_{rw}$  are oil and water relative permeabilities respectively, and  $\mu_o$  and  $\mu_w$  are oil and water viscosities respectively.

Equation (2.35) can be re-written as:

$$\frac{f_w \mu_w}{k_{rw}} = \frac{1}{\lambda_t} \quad (2.36)$$

where, the total mobility is given by:

$$\lambda_t = \frac{k_{rw}}{\mu_w} + \frac{k_{ro}}{\mu_o} \quad (2.37)$$

Therefore, water relative permeability can be calculated from:

$$k_{rw} = f_w \lambda_t \mu_w \quad (2.38)$$

Using the average fractional flow, average total mobility and average water viscosity, in the equation (2.38) above, the water pseudo relative permeability is given by:

$$\bar{k}_{rw} = \bar{f}_w \bar{\lambda}_t \bar{\mu}_w \quad (2.39)$$

Similarly, the oil pseudo function is given by:

$$\bar{k}_{ro} = \bar{f}_o \bar{\lambda}_t \bar{\mu}_o \quad (2.40)$$

The corresponding average saturations for the calculated pseudos are calculated using pore volume weighting:

$$\bar{S}_w = \frac{\sum_{i=I_1}^{I_c} \sum_{k=K_1}^{K_c} (V_p S_w)_{ik}}{\sum_{i=I_1}^{I_c} \sum_{k=K_1}^{K_c} (V_p)_{ik}} \quad (2.41)$$

where,

$V_p$  is the pore volume,

$S_w$  is the water saturation,

$K_l$  and  $K_c$  are the indices of the first and last fine cells along the interface between adjacent coarse cells,

$I_l$  and  $I_c$  are the indices of the first and last fine cells in the x direction within a coarse cell, and

According to the comparison of pseudo functions generation methods carried out by Darman, Pickup and Sorbie (2001), it was found that Stone's method gave the best results for the case with a horizontal model (i.e. with no dipping), while it gave the worst results for the case with the dipping model (15° dip). This is because the Stone's method ignores gravity and capillary terms, which makes pressure potential in both gas and oil phases equal (i.e.  $\Delta\Phi_g = \Delta\Phi_o$ ). The equal potential assumption can be applicable in the case with the horizontal model. However, for the dipping model, it is supposed to account for the difference in elevation between cells centres, which is ignored in Stone's (1991) method by ignoring the gravity term in his calculations as shown in the equations above.

Application of Stone's method in practice might face the following difficulties (Barker and Thibeau, 1997):

1. Neglecting gravity and capillary pressure limits the use of Stone's method to the cases where flow is not significantly gravity or capillary dominated.
2. If a high contrast in total mobility occurs between grid blocks, averaging total mobility using the method introduced by Stone is not suitable.
3. Even though negative pseudos rarely occur (in comparison to Kyte and Berry) they can occur in cases where two phases flow in opposite directions.

### **2.6.3.6 Transmissibility-weighted method**

This method was introduced in 1999 by Darman, Sorbie and Pickup as a new way of calculating pseudo functions in cases with a large gravity impact such as immiscible gas-oil displacement. As part of this method, a scheme for 2D gridding was also included in order to determine regions of the model which should be kept finely gridded and regions which can be coarsely gridded. This is decided depending on magnitude of the gas saturation variation.

The transmissibility-weighted method (TW) follows the same procedure as the Kyte and Berry (1975) method. However, there are two main differences between the

two methods, both are regarding the way the phase potentials are averaged. In the TW method the potentials are averaged using the product of transmissibility and phase potential as weights, while the Kyte and Berry (1975) method uses product of relative permeability, absolute permeability and grid block thickness weighting. The second difference is that in the TW method the phase potential difference is averaged directly between the coarse cells while in Kyte and Berry potentials are first averaged within coarse cells then the averaged potential difference between them is calculated.

The averaged potential difference is given by:

$$\overline{\Delta\Phi_p} = \frac{\sum_{j=1}^5 [T_{xj} \Phi_{pj} \Delta\Phi_{pj}]_{i=3}}{\sum_{j=1}^5 [T_{xj} \Phi_{pj}]_{i=3}} \quad (2.42)$$

where,

the number 5 denotes no. of layers used in the model and  $\Delta\Phi_{pj}$  is calculated from the equation:

$$\Delta\Phi_{pj} = [\Phi_{pj}]_{i=8} - [\Phi_{pj}]_{i=3} \quad (2.43)$$

The pseudo functions are then calculated using the Darcy's equation as follows:

$$\overline{k_{rp}} = \frac{-\overline{\mu}_p \overline{q}_p \Delta x}{\Delta y \Delta z \overline{kx} \overline{\Delta\Phi_p}} \quad (2.44)$$

where,

$\overline{k_{rp}}$  is pseudo relative permeability of phase p,

$\overline{\mu}_p$  is average viscosity of phase p, and

$\Delta x$ ,  $\Delta y$  and  $\Delta z$  are gridblock dimensions.

The corresponding average saturation to the pseudos in the coarse grid-blocks is calculated using pore volume weighting:

$$\overline{S}_p = \frac{\sum_{j=1}^5 \sum_{i=1}^5 S_{pij} V_{p_{ij}}}{\sum_{j=1}^5 \sum_{i=1}^5 V_{p_{ij}}} \quad (2.45)$$

where,

$\overline{S}_p$  is average phase saturation, and

$V_p$  is the pore volume.

When testing the results of the TW method for immiscible gas-oil displacement in a 2D model, Darman et al. (1999) found that the method provides better results for dipping and non-dipping systems in comparison to vertical equilibrium (e.g. Coats, 1967 and 1971), Kyte and Berry (1975) and Stone's (1991) method. The results of using the TW method (Darman et al. 1999) and the Kyte and Berry (1975) were separately tested and the reason for improved results of TW over KB was attributed to the weighting factors used by TW method (i.e. product of transmissibility and phase potential). The less satisfying results obtained by Kyte and Berry was attributed by Darman et al. (1999) to use of relative permeability as weighting factor.

It should also be mentioned here that in another comparison carried out by Darman et al. (2001) for pseudo upscaling methods, they found that in the case of a horizontal model (no dipping), the fractional flows calculated by both the transmissibility weighted and the Hewett and Archer (1997) methods are very similar, even though the shape of the pseudo functions generated by those methods were different. This is because the phase potential is equal.

Generally, pseudos calculated by methods that average pressures in coarse cells are unlikely to produce good results in the case of very heterogeneous reservoirs. This is because these methods are based on the assumption of one-direction flow (no reversal) within each coarse cell, which may not be applicable in case of heterogeneous reservoirs. (Cao and Aziz, 1999).

#### **2.6.3.7 Multiple-step pseudo functions method**

In this method, the pseudo functions are generated in a multistep upscaling process, which starts with an almost homogeneous model with rock curves (relative permeability and capillary pressure) at a small scale and after many steps of upscaling and generating pseudos, it ends up with coarse simulation model with pseudos that capture the heterogeneity and should also be capable of reducing the numerical dispersion, see Figure 2-7.

The multistep pseudo generation method was introduced by Lasseter et al. (1986), and was then extended and studied in detail by Kossack, Aasen and Opdal (1990). The procedure of the multistep upscaling in Figure 4.2 can be explained as follows:

**STEP1:** The permeability variation in the grid blocks is ignored so that a constant value of permeability is set in all grid blocks. The rock curves (relative permeabilities and capillary pressure) are used for this grid. Afterwards, the grid blocks are grouped into flow units, each replaced by one coarse grid block by generating a pseudo function. This coarse grid block will act as fine grid block in the second step of this upscaling process.

**STEP2:** The coarse grid blocks obtained from step 1 will be assigned to a larger scale of permeability variation in this step. The resulting coarse grid will act as the fine grid in this step and use the pseudo functions generated in step 1. As in step1, the grid blocks are grouped into flow units, each replaced by one coarse grid block by generating a pseudo function. Again this coarse grid block will act as fine grid block in the third step of this upscaling process.

**STEP3:** The same process as in step 2 will be repeated here. This multistep upscaling process can proceed until size of grid blocks required for reservoir simulation is obtained. The number of steps will be confined by heterogeneity level.

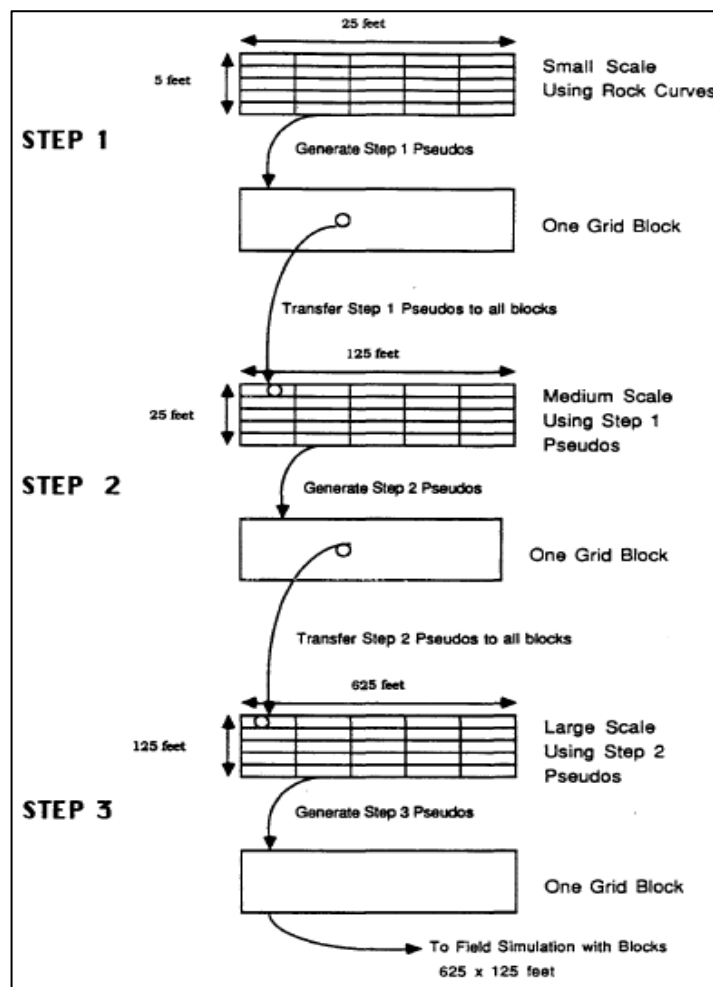


**Figure 2-7:** Multi-step pseudo functions, adapted from Kossack, et al. (1990).



### **2.6.3.8 Ensemble-Level upscaling approach**

This approach was introduced by Chen and Durlofsky (2008) in order to generate pseudo functions using combined numerical and statistical procedures for models with geological uncertainty. Generally, the models with geological uncertainty require running multiple realisations to investigate the geological uncertainty. Applying conventional two phase upscaling methods for these types of models would require large computation time. This is because the conventional two phase upscaling methods would require agreement between the fine and coarse models for each realization. On the contrary, the ensemble-level upscaling, as its name indicates, aims to reproduce the fine grid results such as cumulative oil recovered at the ensemble level (e.g. P90, P50 and P10), rather than matching results of each realisation separately. Therefore, the ensemble-level approach can speed up the two phase upscaling process.

The approach followed in the ensemble-level method (Chen and Durlofsky, 2008) calculates numerically the pseudo functions for only part of the coarse grid blocks in the coarse model, while for the rest of the coarse model(s), the pseudo functions are generated using a statistical method (based on cluster analysis). The statistical method uses the velocity attributes obtained during the single-phase upscaling applied for the same portion of the coarse blocks mentioned above.

The ensemble-level method (Chen and Durlofsky, 2008) was applied to 2D synthetic models with different levels of heterogeneity and total mobility ratios then several realisations were performed in order to investigate the uncertainty. It was found that the ensemble-level approach can give results as close as the two phase upscaling methods but with much less time required to complete the calculations. Similar efforts to speed up the two phase upscaling method were made by Dupouy et al. (1998), who introduced approach to use statistics to group the pseudo functions together. However, the method did not involve calculation of pseudos.

### **2.6.3.9 Combined global absolute permeability upscaling and pseudo functions generation method**

This method was introduced by Li, Cullick and Lake in 1996 to generate pseudo functions that can be combined with global absolute permeability upscaling method, which was also introduced by the same authors in 1995. The target of this combined method was to improve the results of pseudo functions and at the same time to reduce the computational expense by avoiding running fine grid simulation.

The procedure of the method can be described as follows:

1. Upscaling the absolute permeability by using a global scale up method that transports the important heterogeneity in the fine grid cells to the coarse grid cells. The result of this upscaling process is an upscaled permeability field and a residual permeability field (i.e. the permeability that results from the difference between the reference fine grid permeability and the upscaled permeability).
2. Averaging the rock relative permeability and capillary pressure curves within each coarse grid cell using permeability spatial correlation weighting. If the same relative permeability curves are the same all over the model, this averaging step could be by passed.
3. Pseudo functions are determined analytically using superposition of the shock velocities for the residual permeability and fine grid.

The combined global absolute permeability upscaling and pseudo function method Li et al. (1996) was demonstrated by 2D and 3D water flood models. Though a scale up factor of 6 was used to scale up the 3D model, only slight change of water breakthrough time was achieved by using the pseudo functions generated by the Li et al. (1996) method.

#### **2.6.3.10 History matching methods**

The history matching pseudoization methods use algorithms to regress on the pseudo functions until the coarse grid model reproduces results of the fine grid model. Parameterization of pseudos was investigated by Hales in 1983, where pseudos were parameterized in terms of water breakthrough time and pressure drop. Yang and Watson (1991) used a Bayesian methodology to estimate two phase relative permeability curves using a cubic B-spline function.

In 1995, Tan used linear regression to generate a single set of pseudo functions by altering the relative permeability values until the saturation and production rate values of the coarse grid match those of the fine grid. This method was tested by Tan (1995) against the results of Stone (1991) using a model with non-communicating layers, which demonstrated the validity of this history matching method. The method was then extended to three dimensions to account for areal heterogeneity.

The goal of the history matching process of Tan (1995) was to estimate the oil-water relative permeability, gas-oil relative permeability and grid cell permeability so that the objective function  $S$  is minimized.

$$S = \sum_{i=1}^{n_o} [\hat{y}(t_i) - y(t_i)]^T Q_i [\hat{y}(t_i) - y(t_i)] \quad (2.46)$$

where,

$\hat{y}$  represents a vector of  $m$  measurements at observation times  $t_i$ ,

$n_o$  is the number of observation times,

$y$  represents the vector of corresponding calculated values, and

$Q$  is an  $m \times m$  matrix of weighting factors which may vary with time.

It should be noticed that if this automatic matching process occurred only at wells, the results will be affected by changing wells positions and production rates. This is because the block to block flow or average pressure between grid blocks is not matched. Running this matching process at the level of individual grid blocks makes these methods difficult to apply (Barker and Thibeau, 1997).

#### **2.6.3.11 Renormalization method**

The renormalization approach is based on replacing the direct upscaling process of a fine model to a coarse model by series of upscaling steps in which the initial grid is coarsened by merging cells to obtain successively coarser grids until a grid with one block only is built. Renormalization method was first used for single-phase flow upscaling and demonstrated to give accurate results (King and Muggeridge, 1993). Afterwards, the method was extended to be used as two phase flow upscaling method by King and Muggeridge (1993), who compared the results to those obtained by using conventional pseudo functions generation methods. They found that the renormalization approach gives as accurate results as the conventional pseudoization methods. The renormalization method was again extended to multi-phase flow by Christie et al. (1995) in order to upscale Water-Alternating-Gas (WAG) floods in heterogeneous reservoirs.

The procedure of the renormalization method introduced by Christie et al. (1995) is described as follows:

1. Pseudo functions are generated for each coarse grid block for the x, y and z directions by running three WAG fine grid simulations on the part corresponding to the coarse grid for which pseudo functions will be generated.
2. The renormalization approach is used in order to speed up the calculation of the pseudo functions in step 1. The renormalisation method involves series of simulations in which pseudo functions are generated to retain the grid features before proceeding to the next simulation of a coarser grid.
3. An empirical viscous fingering model is used to allow for unstable mobility ratio displacement floods.

Results of this multi-phase upscaling method showed good agreement with commonly used pseudo functions generation methods.

Although the renormalization approach does averaging only over regions of the fine grid (similar to Kyte and Berry (1975) procedure) and averages total mobility instead of phase potential (similar as Stone (1991) method), it differs from the previously mentioned two methods in that it averages quantities (e.g. saturation) only over the outlet face of the renormalization cell, while the Kyte and Berry (1975) and Stone (1991) average only flow rate over the outlet face of the cell but saturation (for example) is averaged over the whole coarse cell.

#### **2.6.3.12 Steady-state pseudoization methods**

Fluid is said to be at steady-state conditions when its saturation does not change with time. This assumption is the base of steady-state upscaling methods which can be divided depending on balance of forces, for example, to capillary-dominated steady-state method (e.g. Smith 1991; and Pickup and Sorbie 1996) and viscous-dominated steady-state method (e.g. Pickup et al. 2000). The steady state methods are used as an approximation to make the generation of pseudo functions easier and quicker than that when using dynamic methods such as the Kyte and Berry (1975) method and Stone (1991) method. However, in many cases neither capillary- nor viscous-dominated assumptions can be applied; instead intermediate steady-state upscaling methods are more appropriate such as that proposed by Stephen and Pickup (1999) and Lohn et al. (2004). Efforts have been made in order to quantify the validity range of the steady-state upscaling methods, such as Jonoud and Jackson (2006).

Deciding which type of steady-state method to use (e.g. capillary-dominated or viscous-dominated) depends on the scale for which it will be applied. For cases with very small scales (e.g. when upscaling from lithofacies-scale to geological model scale) capillary equilibrium can be achieved provided that the injection rate is very low and flow is over a small distance. In this case, using the capillary-dominated steady state methods to generate pseudo functions should be appropriate and help to decrease the time required to complete the upscaling process, Pickup et al. (2000). For other cases with larger scales, the use of viscous-dominated steady state methods for pseudoization was demonstrated to be more appropriate. However, in this case, it is important to assure that the number of cells between the injection and production wells is sufficient to avoid problems of numerical dispersion, Pickup et al. (2000), because the steady state methods do not account for numerical dispersion.

The main assumptions and calculation procedure of the capillary- and viscous-dominated methods are described as follows:

(1) Capillary Limit scale-up method:

In this method, it is assumed that capillary equilibrium may be reached when flow rate is very low and over small flow distance. When rock curves (relative permeability and capillary pressure curves) are known for each lithofacies type, the calculations start with selection of capillary pressure level, which is then used to calculate water saturation ( $S_w$ ). The water saturation is then averaged using pore-volume weighting. The water relative permeability ( $K_{rw}$ ) and oil relative permeability ( $K_{ro}$ ) are calculated using the relative permeability curves. Afterwards, the values of  $K_{rw}$  and  $K_{ro}$  are multiplied by the absolute permeability in order to calculate the phase permeabilities  $k_w$  and  $k_o$  respectively. In order to calculate the effective phase permeabilities, it is necessary to run a single-phase simulation for each phase separately. Finally, the effective relative permeabilities (Pseudos) are calculated by dividing the phase permeabilities by absolute effective permeability and repeating all the above mentioned steps for various capillary pressure curves.

(2) Viscous Limit scale-up method:

This method can be used for high flow rates and over large flow distance. The method assumes that capillary pressure is zero or very small so that it can be neglected, which means that fractional flow can be calculated from:

$$f_w = \frac{k_{rw}\mu_o}{k_{rw}\mu_o + k_{ro}\mu_w} \quad (2.47)$$

This steady-state method assumes that water saturation in grid cells is constant with time, and the water fractional flow is constant. The calculations of this method start by selecting a fractional flow level ( $f_w$ ) which is then used to calculate the water saturation ( $S_w$ ). The average water saturation is calculated using pore-volume weighting. Afterwards, the relative permeabilities are calculated, and then used to calculate the total mobility as follows:

$$\lambda_t = \frac{k_{ro}}{\mu_o} + \frac{k_{rw}}{\mu_w} \quad (2.48)$$

In order to calculate the effective total mobility, it is required to run a single-phase simulation. The effective relative permeabilities are calculated from:

$$\bar{k}_{rw} = \frac{\mu_w f_w \bar{\lambda}_t}{\bar{k}_{abs}} \quad (2.49)$$

$$\bar{k}_{ro} = \frac{\mu_o (1 - f_w) \bar{\lambda}_t}{\bar{k}_{abs}} \quad (2.50)$$

where,

$\bar{k}_{rw}$  and  $\bar{k}_{ro}$  are effective water and oil relative permeabilities respectively,

$\bar{\lambda}_t$  is effective total mobility,

$\bar{k}_{abs}$  is effective absolute permeability.

Repeating the above mentioned steps for various fractional flow levels, we can construct effective permeability curves.

Pickup et al. (2000) carried out two case studies in order to demonstrate the possibility of using steady-state methods to generate pseudo functions in order to scale-up from lamina-scale (where the permeability contrast may be strong and important to be captured) to full model scale using an easier and quicker process than when using dynamic methods. The first case study used a three-stage upscaling process of fluvio-aolian model in order to simulate a water flood. In the first two scale-up stages, the flood was assumed to be capillary-dominated, while for the third stage the flood was assumed to be viscous dominated. The second case study included a two-stage upscaling process of a model representing a tidal deltaic reservoir with gas injection into

the oil leg. The gas flood was assumed to be viscous-dominated in both stages. The first stage involved scale-up from lithofacies scale to geologic model. The second stage involved scale-up from the geological model to the simulation model. Performing these calculations, Pickup et al. (2000) showed that the use of steady-state methods enabled generation of pseudo functions in a simple and accelerated process. By using these pseudos in the simulation model, Pickup et al. (2000) found that it caused the oil recovery to decrease. For the case study with the water flood, the recovery reduction was due to capillary forces which trapped the oil between lithofacies-scale structures; especially in case of water wet rocks. For the case study of the gas flood, the oil recovery reduction was due to fine-scale layering in which the gas was more mobile than the oil. These results reflect two facts. The first is that the scale-up of lamina-scale effects, before use into simulation model, can be important, especially in case of strong permeability contrast (even though this is ignored by many engineers). The second is that generation of pseudo functions can be simplified by applying steady-state methods.

As already mentioned, in many cases neither capillary- nor viscous-dominated assumptions can be used. For these cases, the dynamic simulation can be run until steady state is achieved. However, this is a time consuming process and difficult to apply. Stephen and Pickup (1999) introduced a method to obtain the steady-state solutions directly using implicit steady-state solver. A similar method was introduced by Lohne et al. (2004) to calculate rate-dependent effective properties rather than assuming capillary-dominated or viscous dominated flow.

In order to check the validity of steady state upscaling methods, dimensionless quantitative criteria were defined by Jonoud and Jackson (2006). They developed set of limits and conditions were tested using three realistic models with heterogeneity range from small to intermediate. It was generally found that the criteria for capillary-dominated flow methods application are difficult to meet in practice. On contrary the criteria for application of viscous-dominated flow are more realistic.

### **2.6.3.13 Upscaling for EOR processes**

When applying immiscible EOR processes such as polymer flooding in a 1D homogeneous medium, two shock fronts are formed, one (leading), caused by the displaced connate water and the second (trailing), formed by the EOR fluid displacing both oil and connate water, (Muggeridge and Hongtong, 2014). When modelling this

EOR process using a simulation grid, the numerical dispersion arises due to the gridding results wiping out these shock fronts.

A methodology was proposed by Muggeridge and Hongtong (2014) to analytically upscale relative permeability curves, which can compensate for the numerical dispersion in 1D low salinity waterflooding system and in turn capture the behaviour of the shock front.

The workflow of the methodology starts with upscaling absolute permeability using single phase upscaling in order to calculate the pressure gradient across the coarse model. Afterwards, near well upscaling is performed around the wells. Finally, pseudo functions are generated.

#### **2.6.4 Impact of upgridding on pseudo functions results improvement**

Many attempts have been made to define the appropriate coarse grid (upgridding) before using single-phase upscaling methods in order to improve upscaling results, for example Durlofsky et al. (1997) introduced a method in which grid size depended on fluid flow velocity. For the regions where fluid flow velocity is high, the grid was refined to be at high resolution, while for the other regions, the grid was coarsened (i.e. non-uniform upgridding). Another example is the method proposed by Stern and Dawson (1999), in which they worked on optimising the upscaling results by determining the optimum number of layers and locations for layer boundaries, which are required to preserve the fluid flow behaviour and maintain the important geologic details.

A similar effort to investigate the two phase upscaling problems was introduced, for example, by Coll, Muggeridge and Jing (2001) who introduced a method referred to as regional upscaling. In this method, simulation of the fine grid is performed, and then gravity and viscous numbers are calculated to determine the dominant flow regime in each fine cell. Using the calculated “local” gravity and viscous dimensionless numbers, so called forces maps are created, and according to the forces spatial distribution on these maps, the coarse grid is selected, see Figure 2-8. Afterwards, pseudo functions were generated using Kyte and Berry (1975) or vertical equilibrium by Coats (1971), and used to run simulation of the coarse grid, which was defined in the previous step. The regional upscaling method by Coll, Muggeridge and Jing (2001), see Figure 2-8,



showed better results over the global pseudo functions generation methods such as Kyte and Berry (1975) and vertical equilibrium for the tested cases.

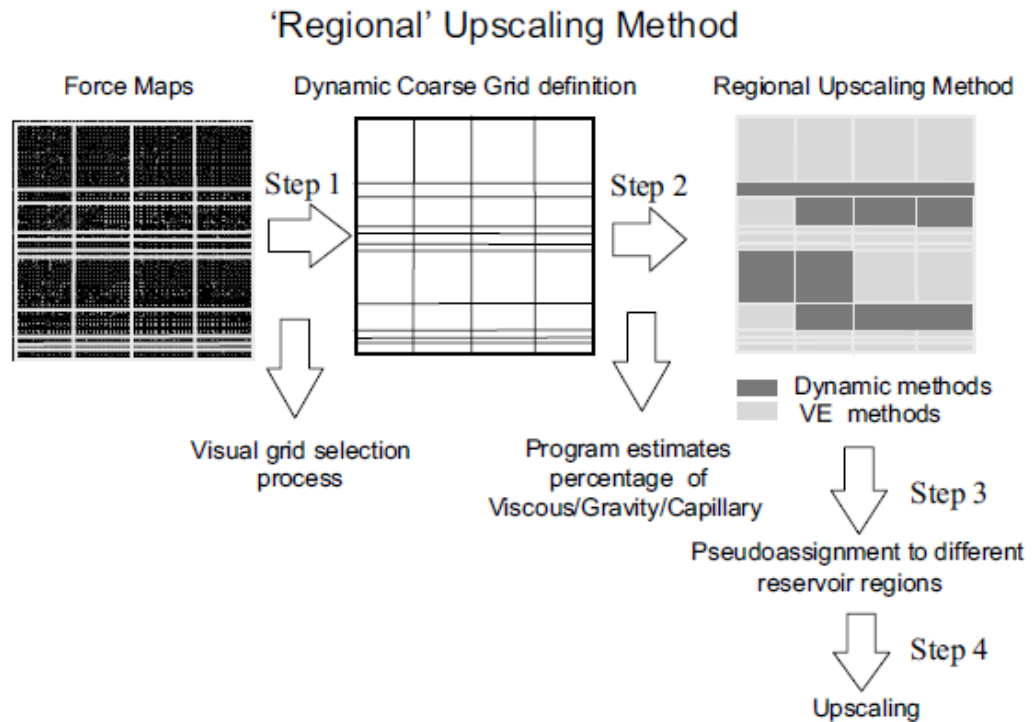


**Figure 2-8:** Regional upscaling method, from Coll et al. (2001).

### 2.6.5 Flow regimes and selection of the proper pseudoization method

Flow regimes can be defined by calculating the capillary and gravity numbers. According to the defined flow regimes, the selection of pseudo functions generation method might be easier and the quality of their results can be predicted. For example, for a reservoir model with significant gravity number, we cannot expect Stone's method to give good results when it ignores the gravity term, etc.

Generally, the capillary and gravity numbers are obtained by dividing capillary and gravity forces by viscous forces respectively. However, there are many definitions of the capillary and gravity dimensionless numbers in the literature, for example Shook et al. (1992) and Zhou and Fayers (1993).

According to Zhou and Fayers (1993) the capillary and gravity numbers are calculated as follows:

Capillary number is given by:

$$N_c = \frac{\text{Capillary force}}{\text{Viscous force}} = \frac{L \bar{K}_z \bar{P}_c}{u \mu_o H^2} = \frac{\bar{K}_z \bar{P}_c B L}{Q_o \mu_o H} \quad (2.51)$$

where,

$\bar{K}_z$  is the average vertical permeability,

$L*B*H$  is the size of the reservoir,

$u$  is the Darcy velocity,

$Q_o$  is the volumetric flow rate, and

$\bar{P}_c$  is the average capillary pressure and is given by:

$$\bar{P}_c = \int_{S_w}^{1-S_{or}} P_c(S_w) dS / (1 - S_{or} - S_{wc}) \quad (2.52)$$

Gravity number is given by:

$$N_g = \frac{\text{Gravity force}}{\text{Viscous force}} = \frac{\Delta\rho g L \bar{K}_z}{q \mu_o H} = \frac{\Delta\rho g \bar{K}_z B L}{Q_o \mu_o} \quad (2.53)$$

where,

$\Delta\rho$  is the fluid density difference, and

$\bar{K}_z$  is the average vertical permeability.

The gravity number measures the strength of the gravity effect. If  $N_g \geq 1$ , it means that water slumping will be strong, while if  $N_g < 0.1$ , the water shock front will be almost vertical. An intermediate gravity effect occurs if  $1 > N_g \geq 0.1$  (Cao and Aziz, 1999). Changing flow rate and permeability will cause change of both  $N_g$  and  $N_c$ , while changing reservoir thickness will affect only  $N_c$ .

Even though the use of gravity and capillary numbers can help in selection of the appropriate pseudoization method according to the determined flow regimes, it may be difficult to identify the flow regimes using the same numbers in the case of heterogeneous reservoirs. This is because there may be different flow regimes in different regions in the reservoir. This means that the use of gravity and capillary numbers to determine the flow regimes may only yield a global definition of the flow regime which in turn leads to erroneous flow modelling (Coll and Muggeridge 2001). In order to overcome this problem, Coll and Muggeridge (2001) proposed a method to

calculate “local” dimensionless numbers that can improve the characterization of flow regimes in heterogeneous reservoirs. In this method, the gravity number is calculated by using the same equation as Shook et al. (1992):

$$N_{gv} = \frac{K_x \lambda_{ro}^o \Delta\rho g \cos \alpha}{U_T} \frac{L}{H} \quad (2.54)$$

where,

$K_x$  is the absolute permeability in the x direction,

$U_T$  is the total fluid velocity,

$\lambda_{ro}^o$  is the endpoint mobility of the oil phase,

$\Delta\rho$  is the fluid density difference,

H & L are the reservoir thickness and length respectively,

$\alpha$  is the dip angle.

The capillary numbers are given by:

$$N_{pcvt} = \{ [k_x (dP_c/ds_{wd}) k_{rw}^o] / (u_T l \mu_w) \} \quad (2.55)$$

and

$$N_{pcvt} = N_{pcvl} \left( \frac{l}{h} \right) \sqrt{\frac{k_z}{k_x}} \quad (2.56)$$

where,

$k_x$  and  $k_z$  are the gridblock permeability in the x and z directions,

$k_{rw}^o$  is the endpoint water relative permeability for the gridblock,

$u_T$  is the total velocity through the gridblock in the x direction, and

l & h are the gridblock length and thickness respectively.

Subscripts t and l are for transverse and longitudinal.

### 2.6.6 Well pseudo functions

Well pseudo functions are functions that represent the flow from grid blocks to the wellbore and could be used to keep the wells at their original position after upscaling. Azoug and Tiab (2003) studied the effect of using local grid refinement (LGR) instead of well pseudo functions on breakthrough time and length of production rate plateau. They found that results of using LGR are not as good as those obtained when using well pseudo functions. Emanuel and Cook (1974) introduced a method of calculating well pseudo functions as follows:

$$(k_{rp})_A = \frac{\sum_{i=1}^{nc} [k_{rp} C_p (P_e - P_w)]_i}{\left[ \frac{\sum_{i=1}^{nl} (P_e \phi V)_i}{\sum_{i=1}^{nl} (\phi V)_i} - P_{wA} \right] \sum_{i=1}^{nc} C_{pi}} \quad (2.57)$$

where,

the subscript p denotes phase and the subscript A denotes areal model,

$C_p$  is flow coefficient analogous to productivity index,

$k_{rp}$  is phase relative permeability,

$P_e$  and  $P_w$  are formation and wellbore pressures respectively, and

$V$  is the block volume.

The corresponding saturation is given by:

$$(S_p)_A = \frac{\sum_{i=1}^{nl} (S_p \phi V)_i}{\sum_{i=1}^{nl} (\phi V)_i} \quad (2.58)$$

where,

$S_p$  is the phase saturation,

$\phi$  is the porosity, and

$V$  is the block volume.

Woods and Khurana (1977) Presented a procedure to obtain well pseudo functions in order to compensate for water coning in a reservoir with bottom water drive and in turn to correct the delay in breakthrough time and to represent the observed water cut values. For reservoirs with many wells, that exhibit similar water coning performance, so that they can be divided into groups, the pseudo functions generated by Wood and Khurana (1977) can speed up the simulation process. However, if each well requires an individual well pseudo function, then using radial well models are more convenient.

### 2.6.7 Directional pseudo functions

Directional pseudo functions mean generating pseudo functions in each direction x, y and z. Azoug and Tiab (2003) suggested using directional pseudo functions because they give better or at least the same results as when using non-directional pseudo functions. A similar finding was introduced by Darman, Pickup and Sorbie (2003) when they upscaled a 3D quarter 5-spot model to a 2D model and obtained good results using directional pseudos. We can conclude from this that it is worth using directional pseudos to improve the upscaling results. This was considered when generating the

pseudos by the method proposed in this thesis, and applying them to test models, see Chapters 4 and 5.

### 2.6.8 Comparison between pseudo generation methods:

A comparison between some of pseudo functions generation methods, mentioned above, is illustrated in Table 2.2.

Method	Example	Type	Flow regime	Use Limitations
Vertical Equilibrium	(Coats et al. 1967&1971)	Analytical	gravity-capillary equilibrium	Very low flow rate
Hearn	Hearn (1971)	Analytical	Viscous - dominated	Stratified reservoirs
Stone	Stone (1991)	Dynamic	Viscous-dominated	Horizontal reservoirs (no dip)
Kyte & Berry	Kyte & Berry (1975)	Dynamic	All flow regimes	dipping reservoirs (not horizontal)
Transmissibility-Weighted (TW)	Darman et al. (1999)	Dynamic	All flow regimes	No known limitations
Steady state methods	Pickup et al. (2000)	Steady state	Viscous or capillary dominated	Very low rate for CL method and high rate for VL method
History matching by non-linear regression	Tan (1995)	History matching	All flow regimes	No known limitations

**Table 2-2:** Comparison between some of pseudo functions generation methods.

### 2.6.9 Review of pseudo functions generation methods

Many reviews and comparisons were made in order to evaluate the validity of the methods used to generate the pseudo functions for different cases. Some of the reviews examined the pseudo functions ability to maintain fractional flow, fluid mobility and pressure distribution between the fine and coarse models, e.g. Darman et al. (2001). Other reviews checked the results of using pseudo functions under different conditions of gravity and capillary pressure numbers, e.g. Azoug and Tiab (2003). A brief summary of the results of some of the pseudo functions reviews will be introduced in this section.

The review carried out by Darman et al. (2001) included comparison between results of upscaling two 2D cross-sectional immiscible gas/oil displacement models to 1D models using pseudo functions. Furthermore, a comparison between results of upscaling one 3D quarter 5-spot model to a 2D model, using pseudo functions, was made. The pseudo functions used to adjust the results of the coarse grid were generated by the Kyte and Berry (1975), Hewett and Archer (1997), transmissibility weighted method (Darman et al., 1999) and Stone (1991) upscaling methods. The authors found that the Hewett and Archer and Transmissibility weighted methods give good results for the 2D models and, when directional pseudos are used, they produced good results even for the 3D model. They also found that Stone's (1991) method gives the worst results for the case with a dipping reservoir, which is expected because Stone's method does not account for gravity. Finally, it was also found that the Kyte and Berry (1975) method (which accounts for gravity) gives the worst results for the case with no dip. See the Figures 2-9 and 2-10.

Another comparison that showed the impact of gravity forces on the effectiveness of pseudo functions is that made by Azoug and Tiab (2003). In this comparison, homogeneous fine models were used to test pseudo relative permeabilities calculated by the Kyte and Berry (1975), Stone (1991), pore volume-weighted method and transmissibility weighted method (Darman et al., 2001). Afterwards, a real field heterogeneous 3D model was also used to repeat the same comparison mentioned above. The authors found that all the pseudo functions calculation methods succeeded in reproducing the fine grid results for the capillary and viscous dominated flows. However, the results were less accurate for gravity dominated flows.

In 1999, Cao and Aziz used 2D homogeneous model of a water flood and 3D heterogeneous quarter 5-spot model to test the pseudo functions calculated by Jacks et al. (1973), Kyte and Berry (1975), Pore volume-weighted, Flux weighted potential method (Guzman et al. 1994), Stone's (1991) and streamline methods (Hewett and Archer, 1997), for different gravity and capillary numbers in addition to different scale up levels. It was found that for the 2D homogeneous model, all the pseudo functions give similar improved results of the coarse grid over those obtained by using rock curves alone, except for strong gravity and capillary forces. For the quarter 5-spot 3D heterogeneous model, only pseudos calculated by Jacks et al. (1973) gave reasonable results. The authors attributed the reason for this to the way pseudos were calculated using the Jacks et al. (1973) method in which pseudos are calculated using transmissibility weighted relative permeabilities and that they are not dependent on pressure averaging, which means that the results are not affected by flow reversal if this occurs.

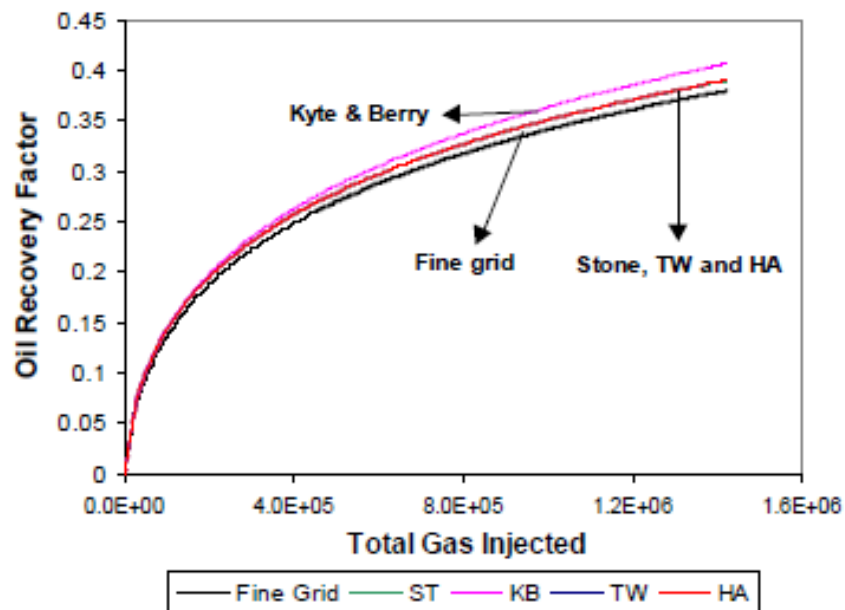


**Figure 2-9:** Comparison between results of using pseudo functions to upscale 2D horizontal model to 1D, adapted from Darman et al., 2001.

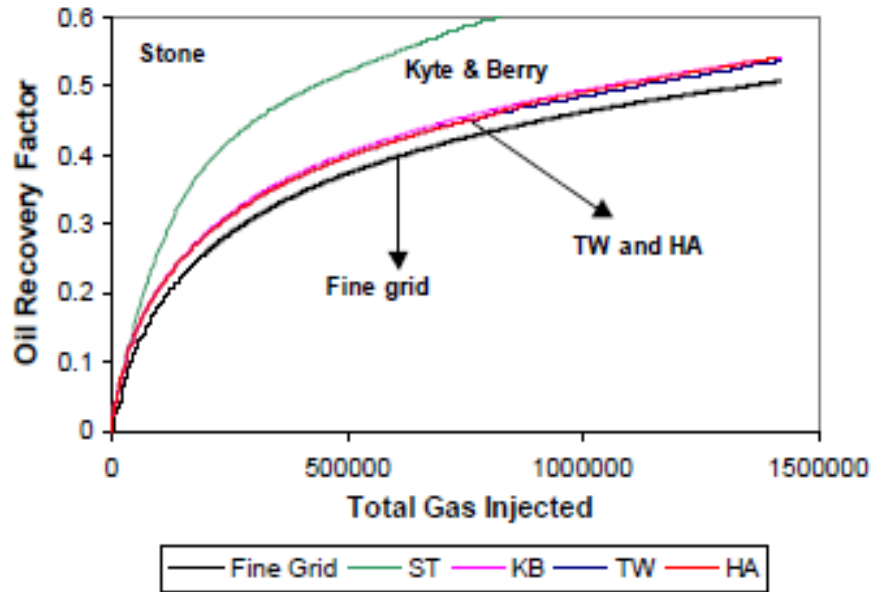


**Figure 2-10:** Comparison between results of using pseudo functions to upscale 2D dipping model to 1D, adapted from Darman et al., 2001.

In summary, there are many challenges and limitations that might arise when using the pseudo functions approach in upscaling. Without regard to the method used to generate the pseudos, the following difficulties can be met when applying the pseudo functions (Barker and Thibeau, 1997):

1. It is impractical to use many sets of pseudos for each coarse grid block, especially in large models. Instead, one set of pseudos should be used for a selected region (group of cells) in the model.
2. It is unfeasible to keep regenerating pseudos after changing well positions and boundary conditions (such as flow rate). Reliable pseudos should account for different conditions.
3. Different sets of pseudos are required even for gridblocks with similar permeability distributions but with different positions in the model. This is because different positions could mean different boundary conditions.

Based on the limitations of the use of pseudos, Barker and Thibeau (1997) concluded that it is necessary to account for gravity and capillary pressure forces when using pseudos, otherwise pseudos become an unreliable approach for upscaling from fine grid model to coarse grid model.



### **2.6.10 The use of pseudo functions generated from a specific case to another**

The issue of applying pseudo functions to cases similar to but other than those from which they were generated, was studied by Ekrann and Mykkeltveit (1995). The authors referred to the case from which the pseudo functions were derived as “Parent case”. For this purpose, 1D homogeneous and heterogeneous water-oil displacement models were used. In these models, different ranges of viscosities, injection rates and realisations were examined. The true solution of the problem in all cases was provided by using Buckley-Leverett equations. The pseudos generated using the parent case(s) were used to run simulations of the child cases and compare the results to the true analytical solution of the off-parent cases.

Ekrann and Mykkeltveit (1995) found that there are differences between the analytical and simulated solutions. However, the relative error between results is almost constant and does not change a lot with change of the tested parameters (i.e. viscosity, velocity or realisation), where each parameter was tested separately. A general relative error of 10% or more was noticed. The authors concluded that pseudos which have been generated for one case may give good results when used for another cases only if they (the pseudos) are not dependent on the parameter, which forms the difference between the two cases. The good results can be also obtained if simulations do not depend on the shape of pseudos. We can conclude from this that pseudos should be used for the case from which they were derived and moreover for the same condition at which they were generated, because even when using pseudos for its parent case but with change for example of boundary conditions, results may be affected (Barker and Thibeau, 1997).

### **2.6.11 Grouping the pseudo functions**

Generating pseudo functions to adjust the results of a coarse model is usually performed by computing one pseudo for each coarse cell. This provides a large number of pseudos, which are not feasible to work with in practice. Instead of assigning one pseudo for each coarse cell, one pseudo should be assigned to a number of coarse cells or a region (Barker and Thibeau, 1997). This can be achieved by grouping similar pseudos together, then using only one of them as a representative of the group.

Some attempts have been introduced in the literature in order to group the pseudo functions. For example, Saad et al. (1995) suggested a method to group the

pseudos according to its endpoint relative permeabilities. In the example presented in their paper, Saad et al. (1995) built a histogram of water endpoint relative permeabilities, which included seven bins representing seven groups of pseudos. Afterwards, the pseudo at the middle of each bin is used as representative of each group. However, using only endpoint relative permeability to group the pseudos means that the shape of the curves themselves is ignored with all information included. Saad et al. (1995) used this method to group the pseudos that were generated to upscale measured data to geological model. If the same method is applied to group pseudos that were generated to upscale from geological model to simulation model, it might mistakenly place pseudos with completely different shapes and different functions in one group. For example, pseudos generated to control numerical dispersion and those generated to compensate for physical dispersion could have similar endpoint relative permeabilities (assuming the same rock type), but they will have different shapes. Placing these pseudos in the same group is expected to give rise to error when used for coarse scale simulations. Saad et al. (1995) also pointed out that pseudos could be grouped by fitting functional models to the curves.

Another approach to group pseudos was provided by Christie (1996), in which parametrization of pseudos was applied. The idea was to calculate fractional flow and total mobility curves then to use shock front saturation, slope of the fractional flow curve at the shock front saturation, and minimum of the total mobility curve as three criteria to group pseudos. Dupouy et al. (1998) presented a cluster analysis approach to group the pseudos. In this approach, they divided water saturations between  $S_{wc}$  and  $1 - S_{or}$  into equal intervals and discretised the pseudos in them. Principal Component Analysis (PCA) was used to reduce the number of parameters to represent each pseudo. Afterwards, cluster analysis was performed to group the pseudos, followed by choosing a representative of each group. Averaging of pseudos included in a group was considered by Dupouy et al. (1998) as a better way how to represent the group rather than to vote one of the pseudos as a representative.

A new method to group the pseudos based on curve fitting to Chierici (1984) functional models is introduced in Chapter 3. Testing of the grouping method was carried out using 2D and 3D models in Chapter 4.

### 2.6.12 Summary and Conclusions

Upscaling generally means the process of coarsening the grid and averaging reservoir properties within them, and it is used to build reservoir models that are feasible for running simulations, referred to as simulation models.

There are several upscaling methods such as analytical methods, single phase and two phase methods. Selection of the appropriate upscaling method depends on the complexity of the problem, the desired level of accuracy and practicality. The single phase upscaling methods are more practical but less accurate for the very heterogeneous reservoirs because its results are dependent on selection of the appropriate boundary conditions. On the other hand, the two phase upscaling methods may give better results in some cases but are less practical for large field models due to the high computation time required. Also, near well upscaling is important and may have great impact on upscaling results because the flow in vicinity of wells is rather radial than linear.

Measured or calculated rock curves should not be used alone to simulate the behaviour of a heterogeneous reservoir because this can lead to remarkable loss of heterogeneity features. Instead upscaled relative permeability and capillary pressure curves (referred to as pseudo functions) should be used to capture flow features and compensate for numerical and/or physical dispersion. Selection of the appropriate two phase upscaling method to generate pseudo functions depend on balance of forces.

Using directional pseudo functions is recommended because they would give better or at least the same results as when using non-directional pseudo functions. Also, using well pseudos would have significant impact on the upscaling results by adjusting well results and preserving well location in the coarse grid.

Assigning one pseudo for each coarse cell is very time consuming when applied for large models. Instead, grouping the pseudo functions then using one pseudos as a representative for each group is more practical and should make using pseudo functions more feasible in practice.

## **Chapter 3 : Transmissibility Weighted Relative Permeability (TWR)**

### **3.1. Introduction**

It has been learnt from the literature review conducted in Chapter 2 that upscaling absolute permeability alone may not be enough to reproduce fine model results by a coarse model. This is in addition to the problem of selecting the appropriate boundary conditions when applying single phase upscaling methods. Also, it has been learnt that using rock curves alone to run coarse-scale simulations may lead to large errors, especially in heterogeneous reservoirs. Instead, upscaling relative permeability curves (pseudo functions) ought to provide improved results. The upscaled relative permeability curves can capture the sub-grid heterogeneity and compensate for numerical dispersion that arises due to the gridding. Many methods and approaches to generate pseudo functions have been already introduced in the literature (e.g. KYTE and BERRY (1975), STONE (1991), Pore Volume Weighted (PVW), PICKUP et al. (2000), CHEN and DURLOFSKY (2008), etc.). Each of these methods has its advantages and limitations, and only few of them are satisfactory when applied to general problems. This makes the need for developing a new upscaling method desirable.

In this chapter, a new dynamic two phase upscaling method is introduced to upscale relative permeability curves for heterogeneous reservoirs. The proposed method is called Transmissibility Weighted Relative permeability, in short TWR. The TWR method can be used to generate pseudo functions for coarse models corresponding either to fine field models or fine sector models. The TWR method avoids pressure averaging and uses transmissibility weighting to arithmetically average relative permeability values at the interface between adjacent coarse cells. Generation of directional TWR pseudos is also considered and can be performed by employing the transmissibility corresponding to the direction for which pseudos will be generated.

Also, in this chapter a method to generate well pseudos in order to adjust wells results is introduced. The well pseudos are generated by upscaling relative permeability curves using well connection factor as weighting.

Finally, a method to group the TWR upscaled relative permeability curves is introduced in order to make the use of the pseudo functions feasible in practice. The grouping method is based on curve fitting of the Chierici functional model (1984) to the pseudo functions.

The procedure of all the methods mentioned above and the calculations involved are described in detail in the following sections.

### **3.2. The TWR and the well pseudos methods**

This thesis proposes a new dynamic two phase upscaling method called Transmissibility Weighted Relative permeability (TWR) as well as a method to generate well pseudos. Like many of the two phase upscaling methods, the purpose is to upscale relative permeability curves in order to adjust coarse model results to be as close as fine model results. The main issue that was considered when developing the TWR and the wells pseudos methods was to avoid pressure averaging when calculating the pseudos. Although pressure averaging is used in many upscaling methods, which ought to provide good results in some cases (e.g. the Kyte and Berry (1975), Pore Volume Weighted (PVW), etc.), some disadvantages are related to the pressure averaging. For example, since the pressure averaging is non-unique, the applied approaches to average pressure give only an approximation, which may lead to errors when generating pseudo functions, especially in heterogeneous reservoirs. Also, the pseudo functions generated by averaging pressure may not be suitable for use in practice. The critical review about pseudo functions by Barker and Thibeau (1997) explained that when generating pseudo functions using the Kyte and Berry (1975) method, the following may occur:

1. Negative pseudo functions might be generated when the flow direction is opposite to the direction in which average pressure gradient was calculated.
2. Infinite pseudos might be generated in case the average pressure gradient is zero while flow between the cells, for which this average gradient was calculated, is nonzero.

Additionally, in the test carried out by Cao and Aziz (1999) using a 3D heterogeneous quarter 5-spot model, only pseudos calculated by Jacks et al. (1973) gave reasonable results when compared to pseudos generated by the Kyte and Berry (1975), Pore volume-weighted, Flux weighted potential method (Guzman et al. 1994), Stone's (1991) and streamline methods (Hewett and Archer, 1997). The authors attributed the reason for this result to the way in which the Jacks et al. (1973) pseudos were generated (i.e. using transmissibility weighting and avoiding pressure averaging), see Chapter 2, section 2.6.3.3.

For these reasons, it was decided to avoid pressure averaging when generating pseudo functions in this thesis. The stages followed to generate pseudo functions by the proposed two phase upscaling method can be described as follows:

1. Upscaling the absolute permeability using the appropriate upscaling method in order to capture pressure gradient between grid blocks (Renard and Marsily, 1997). The flow-based methods ought to provide better results.
2. Upscaling relative permeability curves at the interface between adjacent coarse blocks using the TWR method. Directional pseudos should be also considered, depending on the flow directions.
3. Upscaling relative permeability curves in the wells blocks (well connections) using well pseudos, one pseudo per each coarse block.
4. Calculate the coarse grid well connection factors and the modified transmissibilities between the coarse well connections and its neighbours using Ding (1995) method.

The workflow of the applied approach is illustrated in Figure 3-1 below. In the following sections, each of the stages mentioned above will be explained in detail.

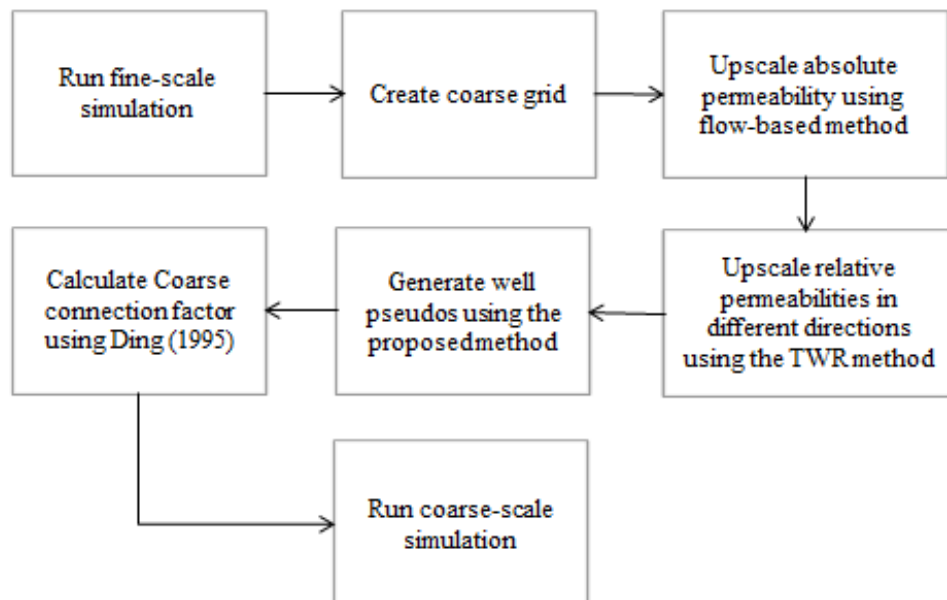


**Figure 3-1:** Workflow of the TWR upscaling method

### 3.2.1. Upscaling the absolute permeability

The first stage in the workflow of the proposed method is to upscale the absolute permeability for the coarse model using the appropriate method. As discussed in Chapter 2, there are many upscaling methods that can be used to upscale permeability or transmissibility. Single phase numerical methods ought to give better results than the analytical methods. However, care should be taken in order to avoid using inappropriate boundary conditions that may lead to large errors.

### 3.2.2. Upscaling relative permeability curves using the TWR method

The TWR method is used to upscale relative permeability curves at the downstream side of the coarse blocks, see Figure 3-2. The idea is to arithmetically average the relative permeability values in the fine cells along the interface between adjacent coarse blocks using transmissibility weighting. The transmissibility weighting was chosen here for two reasons. The first is that transmissibility controls the fluid flow between the grid blocks, which should take control over the shock frontal advance. The second reason is that using transmissibility weighting enables maintaining of the pressure gradient across the model (discussed in Chapter 4, section 4.2.3), assuming that the absolute permeability was already properly upscaled.

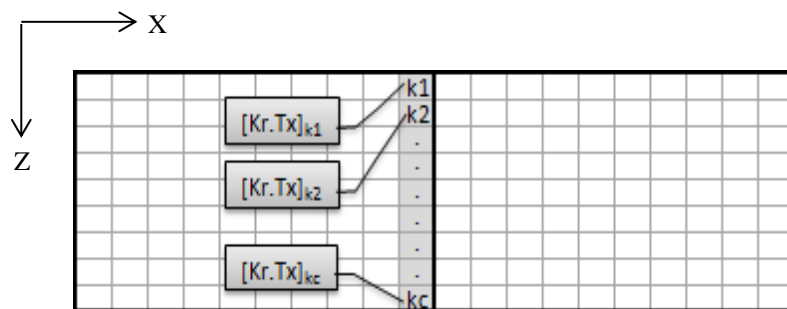


**Figure 3-2:** Upscaling of relative permeability at the downstream edge of coarse blocks (x-z cross-section)

It should be mentioned here that although the transmissibility weighting approach was previously introduced in the literature (e.g. Jacks et al., 1973 and Zhang et al., 2005), the transmissibility weighting approach applied in the TWR method is different as described below:

1. The TWR method differs from that by Jacks et al. (1973) in the approach how the relative permeabilities are upscaled. In the TWR method, relative



permeability curves are upscaled using transmissibility weighting only at the interface between adjacent coarse cells. In Jacks et al. (1973), relative permeability curves are upscaled also using transmissibility weighting but for each column of cells in the x-z direction. Afterwards, each column of cells acts as a single cell in the coarse model (see Jacks et al. method in Chapter 2).

2. The transmissibility weighting approach applied in the TWR method differs from that applied by Zhang et al. (2005) in the purpose of upscaling the relative permeability curves using transmissibility weighting. Zhang et al. (2005) used averaging of the relative permeability curves as an analytical alternative to the majority vote method when upscaling a model with multiple relative permeability curves. On the other hand, the TWR method upscales relative permeability curves in a dynamic two phase upscaling process in order to generate pseudo functions for a coarse model.

The TWR pseudo functions can be generated in the x direction for a 2D cross-sectional coarse model by applying the equations 3.1, 3.2 and 3.3, illustrated below.

Oil pseudo function is given by:

$$\bar{k}_{ro}(S_w) = \frac{\sum_{i=I_1}^{I_c} \sum_{k=K_1}^{K_c} (k_{ro}(S_w) T_x)_k}{\sum_{i=I_1}^{I_c} \sum_{k=K_1}^{K_c} (T_x)_k} \quad (3.1)$$

Similarly, water pseudo function is given by:

$$\bar{k}_{rw}(S_w) = \frac{\sum_{i=I_1}^{I_c} \sum_{k=K_1}^{K_c} (k_{rw}(S_w) T_x)_k}{\sum_{i=I_1}^{I_c} \sum_{k=K_1}^{K_c} (T_x)_k} \quad (3.2)$$

where,

$\bar{k}_{ro}$  and  $\bar{k}_{rw}$  are the oil and water pseudo functions respectively,

$k_{ro}$  and  $k_{rw}$  are the oil and water relative permeabilities of the fine model respectively,

$K_1$  and  $K_c$  are the indices of the first and last fine cells along the interface between adjacent coarse cells, see Figure 3-2,

$I_1$  and  $I_c$  are the indices of the first and last fine cells in the x direction within a coarse cell, and

$T_x$  is the transmissibility in the x direction and is given by  $T_x = K_x \cdot A/dL$ , where  $K_x$  is the harmonic average of the absolute permeability at the interface between adjacent coarse

cells in the x direction, A is the coarse cell face area perpendicular to flow direction and dL is the distance between the centres of two adjacent coarse cells.

The corresponding water saturation is given by:

$$\bar{S}_w = \frac{\sum_{i=I_1}^{I_c} \sum_{k=K_1}^{K_c} (V_p S_w)_{ik}}{\sum_{i=I_1}^{I_c} \sum_{k=K_1}^{K_c} (V_p)_{ik}} \quad (3.3)$$

where,

$\bar{S}_w$  is the average water saturation within a coarse cell,

$V_p$  is the pore volume of a fine cell within the coarse cell,

$K_c$  is the index of the last fine cell in the z direction within a coarse cell,

$K_1$  is the index of the first fine cell in the z direction within a coarse cell,

$I_c$  is the index of the last fine cell in the x direction within a coarse cell, and

$I_1$  is the index of the first fine cell in the x direction within a coarse cell.

The equations 3.1 and 3.2 are used to upscale relative permeabilities in the x direction. However, generating directional TWR pseudos may be required depending, for example, on model dimensions, wells positions, direction of flow, etc. For example, a 2D model with thief zone in the middle may require pseudos in the z direction in addition to that in the x direction. This is because water will advance faster in the thief zone than in the rest of the model, due to the viscous forces. Afterwards, the water will flow in the z direction due to gravity forces. Also, 3D models with injector in the middle may require pseudos in both the positive and negative x and y directions. In Chapter 4, directional pseudos were tested using 2D and 3D models and found to be useful in adjusting the model results.

Therefore, in order to calculate the TWR pseudo functions in the y and z directions, using the equations 3.1 and 3.2, transmissibility in the x direction should be replaced by the transmissibility in the direction for which the pseudos will be generated (e.g. transmissibility in the y direction is used to generate pseudos in the y direction, etc.). Also, the downstream edge along which calculations will be performed should be defined.

It should be noted that it is not possible to calculate TWR pseudo functions for the coarse blocks at the downstream edge of the model because there is no flow. Instead, rock curves should be assigned to these cells when running the coarse-scale

simulation. This should not make difference in the results because there is no flow out of the model. If a well is placed in one of these edge cells, the use of well pseudos (introduced in the following section) could be used to adjust the results of the well.

Procedure of generating pseudo functions using the TWR method:

1. Run fine-scale simulation of the model (or sector model) in order to obtain the relative permeability values and saturations in the fine model.
2. Define the fine cells at the downstream edge between the coarse blocks, and calculate for each cell product of the relative permeability and transmissibility in these cells.
3. Sum the values obtained in step 2 within each coarse cell.
4. Sum the values of transmissibility in all fine cells along the downstream edge of the coarse cell.
5. Divide the values from step 3 by the values from step 4 to calculate the TWR pseudo function for the coarse blocks.
6. Average the water saturation within each coarse block using pore volume weighting.
7. Repeat these calculations at different times throughout the simulation to build up pseudos functions as a function of water saturation.

Calculations used to generate the TWR pseudos were performed using C++ programs, which were written for this purpose using the open source cross-platform Code::Blocks. For more details about the codes of the programs, see Appendices B, C and D.

### 3.2.3. Upscaling well blocks relative permeability curves (The well pseudos)

When building coarse grids, well positions might be different in the coarse blocks than in the fine blocks, which affect the wells results. Adjusting a well's position in the coarse grid can be achieved using the well pseudos presented in this section. The idea is to upscale the well block relative permeability curves by arithmetically averaging relative permeability values in the fine well connections using fine well connection factors as a weighting. See Figure 3-3 and equations 3.4 and 3.5 below.

Well pseudos for oil phase are given by:

$$\bar{k}_{ro}(S_w) = \frac{\sum_{k=K_1}^{K_c} (k_{ro}(S_w)I_w)_k}{\sum_{k=K_1}^{K_c} (I_w)_k} \quad (3.4)$$

Similarly, well pseudo for water phase are given by:

$$\bar{k}_{rw}(S_w) = \frac{\sum_{k=K_1}^{K_c} (k_{rw}(S_w)I_w)_k}{\sum_{k=K_1}^{K_c} (I_w)_k} \quad (3.5)$$

where,

$\bar{k}_{ro}$  and  $\bar{k}_{rw}$  are the well pseudos for oil and water phases respectively,

$k_{ro}$  and  $k_{rw}$  are the oil and water relative permeabilities of the fine model respectively,

$I_w$  is fine scale well connection factor,

$K_c$  is the index of the last fine well connection within coarse well connection, and

$K_1$  is the index of the first fine well connection within coarse well connection.

For a 2D cross-sectional model, the corresponding water saturation is given by the same equation as in the TWR method:

$$\bar{S}_w = \frac{\sum_{i=I_1}^{I_c} \sum_{k=K_1}^{K_c} (V_p S_w)_{ik}}{\sum_{i=I_1}^{I_c} \sum_{k=K_1}^{K_c} (V_p)_{ik}} \quad (3.6)$$

where,

$\bar{S}_w$  is the average water saturation within a coarse cell,

$V_p$  is the pore volume of a fine cell within the coarse cell,

$K_c$  is the index of the last fine cell in the z direction within a coarse cell,

$K_1$  is the index of the first fine cell in the z direction within a coarse cell,

$I_c$  is the index of the last fine cell in the x direction within a coarse cell, and

$I_1$  is the index of the first fine cell in the x direction within a coarse cell.

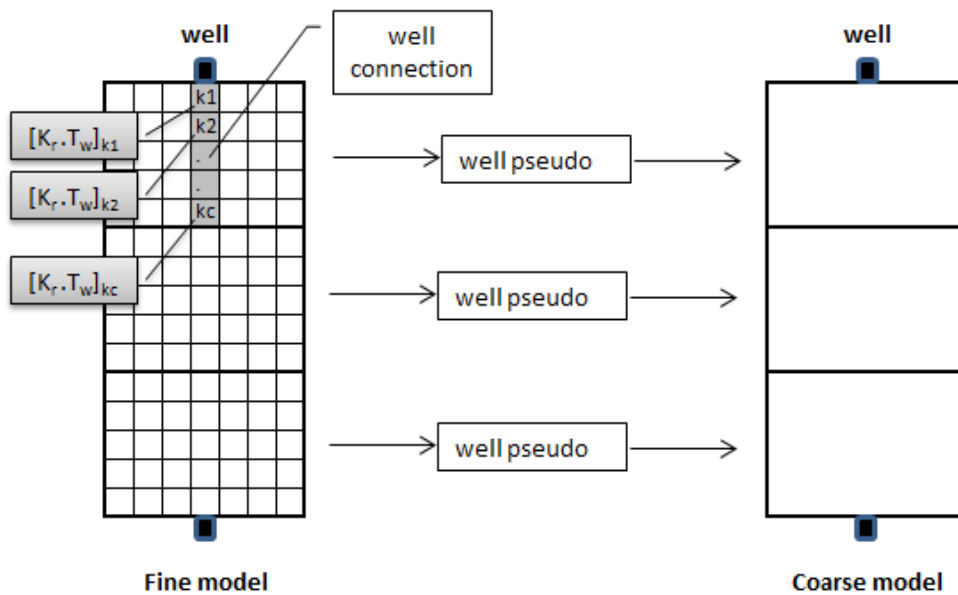


**Figure 3-3:** Upscaling of relative permeability at the well connections using well connection factor as weighting.

The reason for selecting the well connection factor as weighting is because it controls flow from the well connections to the wellbore. The value of well connection factor is dependent on the permeability, the geometry of the connecting grid block and the well position, so that all this information can be captured when generating the well pseudos.

The well connection factor shown in equation 3.4 and 3.5 can be calculated from:

$$I_w = \frac{2\pi kh}{\ln\left(\frac{r_e}{r_w}\right)} \quad (3.7)$$

where,

$I_w$  is the fine scale well connection factor,

$k$  is the geometric mean of the x and y direction permeabilities in the fine connections,

$h$  is the height of the fine well connection,

$r_w$  is the wellbore radius, and

$r_e$  is the pressure equivalent radius of the grid block,

$$r_e = 0.28 \frac{[(k_y/k_x)^{1/2} (\Delta x)^2 + (k_x/k_y)^{1/2} (\Delta y)^2]^{1/2}}{(k_y/k_x)^{1/4} + (k_x/k_y)^{1/4}} \quad (3.8)$$

where,

$k_x$  and  $k_y$  are permeability in the x and y directions respectively, and

$\Delta x$  and  $\Delta y$  are the gridblock dimensions in the x and y directions.

It should be noted that the calculation of well pseudos using the provided equations should be carried out for each coarse grid block connected to the well, which means generating one pseudo per each well connection at the coarse scale, see Figure 3-3. This approach enables better capturing of the dominant flow features that may be present in some but not all fine cells included within the connecting coarse blocks. For example, when a thief zone exists in the model, generating a single well pseudo for all well connections may not be enough to reproduce the fine-scale water influx into the well. Instead generating multiple well pseudos (one for each coarse block connection) would provide better results.

Procedure of generating the well pseudos:

1. Obtain the values of relative permeability in the fine well connections from the fine scale simulation that was previously run to generate the TWR pseudos,
2. Calculate the product of relative permeability and well connection factor in each fine well connection.
3. Sum the values obtained in step 2 within each coarse well connection.
4. Sum the values of well connection factors in all fine connections included within coarse well connection.
5. Divide the values from step 3 by the values from step 4 to calculate the well pseudo for the selected coarse well connection.
6. Average the water saturation within each coarse well connection using pore volume weighting.
7. Repeat the steps above at different times throughout the simulation to build up the well pseudos as a function of water saturation.

Like the TWR pseudos, the well pseudos were tested and the results are described in Chapter 4. The well pseudos were generated using a C++ program, which was built using the open source cross-platform Code::Blocks. More details about the programs are available in Appendix E.

#### **3.2.4. Calculation of the coarse grid well connection factor**

As already been discussed in Chapter 2, the flow in the vicinity of wells is rather radial than linear. Therefore, calculation of the coarse grid well connection factor using Peaceman (1983) formula may not be appropriate (Muggeridge et al, 2002). This is because of the permeability term involved in the formula, which may have been upscaled using conventional upscaling techniques that assume linear flow. Alternatively, a method introduced by Ding in 1995 can be used to calculate the coarse grid well connection factor by using the well flux and pressure drop between the well connection and its well bore (see Chapter 2 for the procedure). Additionally, the method by Ding (1995) modifies the transmissibilities between the well connections and the adjacent cells.

Thus, the method by Ding (1995) is applied in addition to the proposed well pseudos method in order to improve the individual well results.

### 3.2.5. New method to group the pseudo functions

After generating the TWR pseudos, assigning one pseudo for each coarse cell might be impractical and time consuming (Barker and Thibeau, 1997). Instead, grouping the generated pseudos into a manageable number of groups, and assigning a representative of each group to a region (i.e. group of cells) should make the use of pseudos more feasible in practice.

The grouping method presented here is based on curve fitting of Chierici (1984) functional models to the TWR pseudos. Afterwards, the parameters determined from this curve fitting are plotted in order to spot possible clusters of pseudos. The functional model proposed by Chierici in 1984, see equations (3.9) through (3.13) includes four parameters, which are used to compute water/oil imbibition curves. Parameters A and L are used to calculate oil relative permeability curve, while the parameters B and M are used to calculate water relative permeability curve.

The functional models by Chierici (1984) were chosen to perform this pseudos grouping rather than, for example, the modified Brooks-Corey relations (1964), because of the more flexibility provided by the Chierici functions when matching curves with unusual shapes, which is a common characteristic of pseudo functions. This flexibility is attributed to the use of two numerical parameters (A and L for oil or B and M for water), while the modified Brooks-Corey relations (1964) include only one numerical parameter, referred to as Corey exponent.

$$k_{ro}^* = \exp(-A R_w^L) \quad (3.9)$$

$$k_{rw}^* = \exp(-B R_w^{-M}) \quad (3.10)$$

$$k_{ro}^* = \frac{k_{ro}}{k_{ro}(S_{wi})} \quad (3.11)$$

$$k_{rw}^* = \frac{k_{rw}}{k_{rw}(S_{or})} \quad (3.12)$$

where,

$k_{ro}^*$  and  $k_{rw}^*$  are normalized relative permeability to oil and water, respectively,

A, L, B, and M are empirical coefficients,

$k_{ro}(S_{wi})$  endpoint oil relative permeability,

$k_{rw}(S_{or})$  endpoint water relative permeability,

$k_{ro}$  and  $k_{rw}$  are oil and water relative permeabilities respectively, and  $R_w$  is correlation parameter and is given by,

$$R_w = \frac{S_w - S_{wi}}{1 - S_{or} - S_w} \quad (3.13)$$

where,

$S_{wi}$  is irreducible water saturation, and

$S_{or}$  is residual oil saturation.

In order to perform the Chierici (1984) curve fitting to the pseudos, Excel (Microsoft, 2013) spreadsheet with non-linear regression solver was prepared, see Figure 3-4. In this spreadsheet, data of one set of pseudo functions is entered, and the parameters A, L, B and M are assigned an initial value. A curve fitting tool is used to automatically modify the parameters A, L, B and M in order to find the best match of Chierici curves to the pseudo oil and water curves. A graph below the calculation table is used to check the effectiveness of curve fitting.

After determining the Chierici parameters, parameter B is plotted against parameter M in case of water relative permeability grouping, while parameter A is plotted against parameter L in case of oil relative permeability grouping. These plots are used to define possible clusters of pseudo functions. Although water and oil relative permeabilities are interdependent, it is still useful to apply grouping for both oil and water pseudos because it makes it easier to decide which pseudos should be grouped and/or split in order to obtain the best results. After grouping the pseudos according to the method described above, one pseudos is elected as a representative for each group. This could be performed using cluster analysis software. The grouping method introduced here was tested using 2D and 3D models and the results are described in Chapter 4.



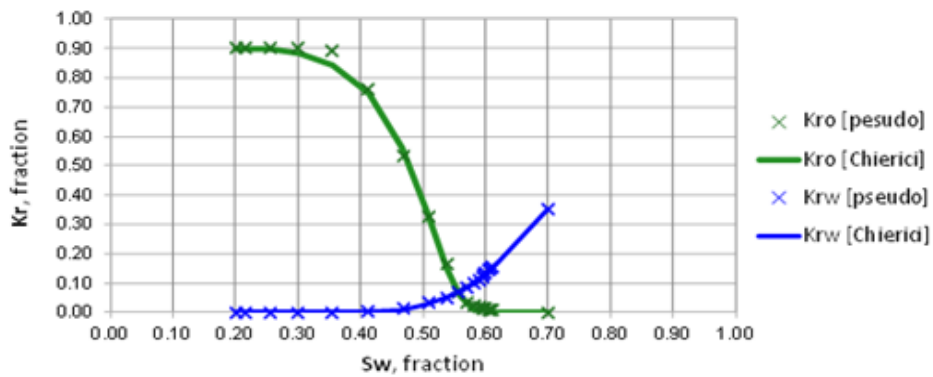
Chierici Parameters :		Rock curve data :		K <sub>rw</sub> Curve Fitting		K <sub>ro</sub> Curve Fitting	
B	4.137	S <sub>wi</sub>	0.2				
M	1.032	S <sub>or</sub>	0.3				
A	0.360	K <sub>ro</sub> (S <sub>wi</sub> )	0.9				
L	2.166	K <sub>rw</sub> (S <sub>or</sub> )	0.35				

	S <sub>w</sub>	K <sub>rw</sub> [pseudo]	K <sub>ro</sub> [pesudo]	R <sub>w</sub>	K <sub>rw</sub> [Chierici]	K <sub>ro</sub> [Chierici]	R2 [K <sub>ro</sub> ]	R2 [K <sub>rw</sub> ]
1	0.200	0.000	0.900	0.001	0.000	0.900	0.000	0.000
2	0.216	0.000	0.900	0.033	0.000	0.900	0.000	0.000
3	0.254	0.000	0.900	0.122	0.000	0.897	0.000	0.000
4	0.303	0.000	0.900	0.258	0.000	0.883	0.000	0.000
5	0.356	0.000	0.892	0.453	0.000	0.844	0.002	0.000
6	0.412	0.000	0.760	0.737	0.001	0.747	0.000	0.000
7	0.466	0.012	0.531	1.138	0.009	0.559	0.001	0.000
8	0.507	0.031	0.326	1.593	0.027	0.336	0.000	0.000
9	0.538	0.051	0.163	2.085	0.050	0.153	0.000	0.000
10	0.559	0.069	0.067	2.540	0.072	0.060	0.000	0.000
11	0.572	0.085	0.035	2.910	0.089	0.024	0.000	0.000
12	0.581	0.099	0.025	3.211	0.101	0.010	0.000	0.000
13	0.588	0.111	0.019	3.475	0.112	0.004	0.000	0.000
14	0.594	0.121	0.015	3.718	0.120	0.002	0.000	0.000
15	0.599	0.129	0.013	3.940	0.128	0.001	0.000	0.000
16	0.603	0.136	0.011	4.142	0.135	0.000	0.000	0.000
17	0.606	0.142	0.010	4.337	0.141	0.000	0.000	0.000
18	0.610	0.148	0.009	4.529	0.147	0.000	0.000	0.000
19	0.613	0.153	0.008	4.720	0.152	0.000	0.000	0.000
20	0.700	0.350	0.000	4999	0.350	0.000	0.000	0.000
21								
22								
23								

Sum of R2	
0.0051	0.0001



**Figure 3-4:** Snapshot of an Excel spreadsheet to perform curve fitting of Chierici (1984) functions to the TWR pseudos

### **3.3. Summary and Conclusions**

To summarize, a new dynamic two phase flow upscaling method has been introduced in this chapter in order to upscale relative permeability curves. The method includes:

- Generating pseudo functions by averaging relative permeability at the downstream edge of coarse cells using transmissibility weighting. The method is called TWR.
- Generating well pseudos by averaging relative permeability in the well connections using well connection factor.

After generating the pseudos, a method to group the TWR pseudos based on curve fitting of Chierici (1984) functional models is provided in order to make using pseudos feasible in practice.

Testing of the proposed methods using synthetic 2D and 3D models is described in Chapter 4.

## **Chapter 4 : Testing of the TWR method and the well pseudos**

## **4.1. Introduction**

In Chapter 3, a new method to upscale relative permeability curves, referred to as the TWR method was introduced. This is in addition to a method to generate well pseudos in order to adjust the well position and results in the coarse grid. In this chapter, the proposed methods are tested by applying the upscaled relative permeability curves for 2D and 3D synthetic models, in order to check the methods performance. Afterwards, the pseudos grouping method (introduced also in Chapter 3), using curve fitting to Chierici functional model (1984), is applied in order to make the use of the generated pseudos feasible in practice. Outlines of the tests considered in this chapter are briefly mentioned below, while details of each test including description of the models, test results as well as discussion about the results are provided in the following sections.

Initially, a synthetic 2D cross-sectional model (40x30) was created to run fine-scale simulation of a water flood problem. Afterwards, the model was coarsened by a scale-up factor of 10x10, followed by upscaling the absolute permeability using a flow-based method. The TWR and the well pseudos methods were used to generate pseudo functions for the coarse model and the wells, respectively. Finally, the results of the coarse model with the pseudo functions were compared to the results of the fine model with rock curves, the coarse model with rock curves, and the coarse model with pseudo functions generated using Stone's (1991) method. Details of this test are provided in section 4.2.

Additional tests were carried out to check the proposed pseudos performance for three cases. First, a case with permeability coarsening upwards where the flow is viscous dominated. Second, a case with permeability fining upwards where water slumping, similar to that caused by gravity effects, is enforced. Third, a case with thief zone with permeability of 10 Darcy is present in the middle of the model. In all cases, comparison between coarse and fine models in terms of water breakthrough time, field water production rates and injector bottom hole pressure was considered. Details of these tests are provided in section 4.3.

Since, most of models built in practice are 3D models, it was necessary to test the performance of the TWR method, the well pseudos and the grouping method when applied to 3D models as well. For this purpose a 3D water flood synthetic model (15x15x9) was built and the TWR method was applied to generate directional pseudo

functions in all flow directions (both positive and negative) for a coarse model of size 5x5x3.

In all tests mentioned above, it was assumed that the fine model represents the “correct” solution of the problem and in turn it can be referred to as the reference or the base model. When the coarse model results were as close as the results of the fine model, the upscaling method was assumed to be successful. Also, in all tests, capillary pressure was assumed to be taken care of during small-scale upscaling from lamina scale to the geological model, so that capillary pressure curves were ignored.

## **4.2. Testing of the TWR method using 2D cross-sectional model**

### **4.2.1. Model description**

For the purpose of initial testing of the TWR pseudo functions, a synthetic 2D cross-sectional model (40x30) was built and referred to as the fine model, see Table 4-1 and Figure 4-1. Afterwards, the fine model was upscaled by scale-up factor of 10 in both the x and z directions to a coarse model of size 4x3. In both the fine and coarse models, two vertical wells (Producer and Injector) were placed at the opposite sides of the model, and were completed throughout the thickness of the model. Reservoir rock and fluid properties used in the fine model are illustrated in Tables 4-2 and 4-3, respectively.

Permeability in the fine scale model was distributed throughout the model using stochastic method (Sequential Gaussian Simulation, PETREL, Schlumberger) with correlation length of 20m (i.e. smaller than the coarse cell size) and standard deviation of 0.5, see Figure 4-3. Permeability range in the x direction was 0.1 - 2000 mD, while permeability in the z direction equalled 10% of the permeability in the x direction. The absolute permeability of the coarse model was upscaled using the flow based method with no flow conditions, see Figure 4-4. Relative permeability curves used in the fine model (rock curves) are illustrated in Figure 4-2. The development strategy applied to this model is based on controlling the producer by bottom-hole pressure of 250 bar, while controlling the injector by water surface rate of 5 m<sup>3</sup>/day, in addition to running simulation for 5 years.

Test models	Reservoir dimensions	Cell dimensions	Model dimensions	No. of cells
Fine model	200m x 15m x 15m	5m x 15m x 0.5m	40x 1x 30	1200 cells
Coarse model	200m x 15m x 15m	50m x 15m x 5m	4x 1x 3	12 cells

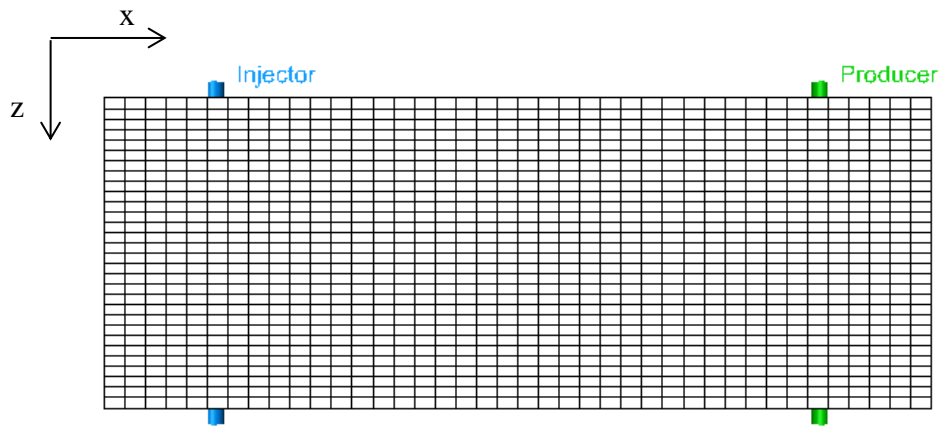
**Table 4-1:** Test models used for initial testing of the TWR pseudos.

Permeability	Porosity	End Point Saturations	Kr at residual saturation	Oil-water contact
Log-normal distribution (Sequential Gaussian Simulation), range (0.1 – 2000mD), mean = 200 mD, correlation length ( $\lambda$ ) = 20m (in all directions) and Standard deviation $\sigma \ln(k) = 0.5$ .	23% (assumed constant throughout the model)	$S_{or} = 30\%$ and $S_{wi} = 20\%$	$K_{rw}@S_{or} = 0.35$ and $K_{ro}@S_{wi} = 0.9$	2500 TVDSS. (Reservoir top @ 1000TVDSS)

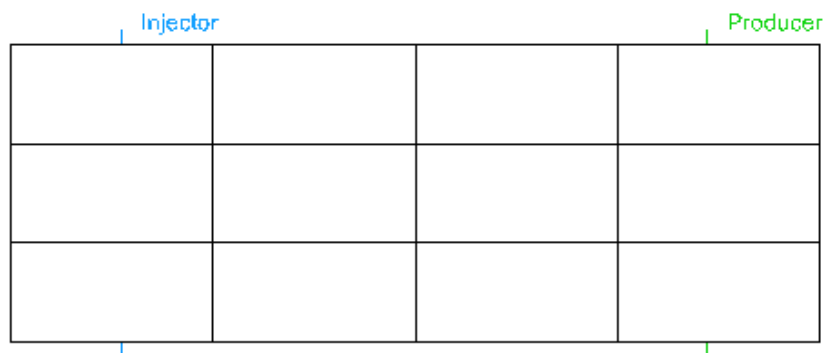
**Table 4-2:** Reservoir properties used in the fine scale model.

Phases	Oil viscosity	Water viscosity	$P_b$ pressure	Initial reservoir pressure	Reservoir temperature
Oil + water	2.12 cp	0.384 cp	80 bar	250 bar @ 1000 TVDSS	80°C

**Table 4-3:** Fluid properties and initial conditions used in the fine and coarse models.



[Fine scale model, 40x1x30]



[Coarse scale model, 4x1x3]

**Figure 4-1:** Fine and coarse synthetic 2D cross-sectional models

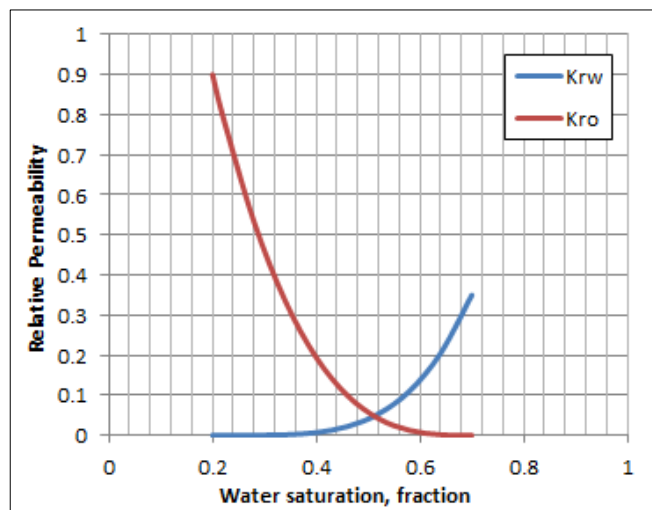


**Figure 4-2:** Relative permeability curves used in the fine model, calculated using the Corey (1954) method.

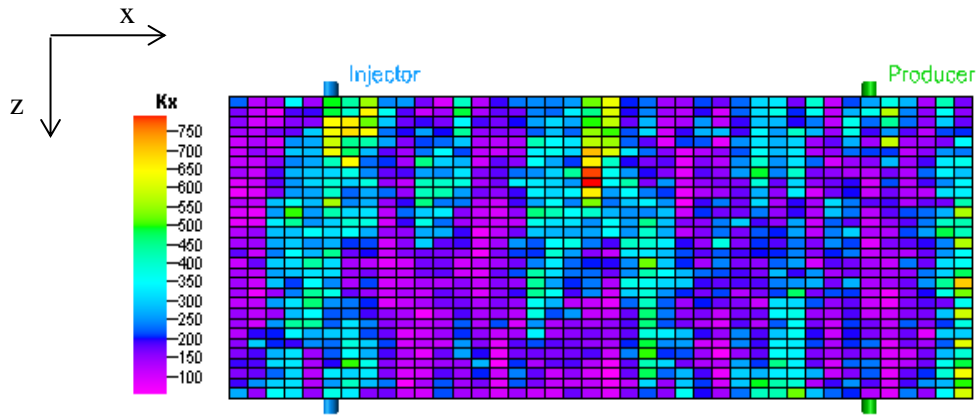


**Figure 4-3:** Permeability distributions in the 2D cross-sectional fine scale model using Sequential Gaussian Simulation (PETREL, Schlumberger), where corr. length ( $\lambda$ ) = 20m (in the x and z directions), mean = 200 mD and std. deviation  $\sigma \ln(k) = 0.5$ . For better visualisation of the model, vertical exaggeration of 5 has been used.

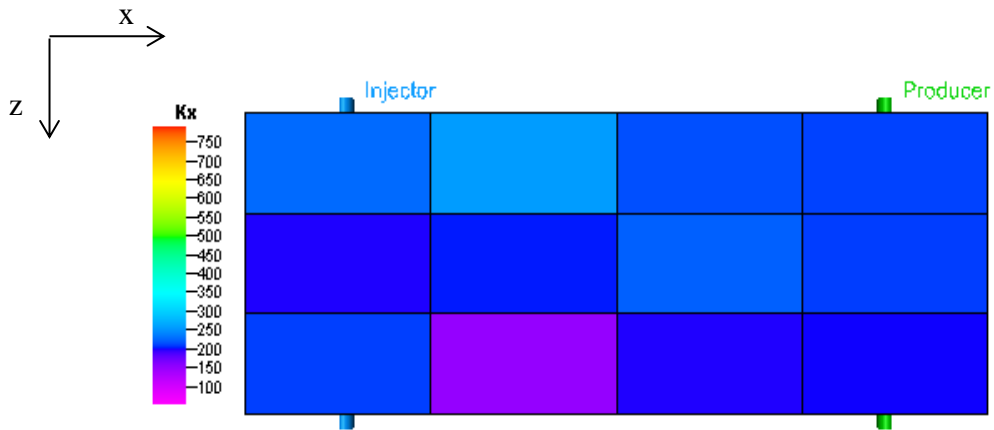


**Figure 4-4:** Upscaled permeability in the x direction in the coarse grid model using flow based method with no flow conditions.

#### 4.2.2. Fine and coarse water flood simulation using rock curves

The fine and coarse models, described in the previous section, were used to run a water flood simulation for 5 years using rock curves, shown in Figure 4-2. Results of the fine model were considered as the reference to which the coarse model results were compared. The simulations cases involved in this study are:

**Fine\_Rock\_Curve:** refers to the fine model with rock curves.

**Coarse\_Rock\_Curve:** refers to the coarse model with rock curves.



In Figure 4-5, comparison between water saturation profiles in the fine and coarse models (both with rock curves) is illustrated at different time steps of the water flood. At the beginning of the water flood, water saturation in both fine and coarse models equalled value of the connate water saturation (i.e.  $S_{wi} = S_{wc} = 0.2$ ). After one year of the water flood, the water shock front proceeded towards the producer and swept oil in both models. It can be noticed that in the fine model the flood front moved slightly faster in the middle and top of the model than in the bottom. This is due to viscous forces that caused water to flow faster in cells with higher permeability than those with lower permeability (See Figure 4-3 for permeability distributions in the x direction in the fine model). At the same time step but in the coarse model, it can be noticed that the water frontal advance had a piston like behaviour. This is because of averaging the permeability of the fine cells within the coarse cells, which washed out the contrast in permeability within them.

At the breakthrough time, in both fine and coarse models, the water reached the producer at almost the same time, along the perforated interval. The effect of numerical dispersion, due to coarsening the grid, was offset by the reduction in physical dispersion due to upscaling the permeability. Therefore, the use of rock curves in this case to run the coarse scale simulation could properly capture the water breakthrough time.

At the end of the water flood, oil has been swept almost everywhere in the coarse model. However, in the fine model, there is still oil trapped in the areas behind the wells, especially in the top corners of the model. This happened because in the fine model the water flowing in the areas behind the wells was very slow, which gave more space for gravity forces to take place. The gravity forces caused the water to flow downwards to the bottom of the model leaving oil trapped in the top corners of the model. This did not occur in the coarse model because the coarse cells where the wells are placed included all fine cells both behind and in front of the wells, so that the water did not have the same behaviour as in the fine model. As a result, the cumulative oil produced in case of the coarse model was higher than that in the fine model, see Figure 4-6.

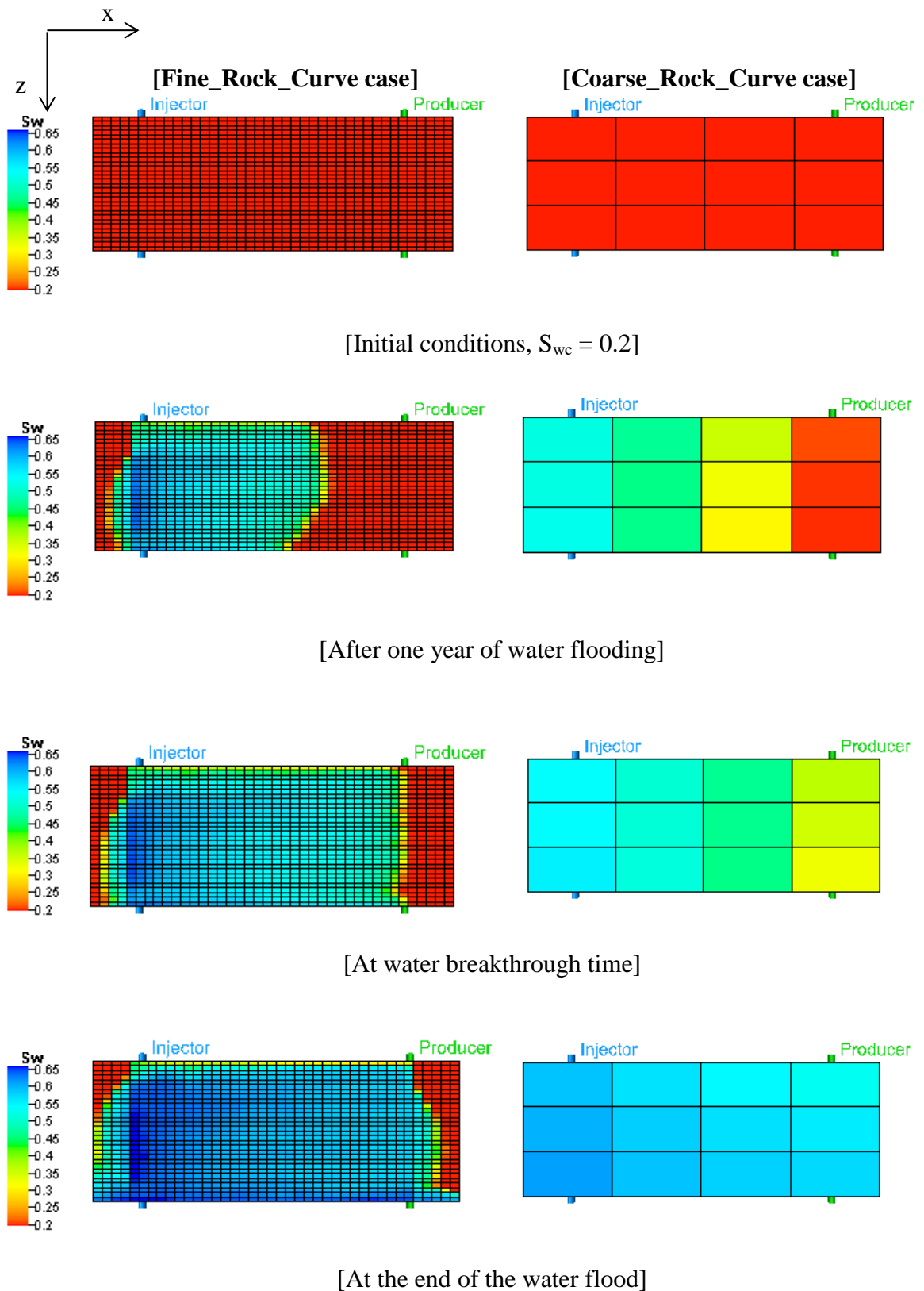


**Figure 4-5:** Comparison between water saturation profiles of the fine and coarse models (both with rock curves) at initial conditions, after 1 year of water flooding, at the water breakthrough time and at the end of the water flood.

In Figure 4-7, comparison between results of the fine and coarse models in terms of field water production rate is illustrated. As already seen in the saturation profiles, the water breakthrough time in the coarse model is very close to that of the fine model. However, after the water breakthrough occurred, the producer's water flow rate in the fine model increased very rapidly compared to that in the coarse model. This indicates that the rock curves used in the coarse model did not capture the fluid flow behaviour from the coarse well connections to the wellbore.

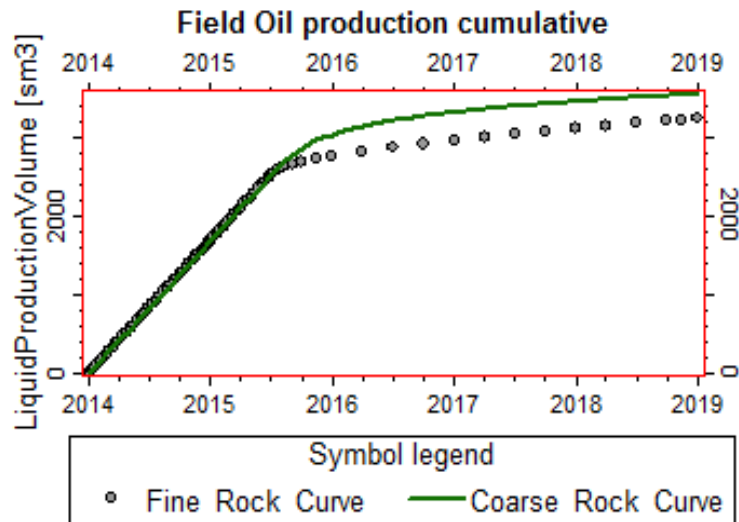


**Figure 4-6:** Comparison between cumulative oil production in case of fine and coarse models (both with rock curves).

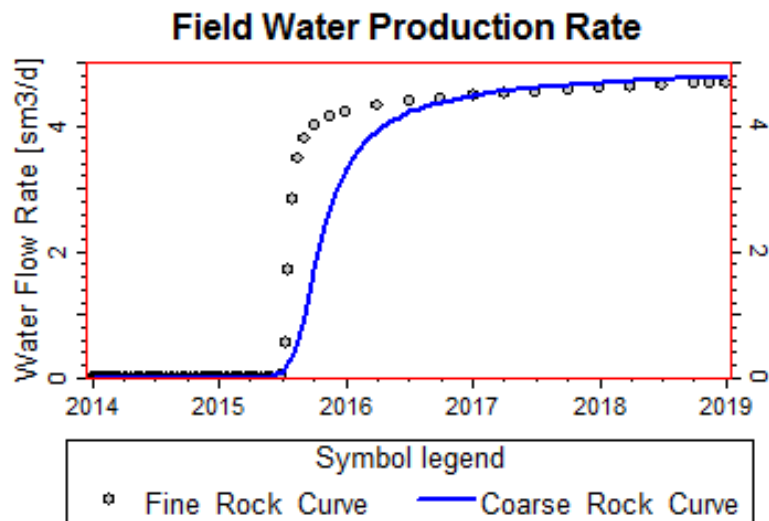


**Figure 4-7:** Comparison between results of the fine and coarse models (both with rock curves) in terms of field water production rate.

Figure 4-8 shows a comparison between results of the fine and coarse models in terms of the injector bottom hole pressure. The results indicate that the coarse model with rock curves did not reproduce the bottom hole pressure of the injector in the fine model. The injector bottom hole pressure increase in the coarse model indicates that the absolute permeability in the injector's blocks has been reduced due to upscaling.

In conclusion, the coarse model with rock curves did not succeed in reproducing the results of the fine model, except for the water breakthrough time. Therefore, the coarse model using the rock curves cannot replace the fine model to run simulations. This shows the need for a tool to adjust the results of the coarse model to be as close as those of the fine model. This could be achieved by using pseudo functions.

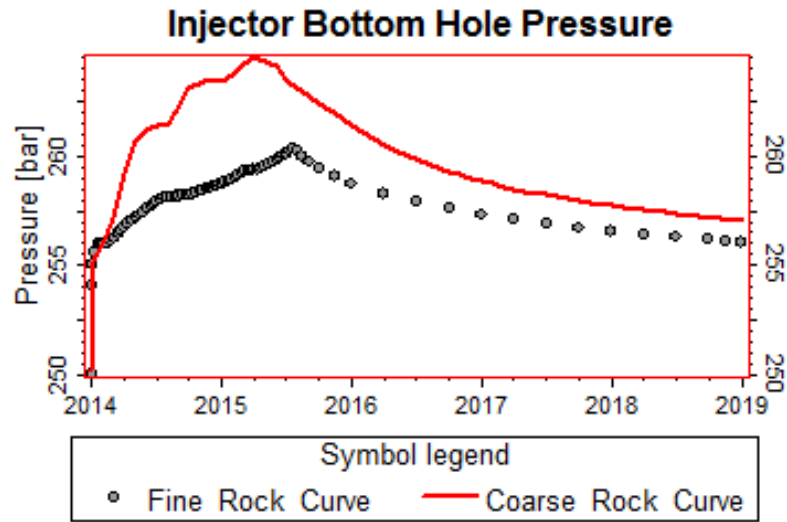


**Figure 4-8:** Comparison between results of the fine and coarse models (both with rock curves) in terms of injector bottom hole pressure.

#### 4.2.3. Coarse water flood simulation using Stone's (1991) pseudo functions

The coarse scale simulation performed in the previous section (using the rock curves) was repeated here but with using pseudo functions. The method selected to generate these pseudo functions is that proposed by Stone in 1991 (explained in detail in Chapter 2). There are two reasons behind this selection. First, the Stone's (1991) method avoids pressure averaging, same as the TWR method. Second, the model used in this study is horizontal (i.e. not dipping) so that the Stone's (1991) method should, according to the review by Darman et al. (2001), see Chapter 2, give better results than for example the method by Kyte and Berry (1975). This is because the Stone (1991)

method assumes that pressure potential in both gas and oil phases are equal (i.e.  $\Delta\Phi_g = \Delta\Phi_o$ ), which can be applicable in the case with horizontal model.

In order to perform the calculations of Stone's (1991) method, C++ codes were written to do so, see the Appendix A in the end of this thesis. The pseudo functions, generated by Stone's (1991) method, were assigned to all coarse cells in the coarse model, except the cells at the right-hand edge of the model, where the producer is placed. This is because the fine cells at the downstream edge of these coarse cells have got no flow and in turn no Stone pseudos can be generated. Instead, the producer coarse connections were assigned rock curves. Afterwards, the coarse scale simulation using Stone's (1991) pseudos was run for 5 years and the results were compared to the fine and coarse models (both with rock curves). The simulation cases involved in this study were:

**Fine\_Rock\_Curve:** refers to the fine model with rock curves.

**Coarse\_Rock\_Curve:** refers to the coarse model with rock curves.

**Coarse\_Stone\_Pseudo:** refers to the coarse model with Stone's (1991) pseudos.

Comparisons between the saturation profile of the cases Coarse\_Rock\_Curve and Coarse\_Stone\_Pseudo is illustrated in Figure 4-9. Comparisons between all three simulation cases mentioned above, in terms of field water production rate and injector bottom hole pressure, are illustrated in Figures 4-10 and 4-11.

In Figure 4-9, at the beginning of the water flood, the water saturation profiles for both Coarse\_Rock\_Curve and Coarse\_Stone\_Pseudo cases are the same, both are at the connate water saturation value ( $S_{wi} = S_{wc} = 0.2$ ). After one year of the water flood, the water shock front in both coarse models moved towards the producer but the water did not breakthrough into the producer yet. Later on, the water breakthrough occurred at the producer almost at the same time in both coarse models, See Figure 4-10. After the breakthrough time the Coarse\_Stone\_Pseudo case provided slight improvement in water production rate over the Coarse\_Rock\_Curve case. However, it failed to give better match to the fine model results. This is because, same as in the Coarse\_Rock\_Curve case, the cells where the producer is placed were assigned rock curves, so that the rock curves alone did not maintain the fluid flow rate from the coarse well connections to the wellbore. This indicates the importance of using well pseudos in order to adjust well results. In the late stage of the water flood, a pseudo steady state was reached and results

of Coarse\_Stone\_Pseudo case are very similar to those of the Coarse\_Rock\_Curve and Fine\_Rock\_Curve cases.

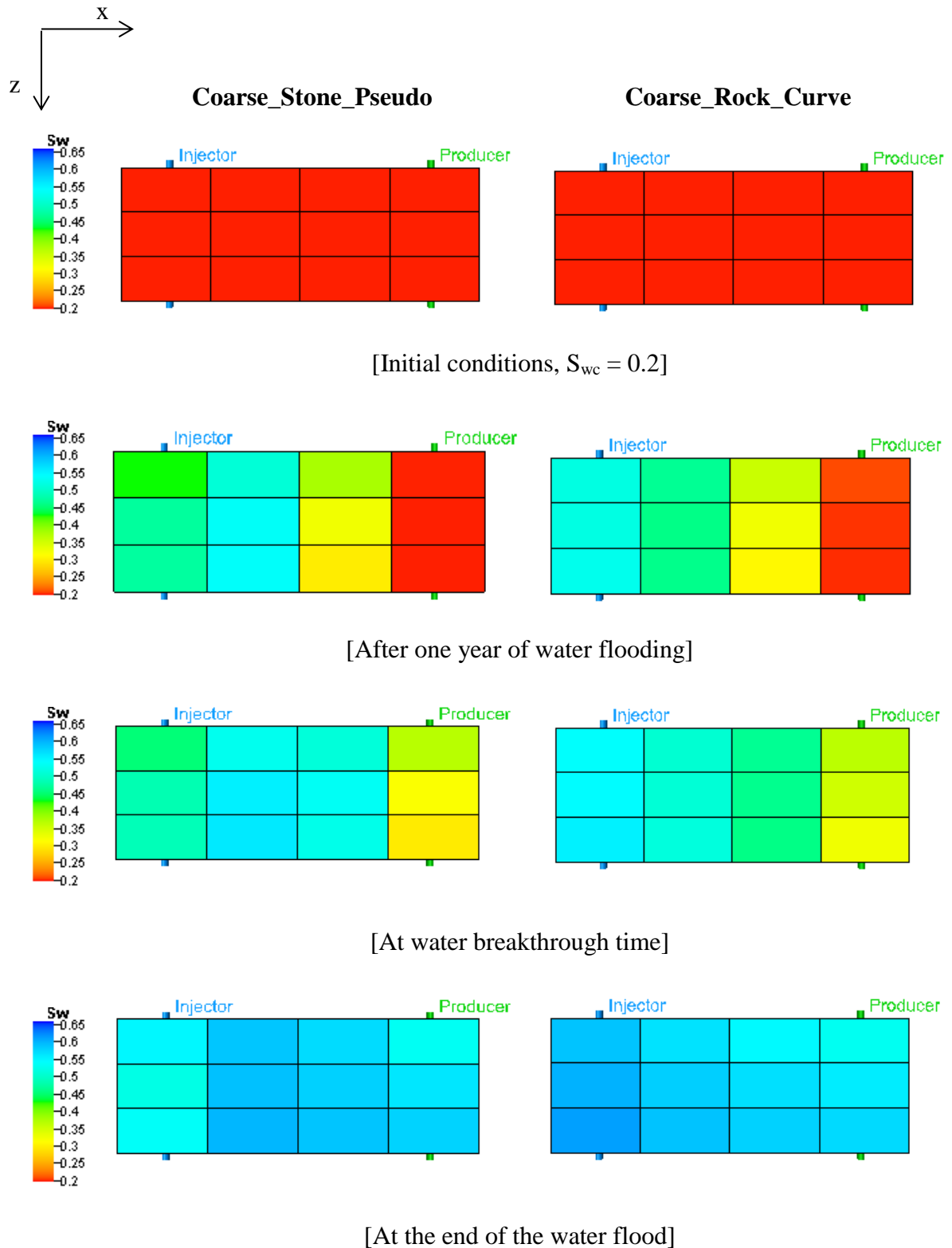


**Figure 4-9:** Comparison between water saturation profiles of coarse model with rock curves and coarse model with Stone (1991) pseudo functions at initial conditions, after 1 year of water flooding, at the water breakthrough time and at the end of the water flood.

In Figure 4-11, it can be noticed that in the Coarse\_Stone\_Pseudo case, the injector bottom hole pressure is very close to that of the fine model. This is, according to Stone (1991), due to using transmissibility weighted total mobility average to calculate the pseudos, which enabled prediction of the pressure gradient across the coarse model. This could be explained as follows:

Since it is assumed that the flow rate of a coarse cell equals the sum of total flow rates of the fine cells at the downstream edge of that coarse cell, which can be expressed as follows:

$$Q = \sum_k q_t \quad (4.1)$$

where,

$Q$  is coarse cell flow rate,

$q_t$  is fine cell total flow rate, and

$k$  is the number of cells at the interface between adjacent coarse cells.

By substituting for Darcy's two phase flow equation for each flow rate, the following is approximately equal:

$$\bar{T} \bar{\lambda}_t \Delta \bar{\Phi}_o = \sum_k (T \lambda_t \Delta \Phi_o)_k \quad (4.2)$$

where,

$\bar{T}$  &  $T$  are transmissibility of coarse and fine cells respectively,

$\bar{\lambda}_t$  &  $\lambda_t$  are total mobility of coarse and fine cells respectively,

$\Delta \bar{\Phi}_o$  is the oil phase potential gradient between adjacent coarse cells, and

$\Delta \Phi_o$  is the oil phase potential gradient between fine cells at the interface between adjacent coarse cells.

Therefore, in order to make the potential gradients of both fine and coarse models equal in equation (4.2) and in turn to match the pressure gradient of the coarse model to that of the fine model, the total mobility at the downstream edge of the coarse cells is arithmetically averaged using transmissibility weighting of the fine grid cells as follows:

$$\bar{\lambda}_t = \frac{\sum_k (T \lambda_t)_k}{\sum_k (T)_k} \quad (4.3)$$

In conclusion, pseudo functions generated by the Stone's (1991) method did not reproduce the production results of the fine model because the producer is placed at the edge of the coarse model, where pseudo functions cannot be calculated, so that rock curves were used instead. Injector bottom hole pressure was well maintained in the coarse model by using Stone's (1991) pseudos.

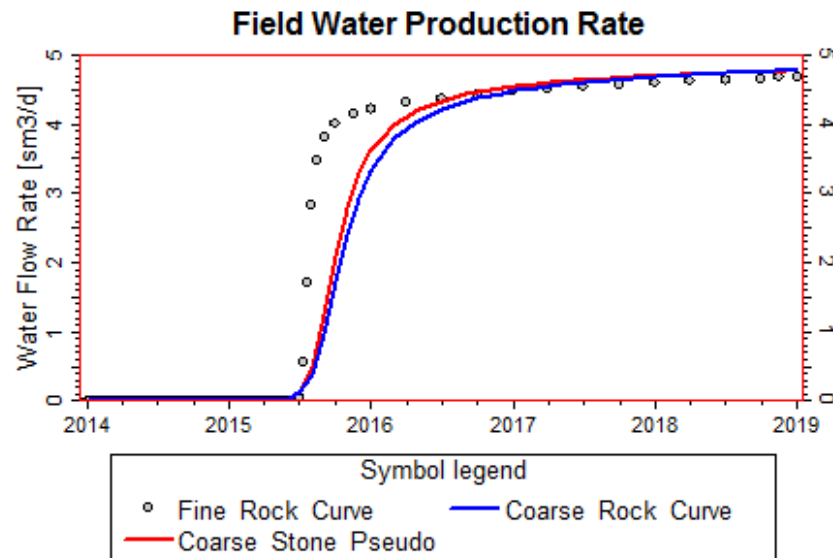


**Figure 4-10:** Comparison between fine and coarse models (with rock curves) and coarse model (with Stone's (1991) pseudo functions) in terms of field water production rate.

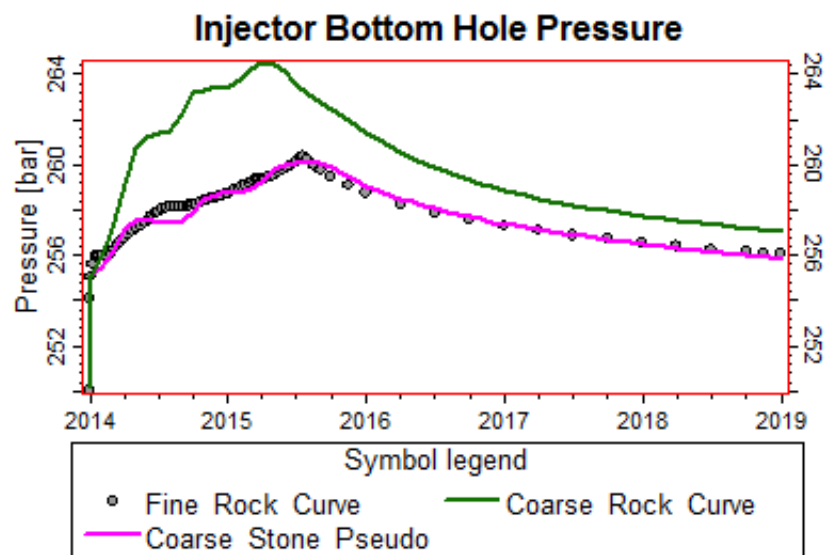


**Figure 4-11:** Comparison between the fine and coarse models (with rock curves) and the coarse models (with Stone's (1991) pseudo functions) in terms of injector bottom hole pressure.



#### 4.2.4. Coarse water flood simulation using TWR pseudo functions

In this test, the TWR pseudo functions were generated for the coarse model using the method described in Chapter 3, see Figure 4-12. The calculations were performed using a C++ program, see the Appendix B in the end of this thesis. Afterwards, each coarse cell was assigned one pseudo. The cells at the edge of the model, where the producer is placed, were assigned rock curves because there is no flow at the edge of the model so that the TWR pseudos cannot be generated. The simulation cases involved in this study are:

**Fine\_Rock\_Curve:** refers to the fine model with rock curves.

**Coarse\_Stone\_Pseudo:** refers to the coarse model with Stone's (1991) pseudos.

**Coarse\_TWR\_Pseudo:** refers to the coarse model with TWR pseudos.

Comparisons between all three simulation cases above, in terms of field water production rate and injector bottom hole pressure, are illustrated in Figures 4-14 and 4-15.

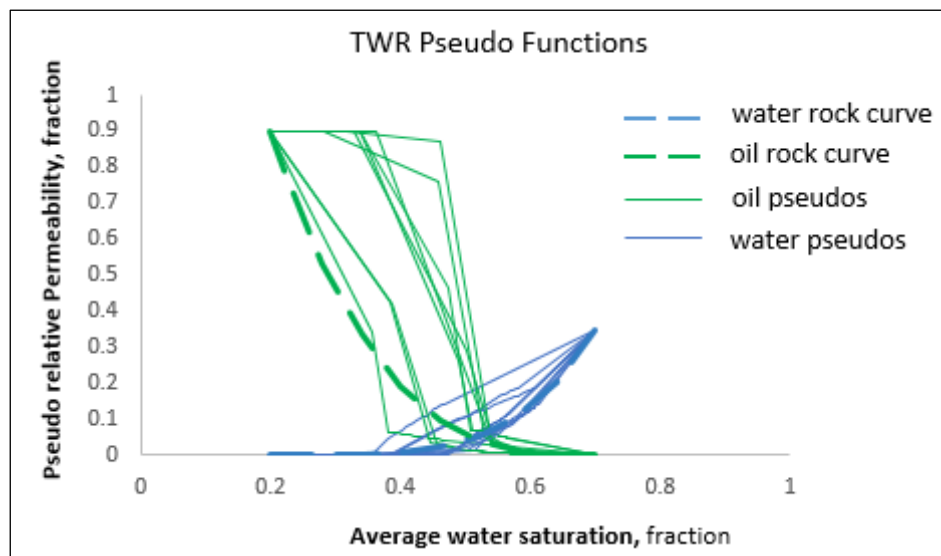


**Figure 4-12:** TWR pseudo functions generated for the 2D cross-sectional model

In Figure 4-13, the water saturation profiles of the Coarse\_Stone\_Pseudo case and the Coarse\_TWR\_Pseudo case at different time steps of the water flood is illustrated. It can be noticed that during all time steps of the water flood, saturation profiles of the two compared simulation cases show almost the same behaviour. This is confirmed in Figure 4.14 where both cases provided almost the same field water production rate. This is because in both cases, the producer's cells were assigned rock curves.

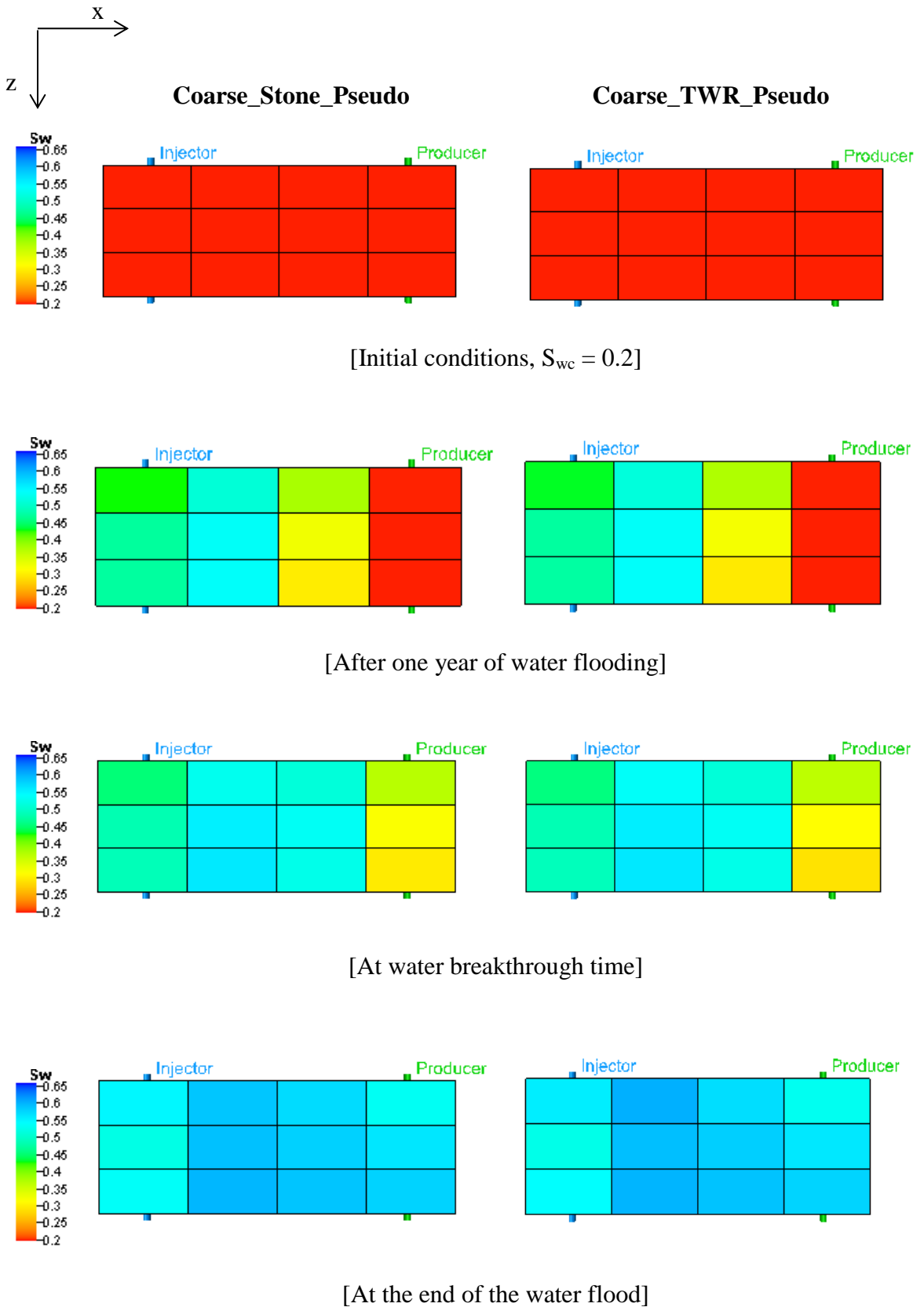


**Figure 4-13:** Comparison between water saturation profiles of coarse model with Stone (1991) pseudo functions and coarse model with TWR pseudos at the initial conditions, after 1 year of water flooding, at the water breakthrough time and at the end of the water flood.

In Figure 4-15, the case with TWR pseudos provides very close values of injector bottom hole pressures to those of the cases with Stone pseudos and the fine model. This is because the TWR method uses transmissibility weighting to upscale the relative permeability curves, which (as discussed in the previous section) should maintain the pressure throughout the coarse model, after upscaling the absolute permeability using the proper method (flow-based upscaling method was used in this test). Also, it can be noticed in Figure 4-15 that in both coarse scale simulation cases before the water breakthrough time, there are few pressure peaks. These pressure peaks are caused by coarsening the grid with high scale-up factor and are not caused by pseudoization. Similar pressure peaks were also present in the case with rock curves only, see Figure 4-8. Since the coarse models consist of 2 coarse blocks between the injector and the producer, the pressure wave propagates across coarse cells forming three peaks before the water breakthrough into the producer.

In conclusion, pseudo functions generated by the TWR method gave similar results to those generated by the Stone's (1991) method for this case study. Although the TWR method generated pseudos that captured successfully the pressure in the fine model, the water flow rate was not reproduced by the coarse model because of using rock curves for the producer cells. This means that pseudo functions generated by the TWR method should be combined with well pseudos in this case study.

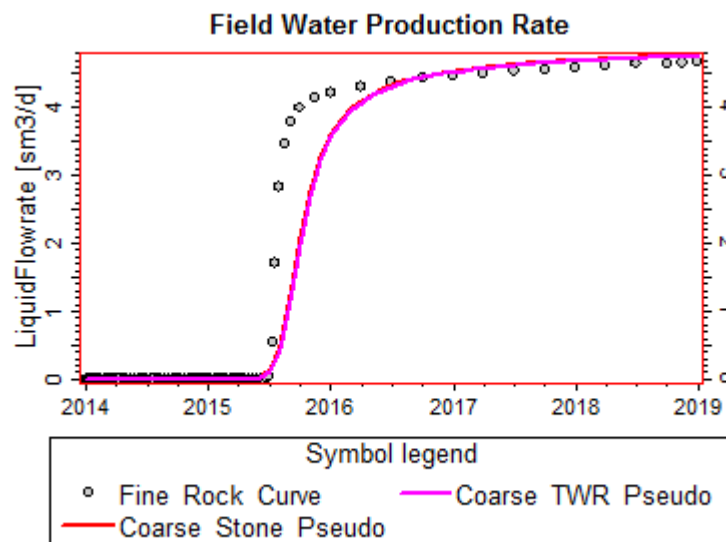


**Figure 4-14:** Comparison between the fine model (with rock curves), coarse model (with Stone's (1991) pseudos) and coarse model (with TWR pseudo) in terms of Field water production rate.

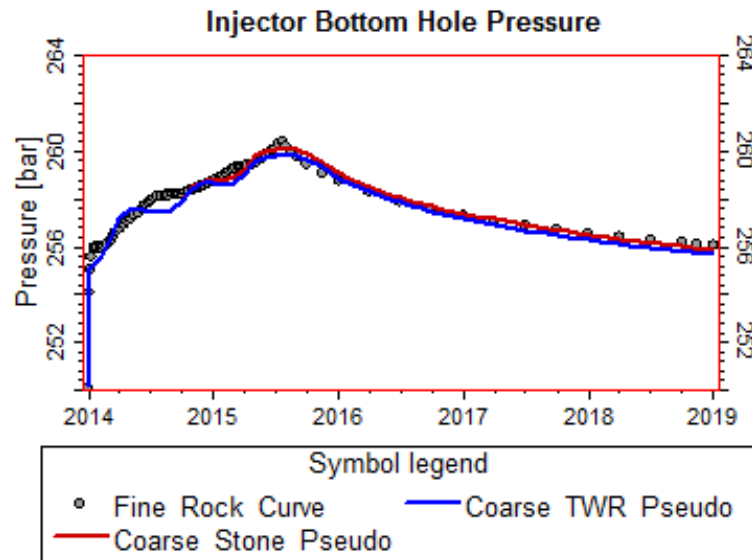


**Figure 4-15:** Comparison between the fine model (with rock curves), coarse model (with Stone’s (1991) pseudos) and coarse model (with TWR pseudo) in terms of injector bottom hole pressure.

#### 4.2.5. Coarse water flood simulation using the TWR and the well pseudos

In this test, the TWR pseudos are combined with the well pseudos, generated by the method described in Chapter 3. The proposed well pseudos should adjust well results by assigning one well pseudo for each coarse cell where the well is placed. This should ensure better compensation for sub-grid heterogeneity than when using only one pseudo per well. The well pseudos, see Figure 4-16, were assigned to both the producer and the injector coarse connections, while the TWR pseudos were assigned to the rest of the model except the edge cells, which were still assigned rock curves. Coarse scale simulation using the TWR pseudos and the well pseudos was run. The simulation cases included in this study are:

**Fine\_Rock\_Curve:** refers to the fine model with rock curves.

**Coarse\_TWR\_Pseudo:** refers to the coarse model with TWR pseudos only.

**Coarse\_TWR\_WP:** refers to the coarse model with the TWR pseudos in addition to the well pseudos.

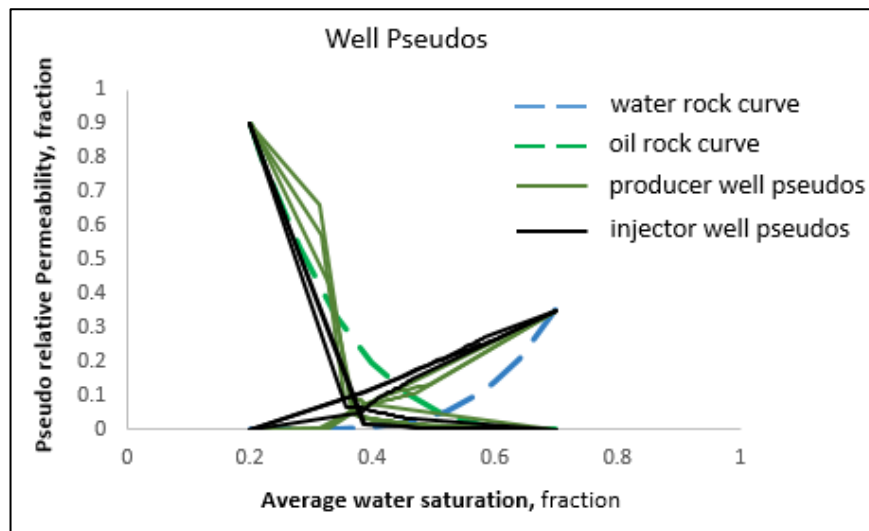


**Figure 4-16:** Well pseudos assigned to the producer and injector well blocks

In Figure 4-16, the well pseudos assigned to the coarse well connections are shown. The injector's water pseudos were shifted to the left of the water rock curve in order to make water flow faster. On the contrary, the injector's oil pseudos were shifted to the left of the oil rock curve in order to make the oil flow slower. Also, the flow of water at the producer was captured by shifting the water pseudo to the left of the water rock curve so that more water can be produced.

In Figure 4-17, water saturation profiles of the Coarse\_TWR\_WP and Coarse\_TWR\_Pseudo cases are illustrated. As expected, the water saturation profiles before the water reaches the producer's blocks are very similar in both simulation cases. However, at the end of the water flood, the water saturation in the producer blocks is less in the Coarse\_TWR\_WP case than that in the Coarse\_TWR\_Pseudo case. This indicates that more water was produced by the producer in the Coarse\_TWR\_WP case, which was enabled by the use of well pseudos. This was also confirmed in Figure 4-18, where it is obvious that the well pseudos have adjusted the results of the producer and provided very close results to those of the fine model in terms of water production rate. This in turn was reflected on providing very close value of cumulative oil production to that obtained by the fine model as shown in Figure 4-19. Also the Figure 4-20 shows that the injector bottom hole pressure was well captured by the TWR pseudos.

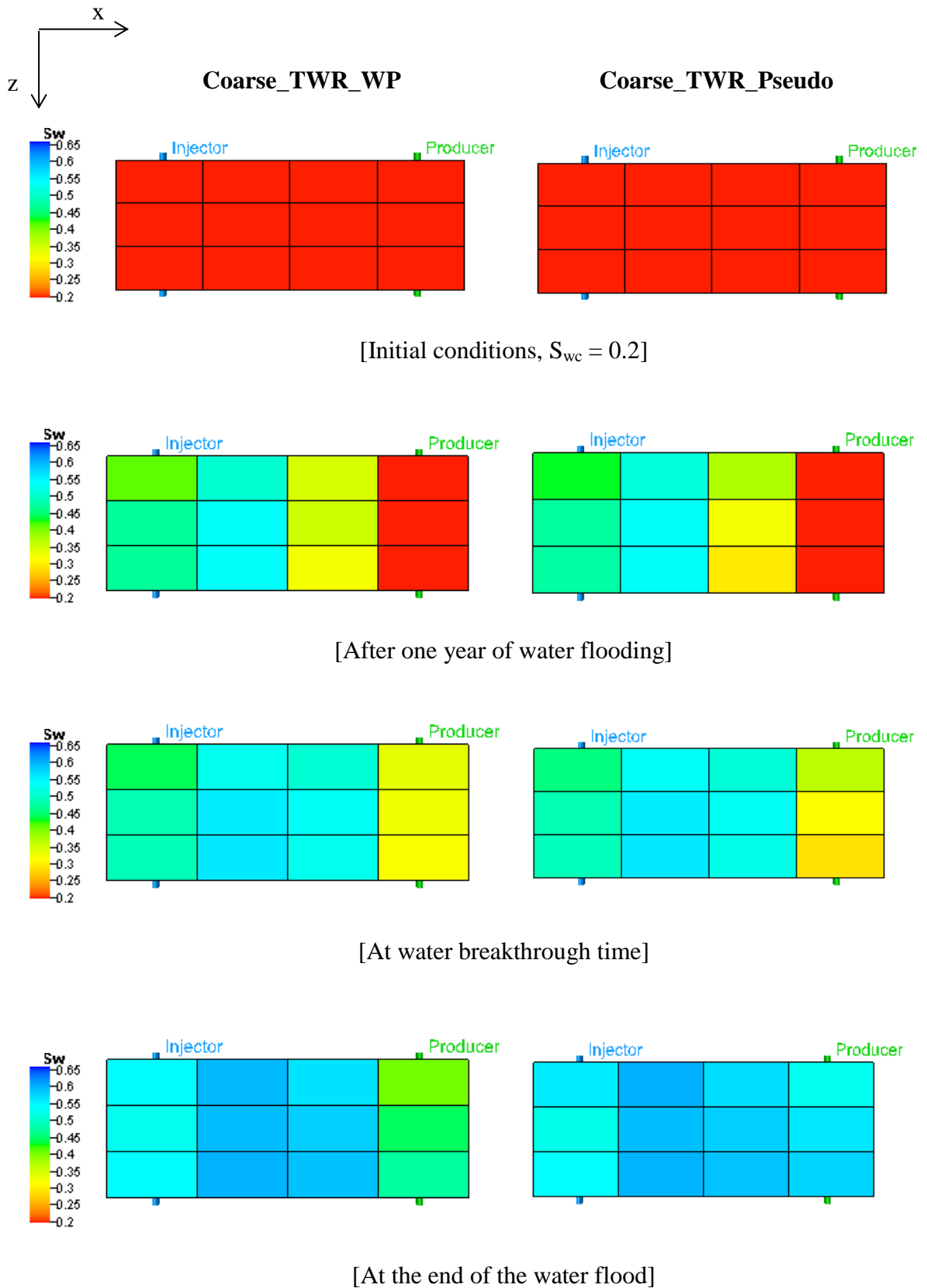


**Figure 4-17:** Comparison between water saturation profiles of coarse model with TWR pseudos and coarse model with both TWR pseudos and well pseudos at the initial conditions, after 1 year of water flooding, at the water breakthrough time and at the end of the water flood.

The results of applying the TWR pseudos and the well pseudos in this case study can be summarized as follows:

1. Pressure throughout the model was maintained by first upscaling the absolute permeability using a flow-based method with no flow boundaries, and then by using the pseudo functions generated by the TWR method (described in Chapter 3).
2. As a result of controlling the water frontal advance across the model by the TWR pseudos, water breakthrough time was well captured. However, in this test model, the rock curves were also able to provide very close water breakthrough time to that of the fine model. Therefore, examining the TWR pseudos for a case with high physical dispersion (e.g. with thief zone) will be considered in the following section.
3. The well pseudos, generated by well connection factor weighting (as described in Chapter 3) enabled adjusting well results so that production rate of the producer in both fine and coarse models were very similar. However, the well's position was the same in both the fine and coarse models (i.e. in the centre of the cell), so that the effect of using the well pseudos on adjusting the well positions in the coarse grid was not tested here.

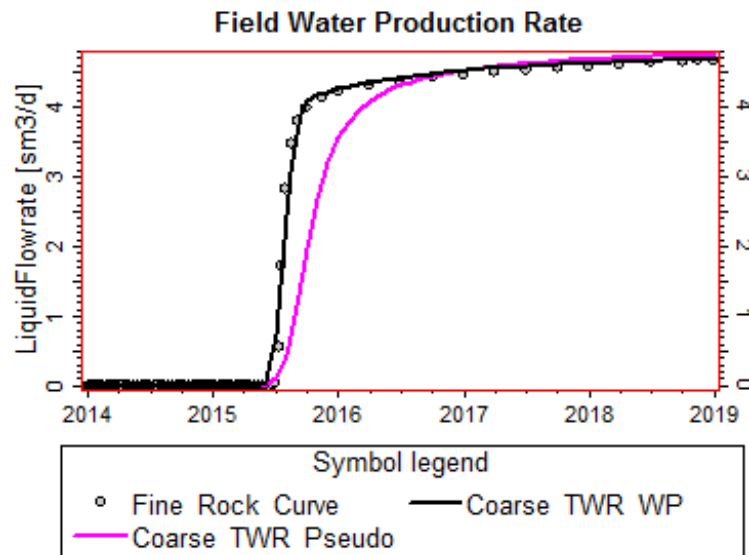


**Figure 4-18:** Comparison between fine model (with rock curves), coarse model (with TWR pseudos) and coarse model (with TWR pseudos + well pseudos) in terms of field water production rate.

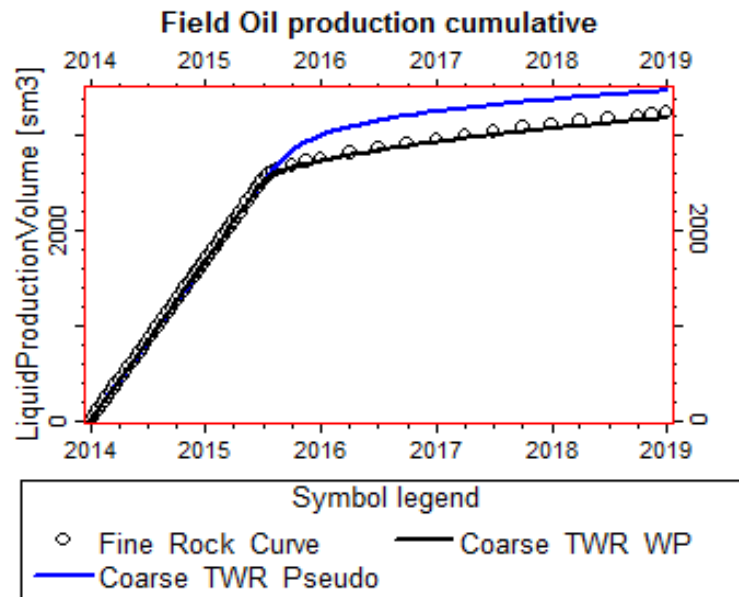


**Figure 4-19:** Comparison between fine model (with rock curves), coarse model (with TWR pseudos) and coarse model (TWR pseudos + well pseudos) in terms of field oil production cumulative.

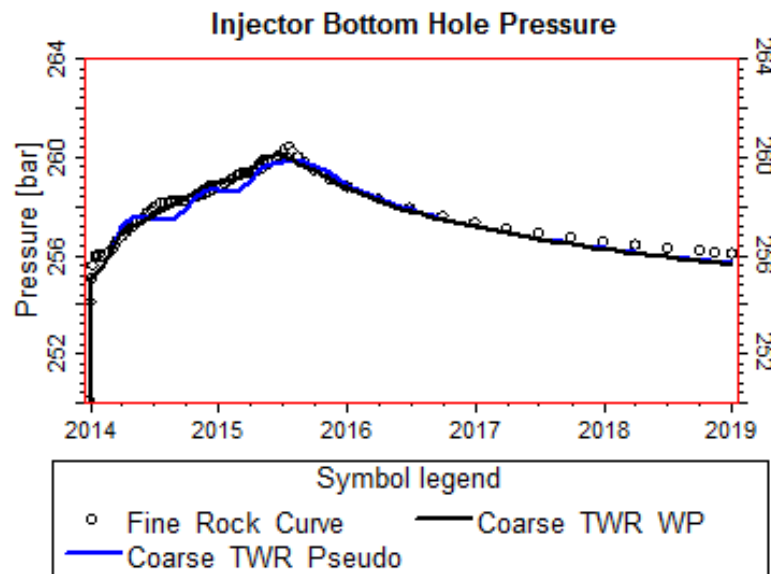


**Figure 4-20:** Comparison between fine model (with rock curve), coarse model (with TWR pseudos) and coarse model (with TWR pseudos + well pseudos) in terms of injector bottom hole pressure.

In conclusion, the pseudo functions generated by the TWR method and the well pseudos provided very close results to the fine model for this case study. Further examinations of the pseudos were carried out and described in the following sections



### 4.3. Additional testing of the TWR method and the well pseudos using 2D model

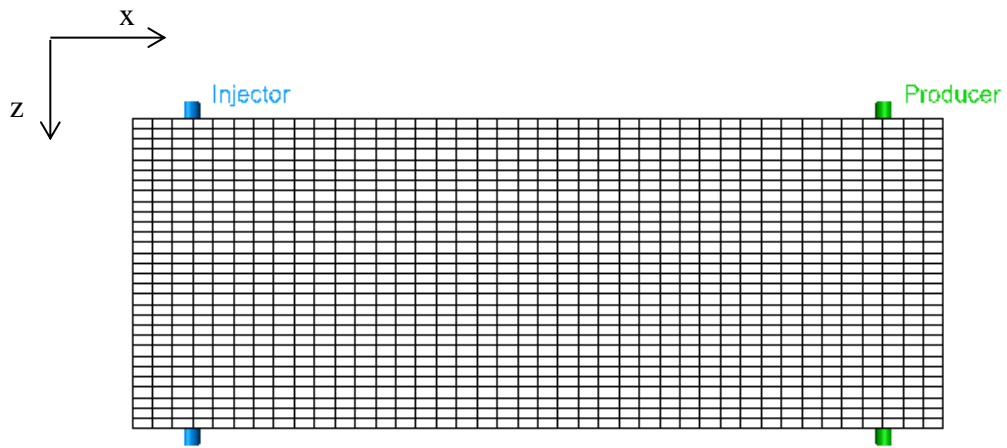
In this section, testing of the TWR method and the well pseudos using a 2D cross-sectional model (described below) is carried out by considering the following case studies:

1. Upward permeability coarsening. In this case, viscous forces dominate the flow and force water to flow faster in the upper layers of the model (i.e. the layers with higher permeability).
2. Upward permeability fining. In this case, the viscous forces make the water flow faster in the lower layers with high permeability. This enforces a water slumping effect similar to that occurring due to gravity forces.
3. Thief zone with permeability of 10D in the middle of the model. The objective of this test is to check the performance of the proposed pseudos in cases of high physical dispersion.

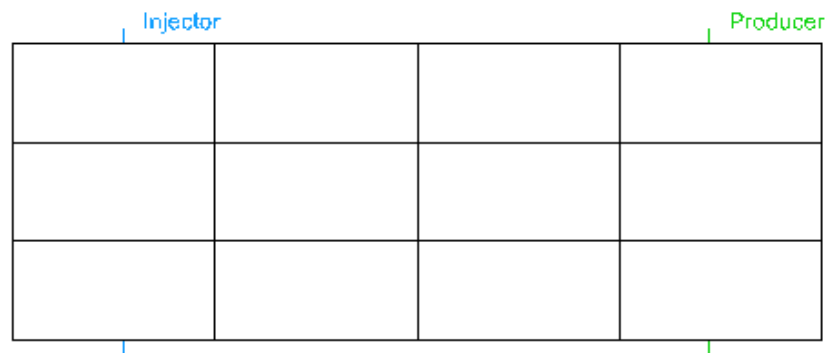
In all cases mentioned above, 2D cross-sectional synthetic fine and coarse models, see Figure 4-21, were used to run simulations of a water flood problem. The fine model (40x1x30) was assigned permeability values according to the tested case, see Table 4-4. The coarse model (4x1x3) was used to run coarse scale simulations of the cases with permeability coarsening and fining upwards, while the coarse model (8x1x6) was used to run coarse scale simulation of the case with thief zone in the middle. Model dimensions in addition to reservoir and rock properties are illustrated in Tables 4-5, 4-6 and 4-7.

In all fine and coarse models, two wells (producer and injector) were placed in the opposite sides of the reservoir and were completed throughout the thickness of the model.

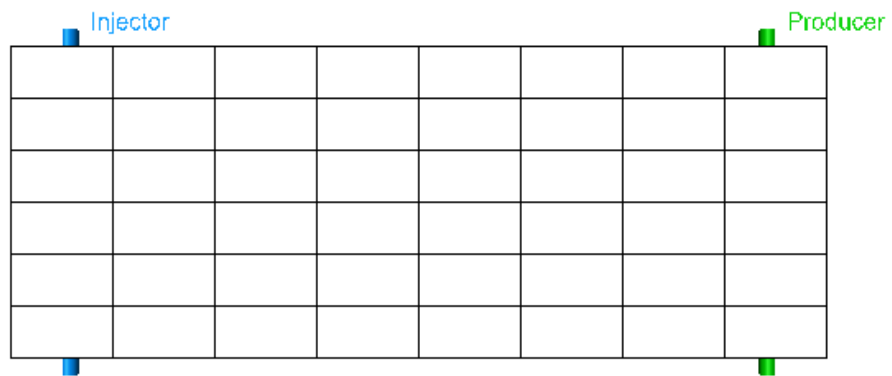
The development strategy of the reservoir was based on controlling the producer by bottom-hole pressure of 250 bar, while the injector was controlled by water surface rate of 5 m<sup>3</sup>/day. The simulation was run for 5 years.



[Fine scale model, 40x30]



[Coarse scale model (4x1x3), used for the cases with permeability coarsening and fining upwards]



[Coarse scale model (8x1x6), used for the case with thief zone in the middle]

**Figure 4-21:** Fine and coarse 2D cross sectional synthetic models

Layer no.	Thief Zone		K [upward coarsening]		K [upward fining]	
	K <sub>x</sub> (mD)	K <sub>z</sub> = 0.1K <sub>x</sub> (mD)	K <sub>x</sub> (mD)	K <sub>z</sub> = 0.1K <sub>x</sub> (mD)	K <sub>x</sub> (mD)	K <sub>z</sub> = 0.1K <sub>x</sub> (mD)
1	200	20	3500	350	50	5
2	200	20	3500	350	50	5
3	200	20	3500	350	50	5
4	200	20	2500	250	200	20
5	200	20	2500	250	200	20
6	200	20	2500	250	200	20
7	200	20	2000	200	400	40
8	200	20	2000	200	400	40
9	200	20	2000	200	400	40
10	200	20	1500	150	600	60
11	200	20	1500	150	600	60
12	200	20	1500	150	600	60
13	200	20	1000	100	800	80
14	200	20	1000	100	800	80
15	10000	1000	1000	100	800	80
16	10000	1000	800	80	1000	100
17	200	20	800	80	1000	100
18	200	20	800	80	1000	100
19	200	20	600	60	1500	150
20	200	20	600	60	1500	150
21	200	20	600	60	1500	150
22	200	20	400	40	2000	200
23	200	20	400	40	2000	200
24	200	20	400	40	2000	200
25	200	20	200	20	2500	250
26	200	20	200	20	2500	250
27	200	20	200	20	2500	250
28	200	20	50	5	3500	350
29	200	20	50	5	3500	350
30	200	20	50	5	3500	350

**Table 4-4:** Permeability distributions for the cases with thief zone in the middle, permeability coarsening upwards, and permeability fining upwards.

Test models	Reservoir dimensions	Cell dimensions	Model dimensions	No. of cells
Fine model	200m x 15m x 15m	5m x 15m x 0.5m	40x1x30	1200 cells
Coarse model	200m x 15m x 15m	50m x 15m x 5m	4x1x3	12 cells
Coarse model	200m x 15m x 15m	25m x 15m x 2.5m	8x1x6	48 cells

**Table 4-5:** Test models used for additional testing of the TWR pseudos & well pseudos.

Phases	Oil viscosity	Water viscosity	$P_b$ pressure	Initial reservoir pressure	Reservoir temperature
Oil + water	2.12 cp	0.384 cp	80 bar	250 bar @ 1000 TVDSS	80°C

**Table 4-6:** Fluid properties and initial conditions used in the fine and coarse models.

Porosity	End Point Saturations	$K_r$ @ residual saturation	Oil-water contact
23% (assumed constant throughout the model)	$S_{or} = 30\%$ and $S_{wi} = 20\%$	$K_{rw} @ S_{or} = 0.35$ and $K_{ro} @ S_{wi} = 0.9$	2500 TVDSS. (Reservoir top @ 1000 TVDSS)

**Table 4-7:** Reservoir properties used in the fine scale model.

### 4.3.1 Upward permeability coarsening

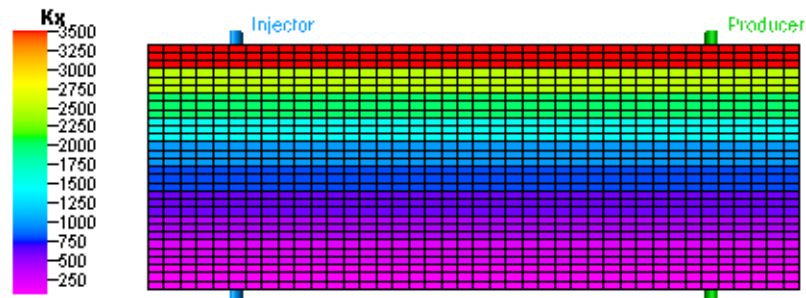
In this simulation study, the permeability is coarsened upwards, starting from 50 mD at the bottom of the model to 3500 mD at the top of the model, see Figure 4-22 for permeability distributions in the fine and coarse models. The simulation cases performed in this study are:

**Fine\_Rock\_Curve\_Kcup:** refers to the fine model with rock curves, the letters Kcup denotes permeability coarsening upwards.

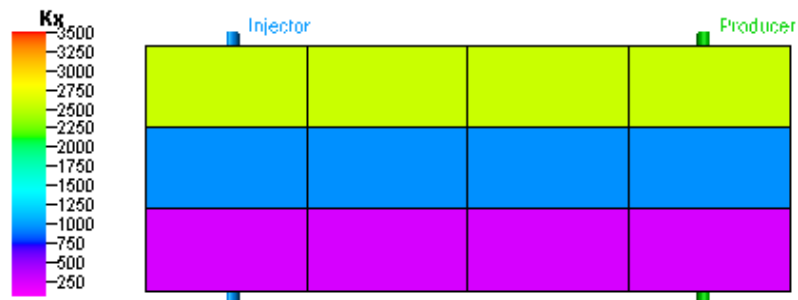
**Coarse\_Rock\_Curve\_Kcup:** refers to the coarse model with rock curves. Permeability was upscaled using flow based method with no-flow boundary conditions.

**Coarse\_TWR\_WP\_Kcup:** refers to the coarse model with TWR pseudos and well pseudos for the producer. Again, permeability was upscaled using flow based method with no-flow boundary conditions.

Results of all simulation cases mentioned above are illustrated in Figures 4-23, 4-24 and 4-25.



[Fine model with permeability coarsening upwards (50 – 3500 mD)]



[Coarse model with permeability upscaled using flow based method with no-flow boundary conditions. Effective permeability range (255 - 2550mD)]

**Figure 4-22:** Permeability distributions (in the x direction) in fine and coarse models with permeability coarsening upwards.

The Figure 4-23 illustrates comparison between water saturation profiles in all simulation cases after one year of the water flood. It is obvious that the water flows faster in the top layers of the fine model. This is due to the viscous forces that make the water flow faster in the layers with higher permeability.

In Figure 4-24, a comparison between the coarse and fine models in terms of field water production rate is shown. The case with pseudo functions and well pseudos (i.e. Coarse\_TWR\_WP\_Kcup) gave very close match to the fine model results, while the case with rock curves (i.e. Coarse\_Rock\_Curve\_Kcup) did not reproduce the fine model results. This is especially because no well pseudos have been used to adjust the producer results.

In Figure 4-25 the case with TWR pseudos matched the injector bottom hole pressure in the fine model, while the case with rock curves failed to do so. The pressure increase in the case with rock curves indicates reduction in the range of the permeability distribution due to upscaling. The TWR pseudos compensated for this permeability reduction by using transmissibility weighting to upscale the relative permeability curves so that the pressure was matched.

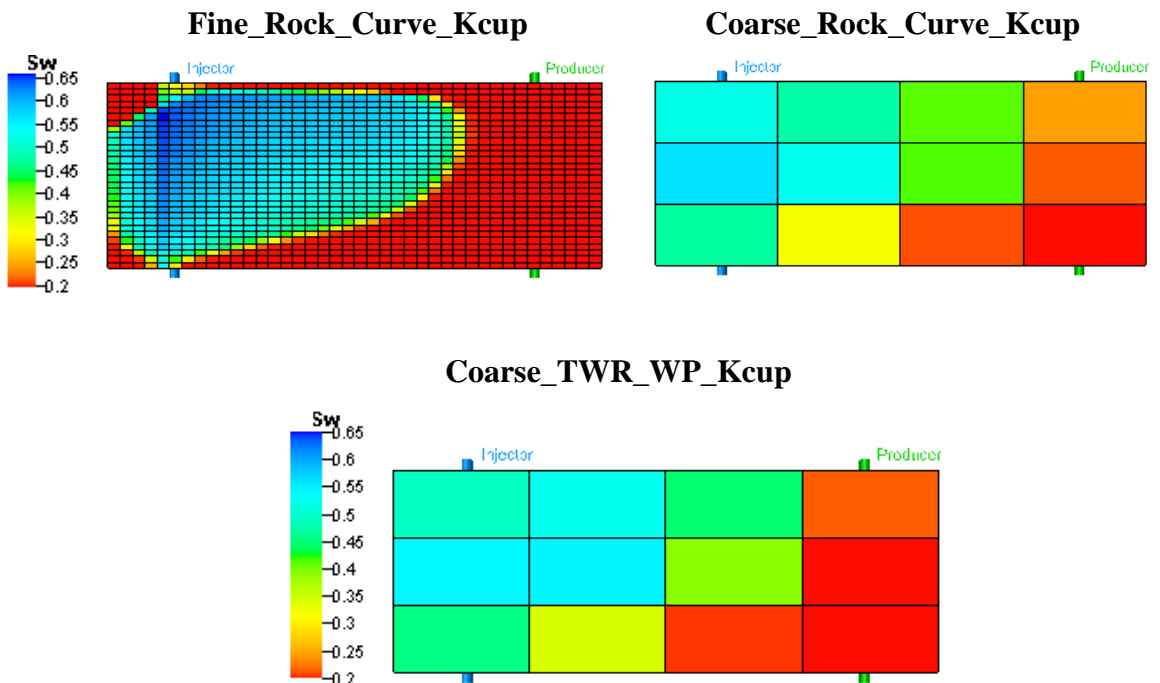


**Figure 4-23:** Comparison between water saturation profiles of fine model (with rock curves), coarse model (with rock curves) and coarse model (with TWR pseudos in the x direction + well pseudos) after 1 year of water flooding.

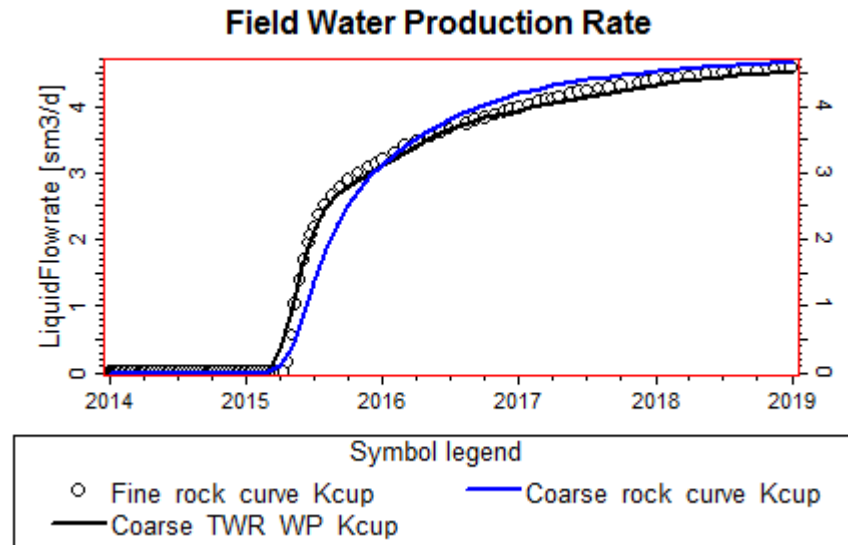


**Figure 4-24:** Comparison between the fine model (with rock curves), coarse model (with rock curves) and the coarse model (with TWR pseudos in the x direction + well pseudos) in terms of field water production rate.

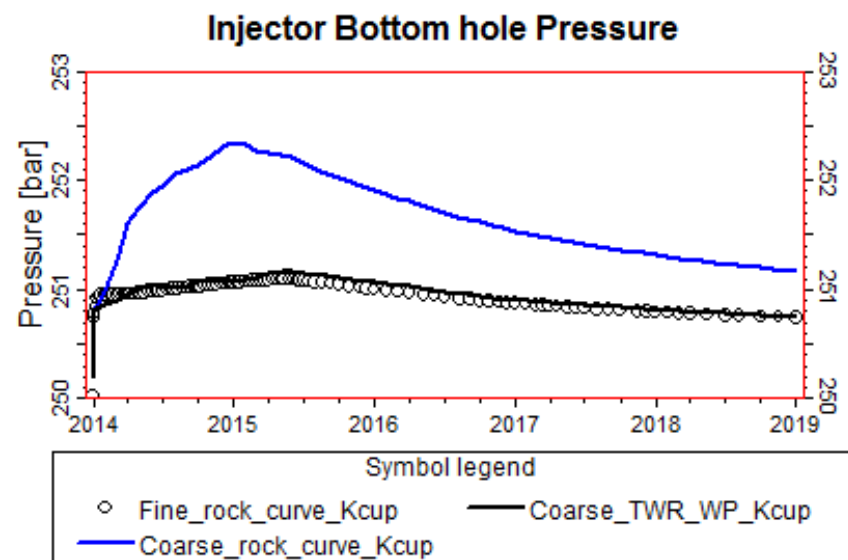


**Figure 4-25:** Comparison between the fine model (with rock curves), coarse model (with rock curves) and coarse model (with TWR pseudos in the x direction + well pseudos) in terms of injector bottom hole pressure.

### 4.3.2 Upwards permeability fining

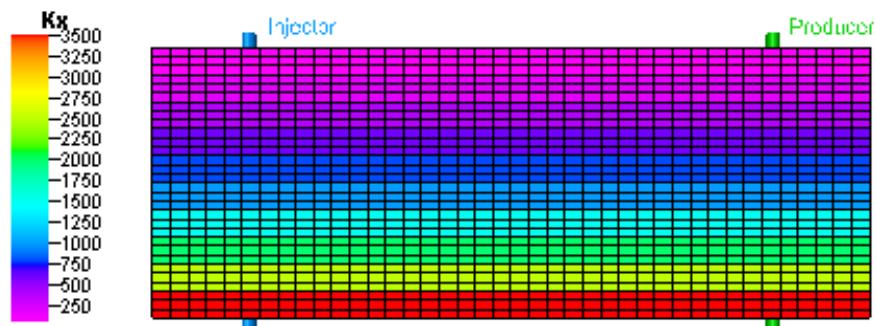
In this simulation study, the permeability is fining upwards, starting from 3500mD at the bottom of the model to 50 mD at the top of the model, see Figure 4-26 for permeability distributions in the fine and coarse models. The simulation cases performed in this study are:

**Fine\_Rock\_Curve\_Kfup:** refers to the fine model with rock curves, the letters Kfup denotes permeability fining upwards.

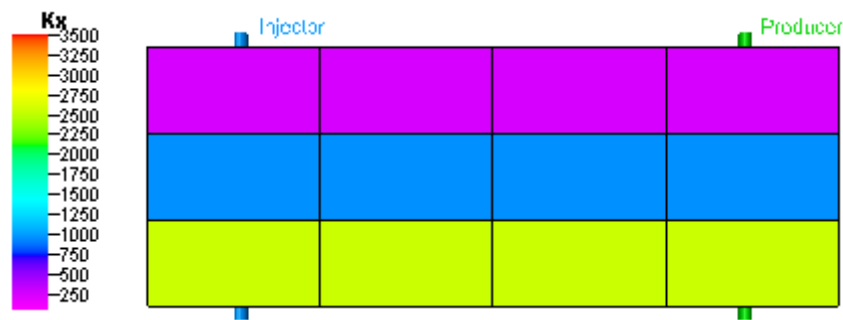
**Coarse\_Rock\_Curve\_Kfup:** refers to coarse model with rock curves. Permeability was upscaled using flow based method with no-flow boundary conditions.

**Coarse\_TWR\_WP\_Kfup:** refers to coarse model with TWR pseudos as well as well pseudos.

Results of all simulation cases mentioned above are illustrated in Figures 4-27, 4-28 and 4-29.



[Fine model with upward permeability fining, (3500 - 50 mD)]



[Coarse model with permeability upscaled using flow based method with no-flow boundary conditions. Permeability range (255 - 2550mD)]

**Figure 4-26:** Permeability distributions (in the x direction) in the fine and coarse models used to simulate the case with permeability fining upwards.



In Figure 4-27 a comparison between saturation profiles in all simulation cases after one year of the water flood is illustrated. Opposite to the case with permeability coarsening upwards, it can be noticed that the water flows faster in the bottom layers of the model with permeability fining upwards, due to the viscous forces. In this case a water slumping effect (caused by gravity forces) is artificially enforced by the viscous forces.

In Figure 4-28, it can be noticed that the water breakthrough in the case with rock curves (i.e. Coarse\_Rock\_Curve\_Kfup) occurred later than that in the case with TWR pseudos (i.e. Coarse\_TWR\_WP\_Kfup). This is because of reduction in the range of the permeability distribution due to upscaling, which caused delay to the water shock front. This shows that using rock curves alone did not compensate for these effects, while using the TWR pseudos in addition to the well pseudos helped in reproducing the fine model water production rate and water breakthrough time.

In Figure 4-29, the case with rock curves failed to match the injector bottom hole pressure while the case with TWR pseudos provided good match to the fine model results.

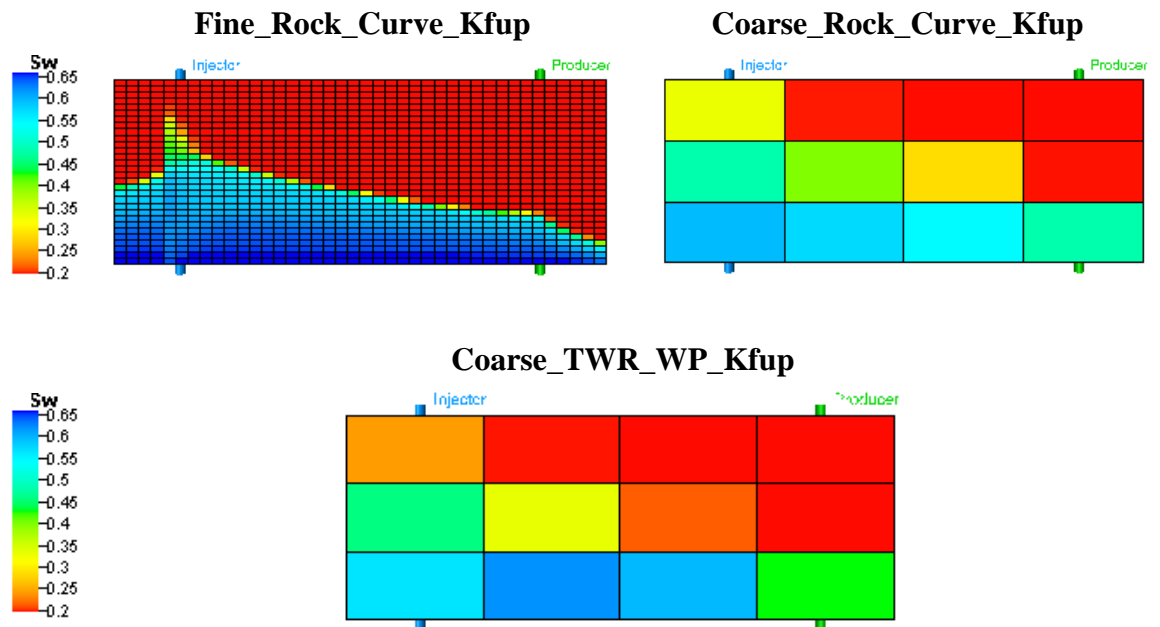


**Figure 4-27:** Comparison between water saturation profiles of fine model (with rock curves), coarse model (with rock curves) and coarse model (with TWR pseudos in the x direction) after 1 year of water flooding.

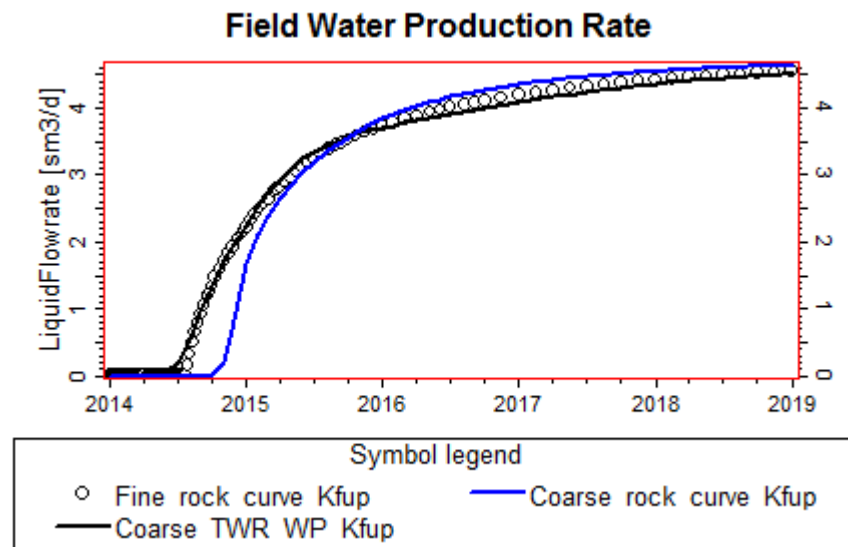


**Figure 4-28:** Comparison between fine model (with rock curves), coarse model (with rock curves) and coarse model (with TWR pseudos in the x direction + well pseudos) in terms of field water production rate.

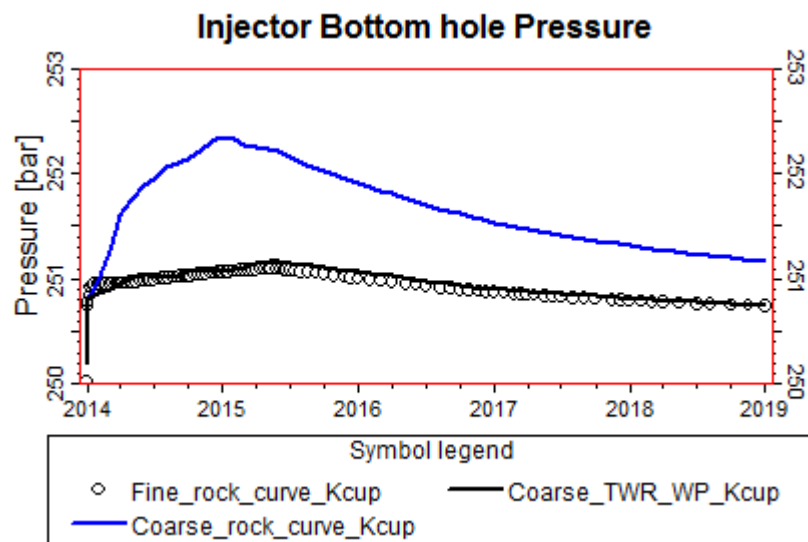


**Figure 4-29:** Comparison between the fine model (with rock curves), coarse model (with rock curves) and coarse model (with TWR pseudos in the x direction + well pseudos) in terms of injector bottom hole pressure.

### 4.3.3 Thief zone in the middle of the model

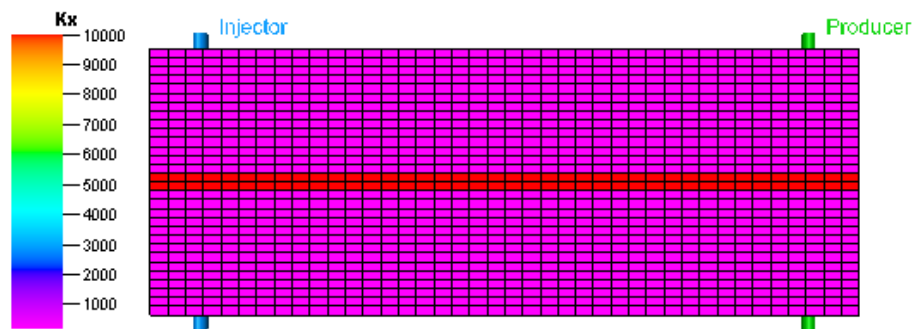
In this experiment, constant permeability of 200 mD was associated to all cells in the fine model except two rows of cells in the middle (Layers 15 and 16), see Figure 4-30, which were set permeability of 10D, in order to represent a thief zone. The simulation cases performed in this case study are:

**Fine\_Rock\_Curve\_TZ:** refers to fine model with rock curves. The letters TZ denote Thief Zone.

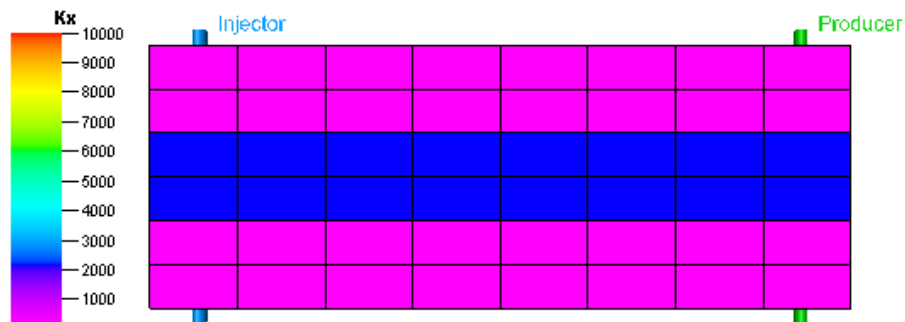
**Coarse\_Rock\_Curve\_TZ:** refers to coarse model with rock curves. Permeability was upscaled in this simulation case and all the cases below using flow based method with no-flow boundary conditions.

**Coarse\_TWR\_WP\_TZ:** refers to coarse model with TWR pseudos in the x direction, in addition to well pseudos for the producer and the injector.

**Coarse\_TWRxz\_WP\_TZ:** same as the Coarse\_TWR\_WP\_TZ case but with additional pseudos in the positive z direction (i.e. directional pseudos were applied).



[Fine model with thief zone,  $K_{\text{thief zone}} = 10D$ ]



[Coarse model with thief zone,  $K_{\text{thief zone}} = 2160\text{mD}$  (flow-based upscaling)]

**Figure 4-30:** Permeability distributions (in the x direction) of fine and coarse models with thief zone in the middle. Permeability was upscaled using flow based method with no flow boundary conditions.

The TWR pseudo functions generated in the x direction for the case Coarse\_TWR\_WP\_TZ is illustrated in Figures 4-31. Three groups of water pseudo functions can be easily identified. The first and second groups belong to the thief zone top and bottom layers, and they are shifted to the left of the water rock curve in order to force the water to flow faster, and in turn to compensate for the large reduction in the thief zone permeability due to coarsening. The third group is similar to the rock curve and belong to the rest of the model.

In the Coarse\_Rock\_Curve\_TZ case, rock curves were assigned to all cells in the model, while in the Coarse\_TWR\_WP\_TZ case, TWR pseudo functions were assigned to all cells except the cells at the edge of the model (i.e. the producer's cells), where the rock curves were used instead. Results of all simulation cases are illustrated in Figures 4-32, 4-33 and 4-34.

Figure 4-32 illustrates a comparison between water saturation profiles in all simulation cases after one year of the water flood. It can be noticed that the frontal displacement is much faster in the middle of the model in all simulation cases. This was expected because permeability of the thief zone is very high in comparison to the rest of the model, so that the viscous forces caused the water to flow faster in the cells representing the thief zone. Therefore, it can be noticed that in all simulation cases the water breakthrough into the producer occurred at the thief zone region. However, the Coarse\_Rock\_Curve\_TZ case has got higher water saturation in the middle of the model than that in the other cases. This occurred because the water breakthrough in the Coarse\_Rock\_Curve\_TZ case was the latest between all the cases, see Figure 4-33. The delay in water breakthrough gave more time for water saturation to increase in the middle of the coarse model with rock curves.

There are two reasons behind the water breakthrough delay in the case of Coarse\_Rock\_Curve\_TZ, the first is the permeability upscaling and the second is the use of rock curves. Due to upscaling, the permeability of the thief zone was reduced from 10,000 mD to 2160 mD, see Figure 4-30. Consequently, the effect of the physical dispersion caused by the thief zone was reduced and the water shock front moved slowly. This initially happened in all coarse scale simulation cases because the same permeability upscaling method was used in all of them. The difference in the Coarse\_Rock\_Curve\_TZ case is the use of rock curves, which did not compensate for the suppression of permeability due to upscaling. Using pseudo functions enabled

compensation for the permeability reduction in the Coarse\_TWR\_WP\_TZ case and adjusted the water shock front speed, so that the water breakthrough time was well captured, see Figure 4-33.

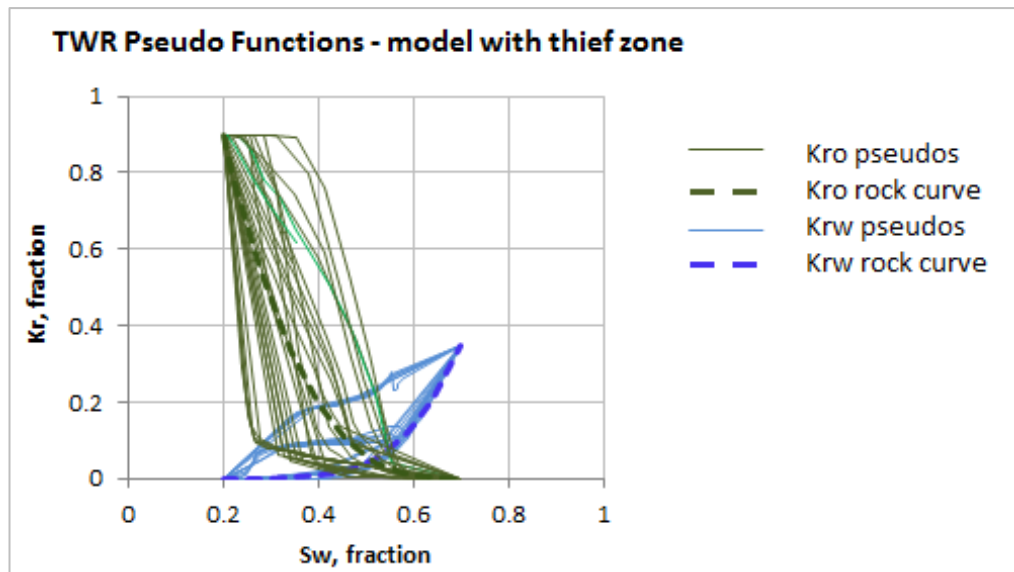


Figure 4-31: TWR pseudo functions generated for the model with thief zone

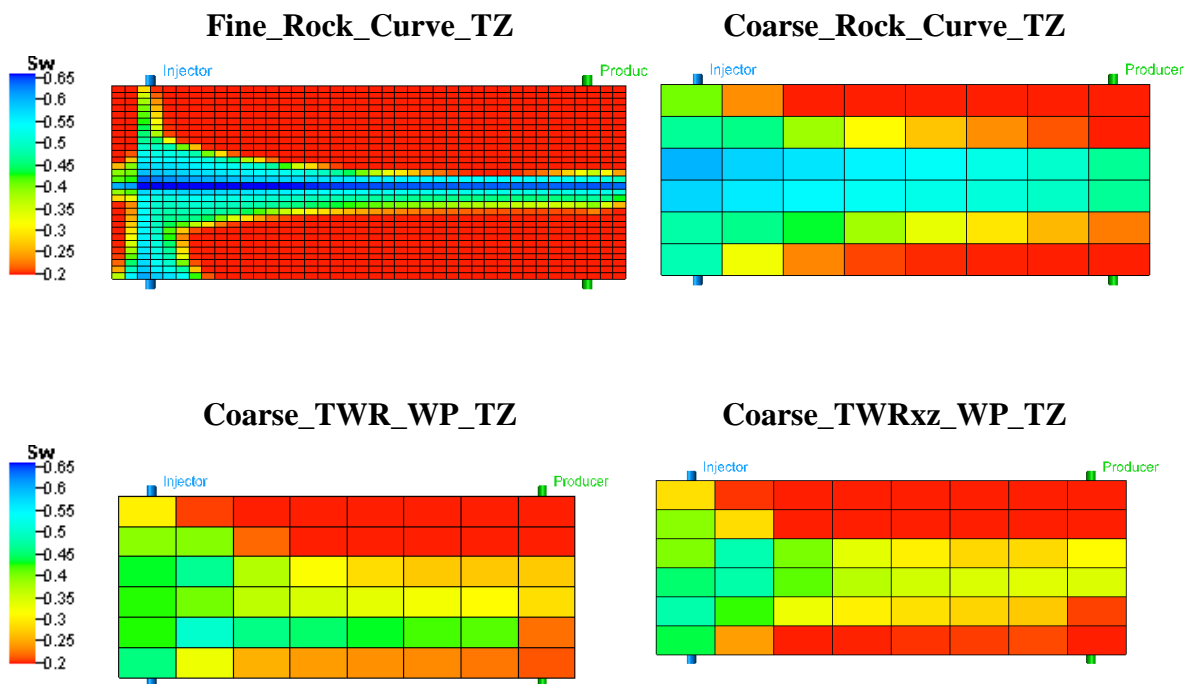
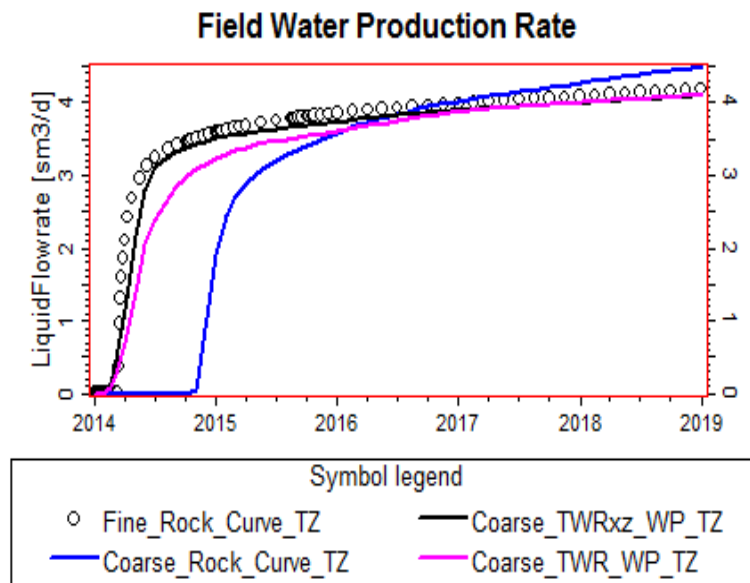


Figure 4-32: Comparison between water saturation profiles of fine model (with rock curves), coarse model (with rock curves), coarse model (with TWR pseudos in the x direction + well pseudos) and coarse model (with TWR pseudos in the x and z directions + well pseudos) after 1 year of water flooding.

Although the Coarse\_TWR\_WP\_TZ case provided a good estimate of the water breakthrough time, the water production rate was not matched, see Figure 4-33. This is because the TWR pseudos were generated only in the x direction, while the water in the fine model flowed in both the x and z directions. Flow of water in the z direction was caused by gravity forces, after being forced to flow in the x direction through the thief zone by the viscous forces, see the water saturation profile of the fine model in Figure 4-32. Since the coarse model has got cells with larger size, the water advanced faster in the z direction than that in the fine model (i.e. numerical dispersion) so that less water reached the producer's connections and in turn less water was produced. This effect was not well captured by using TWR pseudo functions in one flow direction only (i.e. the x direction). This means that pseudos in the z direction should be also used in order to control the flow in the z direction. The case with TWR pseudos was assigned pseudos in the z direction as well as pseudos in the x direction. This case is referred to as Coarse\_TWRxz\_WP\_TZ and as can be seen (the black line in Figure 4-33), it was able to match the water flow rate of the fine model.



**Figure 4-33:** Comparison between fine and coarse models (rock curve), coarse model (TWR pseudos in the x direction + well pseudos) and coarse model (TWR pseudos in the x and z directions + well pseudos) in terms of field water production rate.

In Figure 4-34, it can be noticed that the coarse model with TWR pseudo functions gives better results in terms of injector bottom hole pressure than the coarse model with rock curves only. This again shows that the TWR pseudos can capture the pressure gradient in the fine model.

In conclusion, the coarse scale simulation using the TWR pseudos in the x and z directions in addition to well pseudos succeeded in giving results very close to those of the fine model. Also, this test showed the importance of using directional pseudo functions in order to capture the flow behaviour in the different directions, and in turn to improve the results of the coarse model.

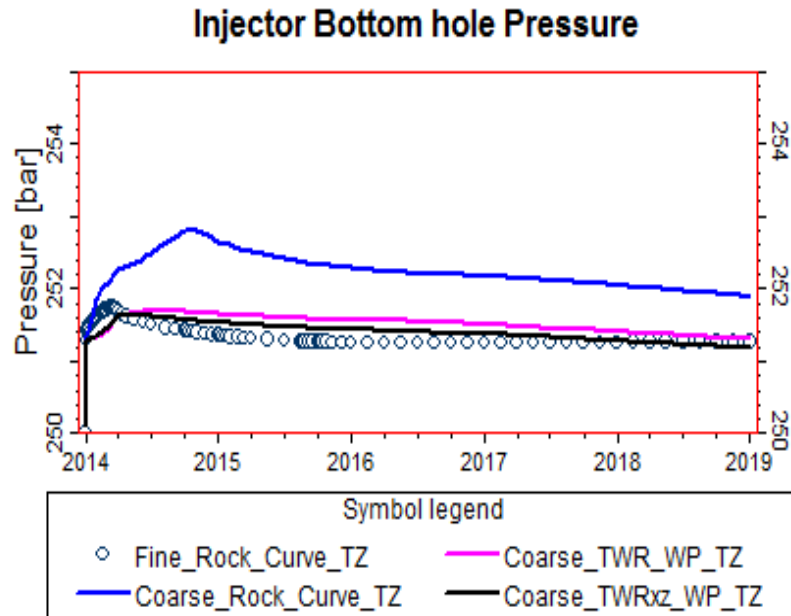


**Figure 4-34:** Comparison between fine and coarse models (rock curve), coarse model (TWR pseudos in the x direction + well pseudos) and coarse model (TWR pseudos in the x and z directions + well pseudos) in terms of injector bottom hole pressure.

**Grouping the pseudos:**

The TWR pseudos generated in both the x and z directions for the model with thief zone, were grouped using Chierici curve fitting (described in Chapter 3). The target of this pseudos grouping is to combine similar pseudos in a manageable number of groups, which would make their use feasible in practice.

First of all, the Chierici parameters (A and L for oil, and B and M for water) were determined by fitting Chierici functional models (1984) to the TWR pseudos. Afterwards, the parameter A was plotted against the parameter L, while the parameter B was plotted against the parameter M. Results are shown in Figures 4-35, 4-36, 4-37 and 4-38.

Even though water and oil relative permeabilities are interdependent, it was decided to apply grouping on both water and oil pseudos in order to check if the selected groups are consistent in both cases.

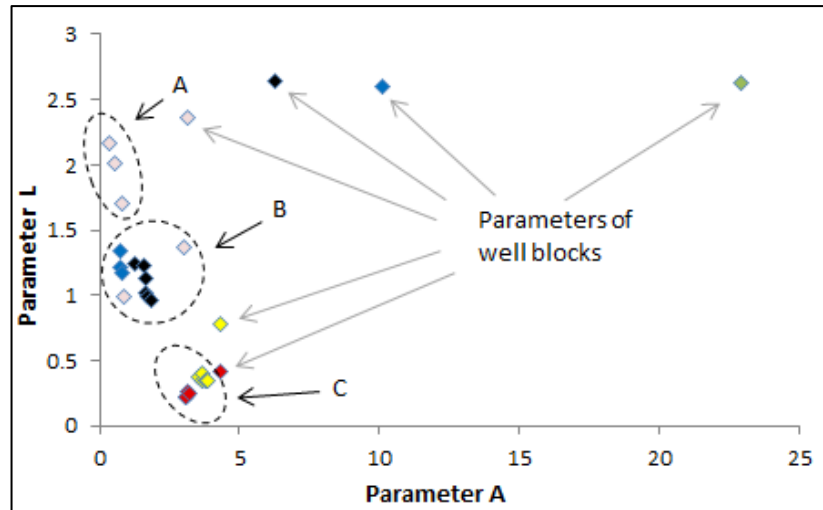


Figure 4-35: Grouping of oil pseudos in the x direction

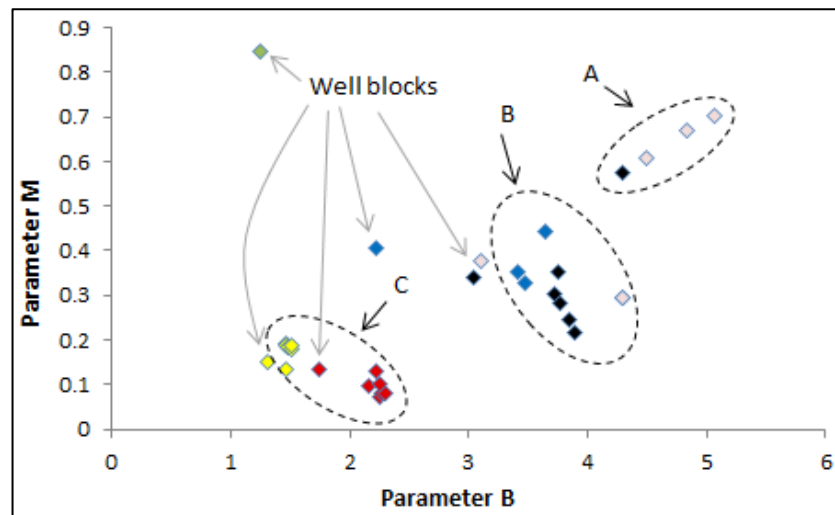
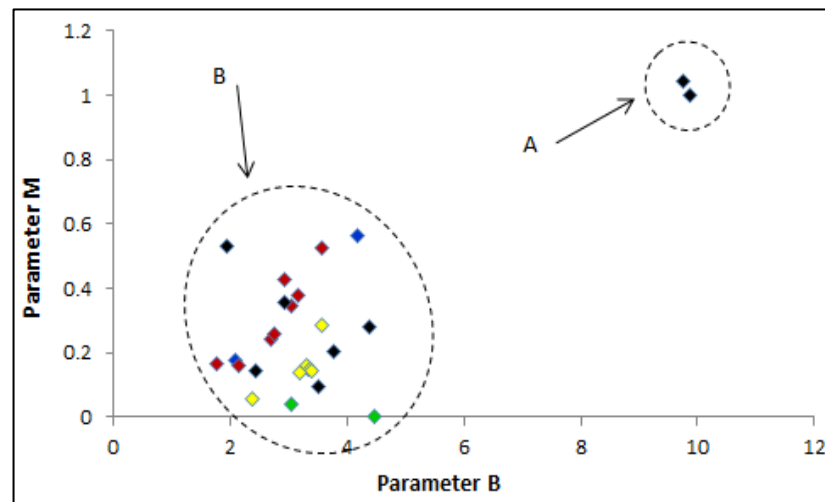
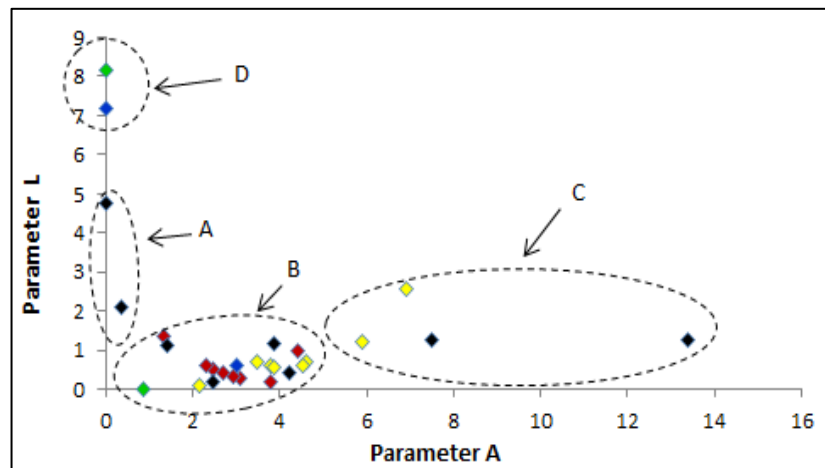


Figure 4-36: Grouping of water pseudos in the x direction





**Figure 4-37:** Grouping of water pseudos in the z direction



**Figure 4-38:** Grouping of oil pseudos in the z direction

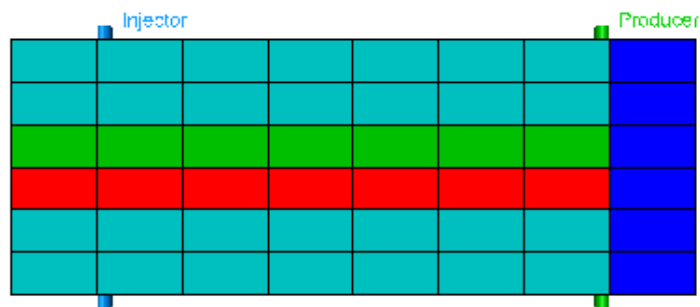
Regarding grouping of the pseudos in the x direction, it can be noticed in Figure 4-35 that three groups of oil pseudos have been formed, A, B and C. However, there are a few scattered points that were difficult to group. These points represent the parameters of the well blocks. The same thing regarding the well blocks was noticed when grouping the water pseudos in Figure 4-36. This indicates that the well blocks might be difficult to group and should be excluded, which was also suggested by Dupouy et al. (1998).

Comparing the results of plotting oil and water parameters, it was found that three groups should provide a good representation for both oil and water pseudos in the x direction.

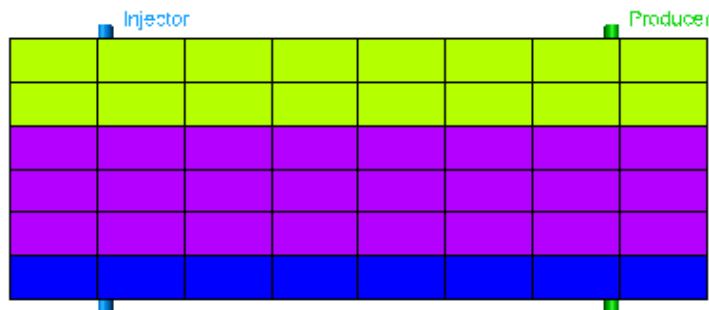
Regarding grouping of the pseudos in the z direction, Figure 4-37 shows that only two groups could be enough to represent the water pseudos in the z direction. However, in Figure 4-38, more groups have been formed. Indeed, the large group B in Figure 4-37, was split into 3 groups B, C and D in Figure 4-38. This is because some oil pseudos exhibited different behaviour than the rest of the pseudos. However, after initial testing of the grouping, only two groups were considered (i.e. based on the water parameters Figure 4-37).

To summarize the grouping procedure discussed above, it is assumed that only 3 pseudos should be enough to represent the 42 TWR pseudos in the x direction (excluding the producer blocks). Also, 2 pseudos should be used to represent the 40 TWR pseudos in the z direction. Additionally, well pseudos will be used explicitly in the coarse model, as suggested by Dupouy et al. (1998).

Figure 4-39 below shows the regions to which the grouped pseudos will be assigned in the x and z directions. Therefore, instead of assigning one pseudo to each coarse cell, one pseudo will be assigned to a region.



Pseudo regions in the +x direction. Three pseudos (green, red and turquoise)  
+ rock curve (blue)



Pseudo regions in the +z direction. Two pseudos (yellow and purple) + rock curve  
(blue).

**Figure 4-39:** TWR pseudos regions in both the x and z directions

Results of using the grouped pseudos in the coarse model are shown in Figure 4-40 and 4-41. The figures show good agreement between the case with grouped pseudos (i.e. Coarse\_TWRxz\_WP\_TZ\_Grouped) and the case without grouping of the pseudos (i.e. Coarse\_TWRxz\_WP\_TZ).

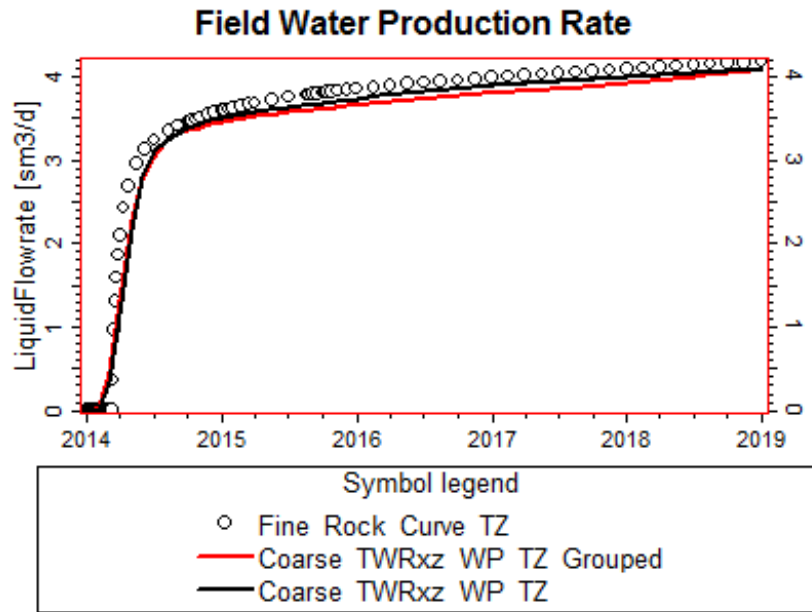


**Figure 4-40:** Comparison between results of the TWR pseudos (with and without grouping) in terms of field water production rate.

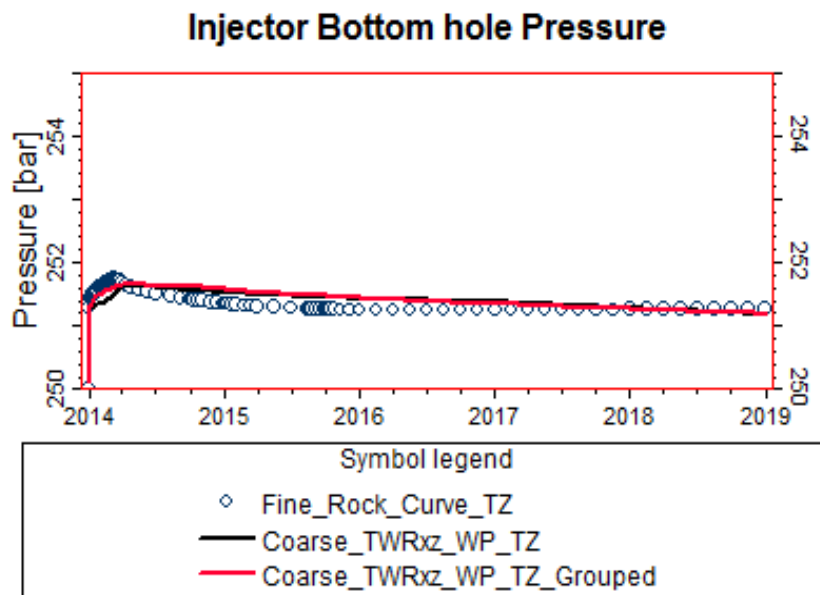


**Figure 4-41:** Comparison between results of the TWR pseudos (with and without grouping) in terms of injector bottom hole pressure.

#### 4.4. Testing of the TWR method and the well pseudos using 3D model

In this section, testing of the TWR pseudos and the well pseudos is performed using a synthetic 3D model to simulate a water flood problem. A 3D model of size 15x15x9 was built and referred to as the fine model. The fine model was then coarsened using scale up factor of 3 in all directions in order to create a coarse model of size 5x5x3, see Table 4-8.

The permeability distributions (in the x direction) in both fine and coarse models are shown in Figure 4-42. Permeability in the fine scale model was distributed throughout the model using stochastic method (Sequential Gaussian Simulation, PETREL, Schlumberger) with correlation length of 20m (i.e. smaller than the coarse cell size) and standard deviation of 0.5. The permeability range in the x and y directions is 0.1 - 2000 mD, while permeability in the z direction equalled 10% of the permeability in the x direction. Permeability in the coarse model was upscaled from that in the fine model using flow based method with no flow boundary conditions. Reservoir rock and fluid properties used in the fine model are illustrated in Tables 4-9 and 4-10, respectively.

In both fine and coarse models, five wells (four producers and one injector) were considered. The four producers were placed in the corners of the models, while the injector was placed in the middle. All wells were completed throughout the thickness of the model. The development strategy of the reservoir was based on running simulation for five years, while controlling the producers by bottom-hole pressure of 200 bar and the injector by water surface rate of 400 m<sup>3</sup>/day.

Test models	Reservoir dimensions	Cell dimensions	Model dimensions	No. of cells
Fine model	240mx240mx90m	16mx16mx9m	15x15x9	2025 cells
Coarse model	240mx240mx90m	48mx48mx30m	5x5x3	75 cells

**Table 4-8:** Test fine and coarse models

Phases	Oil viscosity	Water viscosity	$P_b$ pressure	Initial reservoir pressure	Reservoir temperature
Oil + water	2.12 cp	0.384 cp	80 bar	250 bar @ 1000 TVDSS	80°C

**Table 4-9:** Fluid properties and initial conditions used in the fine and coarse models.

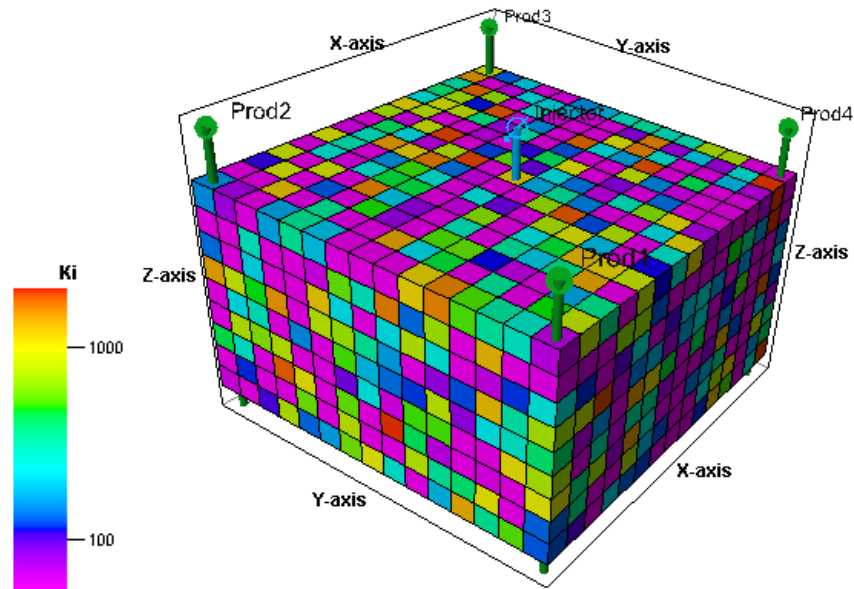
Permeability	Porosity	End Point Saturations	Kr @ residual saturation	Oil-water contact
Log-normal distribution (Sequential Gaussian Simulation). Range (0.1 – 2000mD). Mean = 200 mD. Corr.length ( $\lambda$ ) = 20m (in all directions) Std.deviation $\sigma_{\ln(k)}$ = 0.5.	23% (assumed constant throughout the model)	$S_{or} = 30\%$ and $S_{wi} = 20\%$	$K_{rw} @ S_{or} = 0.35$ and $K_{ro} @ S_{wi} = 0.9$	2500 TVDSS. (Reservoir top @ 1000TVDSS)

**Table 4-10:** Reservoir properties used in the fine scale model.

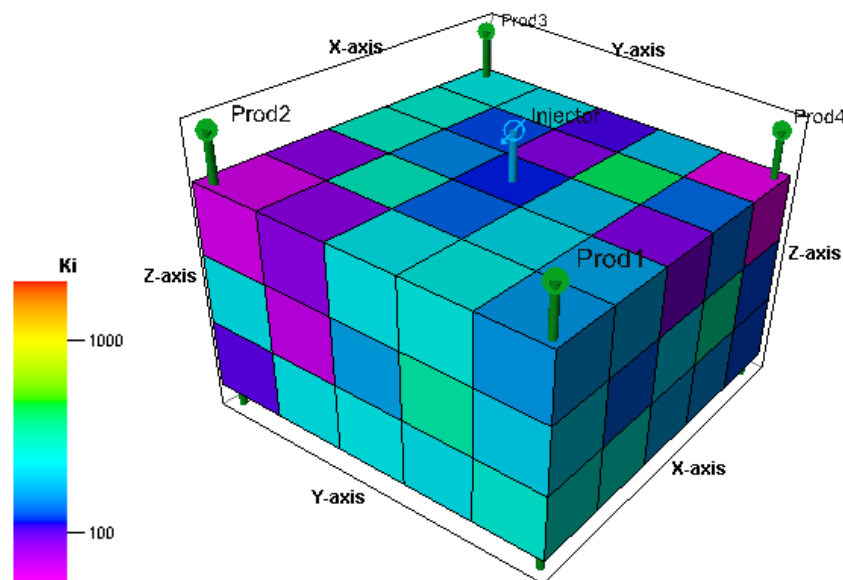
After running the fine scale simulation, TWR pseudo functions were generated in both the positive and negative x and y directions using the TWR method. Generation of directional pseudos for this 3D model is based on what has been learnt from the previous experiments about the importance of generating pseudos in different directions in order to capture the fluid flow behaviour in these directions. In this test, the injector is placed in the middle of the model, which means that the water is expected to flow in both the positive and negative x and y directions towards the producers. No pseudos were generated for the flow in the z direction because there was no significant flow in this direction.

Since the producers are placed in the centre of the connected fine scale cells, they are (after building the coarse model) considered as if they were in the centre of the coarse connection, although they are physically placed in the corner of the model. This

may cause, for example, erroneous early water breakthrough in the wells. Therefore, the well pseudos method (described in Chapter 3) were used to generate pseudo functions that should adjust wells position in the coarse grid, and in turn give better prediction of the water breakthrough time.



[Fine model 15 x 15 x 9]



[Coarse model 5 x 5 x 3]

**Figure 4-42:** Permeability distributions (in the x direction) of the fine and coarse 3D models. Permeability of the coarse model was upscaled using flow based method with no flow boundary conditions.

Three simulation cases were considered in this test:

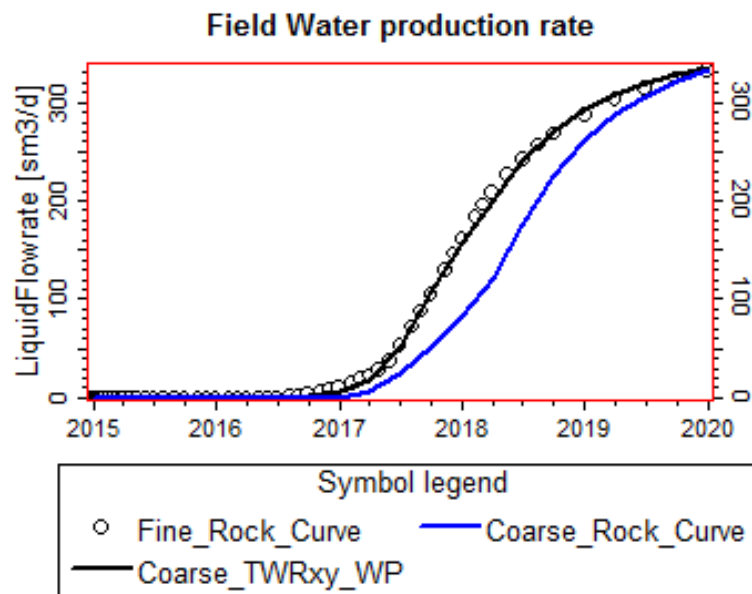
**Fine\_Rock\_Curve:** refers to the fine model with rock curves.

**Coarse\_Rock\_Curve:** refers to the coarse model with rock curves. Permeability is upscaled in this case and in all the coarse scale simulation cases below using flow based method with no-flow boundary conditions.

**Coarse\_TWRxy\_WP:** refers to coarse model with TWR pseudos in the positive and negative x and y direction. The letters PN denotes the positive and negative directions.

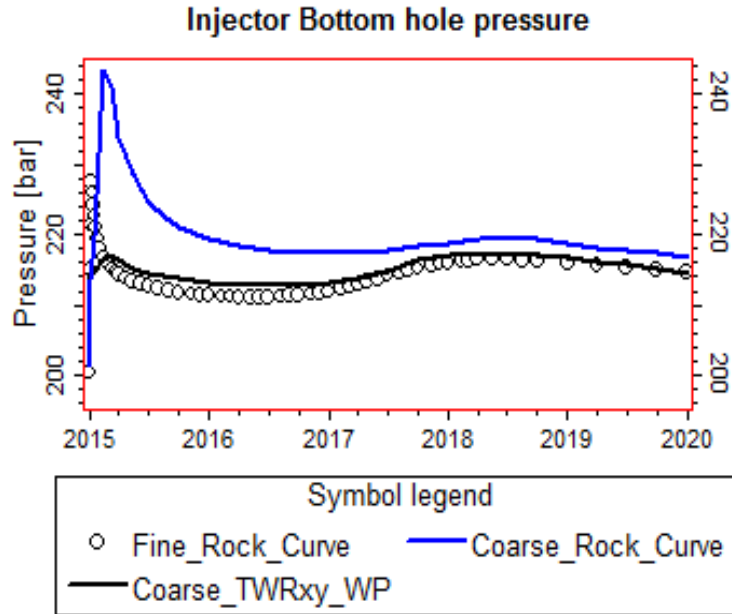
Comparisons between results of the simulation cases mentioned above are illustrated in Figures 4-43 and 4-44.

Figure 4-43 shows that the case with directional TWR pseudos and well pseudos (i.e. Coarse\_TWRxy\_WP case) succeeded in capturing the water breakthrough time as well as the water production rate. This is because the TWR pseudos have compensated for the sub-grid heterogeneity and fluid flow behaviour in all flow directions. Also, the well pseudos have adjusted the wells positions in the coarse grid. On the other hand, the rock curves, represented by the case Coarse\_Rock\_Curve, did not reproduce the fine model results.



**Figure 4-43:** comparison between results of the fine model (with rock curves), the coarse model (with rock curves) and the coarse model (with TWR pseudos in the x and y directions) in terms of field water production rate.

Figure 4-44 shows that the case with TWR pseudos maintained the bottom hole pressure at the injector.



**Figure 4-44:** comparison between results of the fine model (with rock curves), the coarse model (with rock curves) and the coarse model (with TWR pseudos in the x and y directions) in terms of injector bottom hole pressure.

When generating the TWR pseudos for this test, it was found that each coarse cell was assigned 4 pseudos (2 in each flow direction), which means that 270 sets of pseudos (135 in the positive and negative x directions plus 135 in the positive and negative y directions) were assigned to the coarse model. Grouping of the TWR pseudos was considered using the grouping method described in Chapter 3.

### **Grouping the pseudos:**

The grouping method using Chierici curve fitting was applied to the TWR oil and water pseudo functions. Results of plotting the Chierici parameters (i.e. A, L, B and M), which were determined by nonlinear regression on the TWR pseudos are shown in Figures 4-45 and 4-46.

Regarding grouping of the pseudos in the x direction, it can be noticed in Figure 4-45 that two groups of water pseudos (referred to as A and B) have been formed in both the positive and negative directions. However, oil pseudos show that it is possible to split the group B into two groups, B and C. The same observation applies for grouping the pseudos in the y direction, see Figure 4-46.



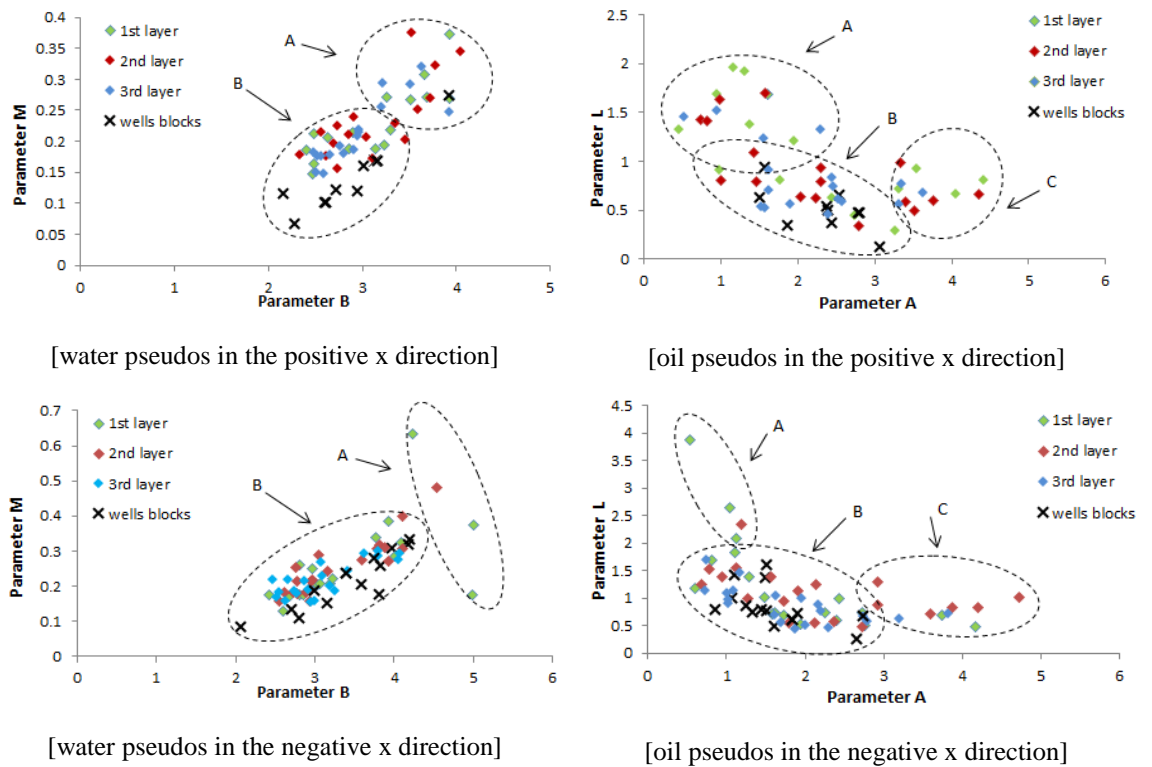


**Figure 4-45:** Grouping of oil and water pseudos in the positive and negative x directions

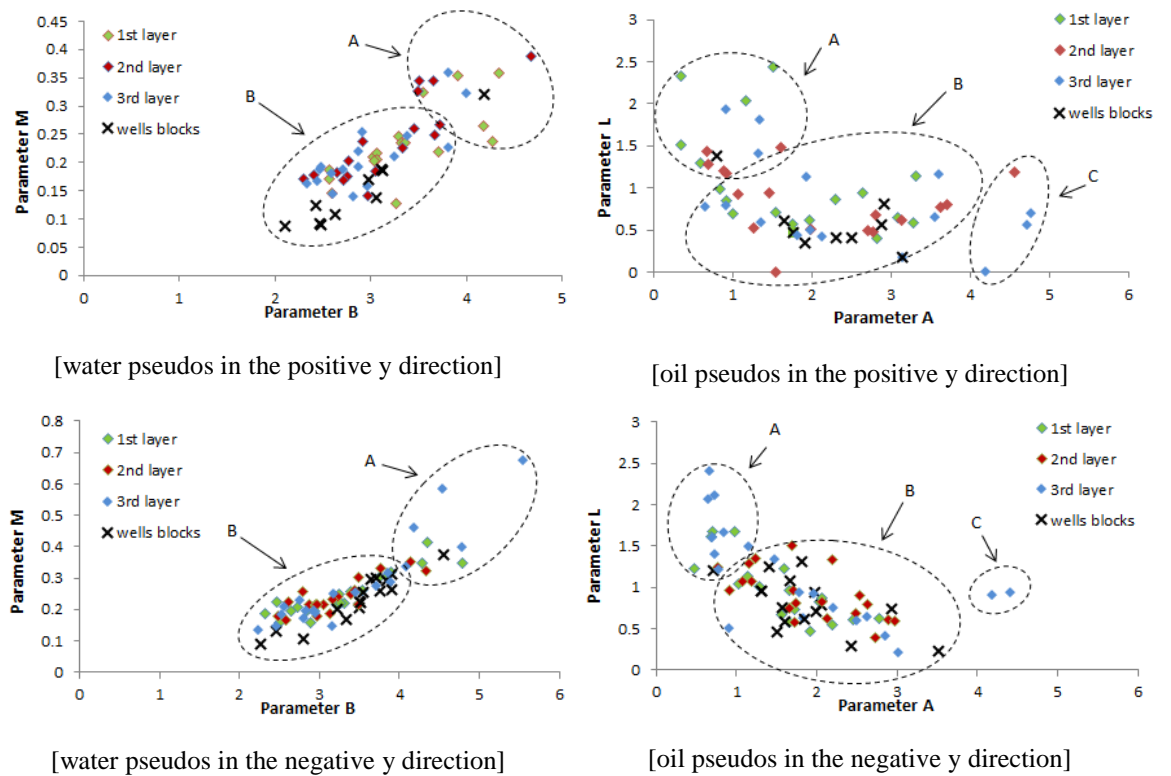


**Figure 4-46:** Grouping of oil and water pseudos in the positive and negative y directions

Since the oil and water pseudos grouping Figures 4-45 and 4-46 show that only two groups of pseudos should represent the TWR pseudos in each flow direction, it was assumed that only eight groups of pseudos should give similar result to the 270 sets of pseudos. Also fifteen well pseudos (i.e. 3 per well) were explicitly assigned to the wells blocks in the coarse model. This grouping approach was tested by running coarse scale simulation using 8 pseudos only. Results are shown in Figure 4-47 and 4-48, which indicate a good agreement between the cases with and without pseudos grouping.

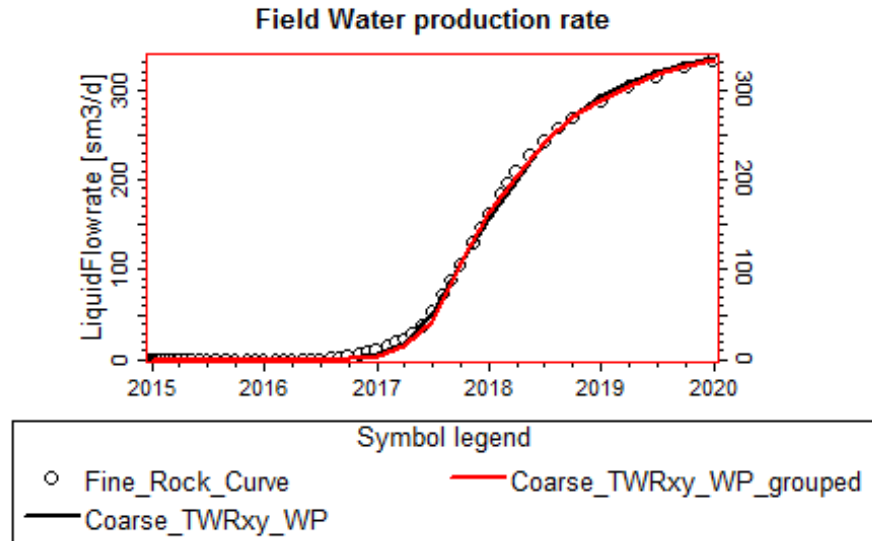


**Figure 4-47:** Comparison between results of the TWR pseudos (with and without grouping) in terms of field water production rate.

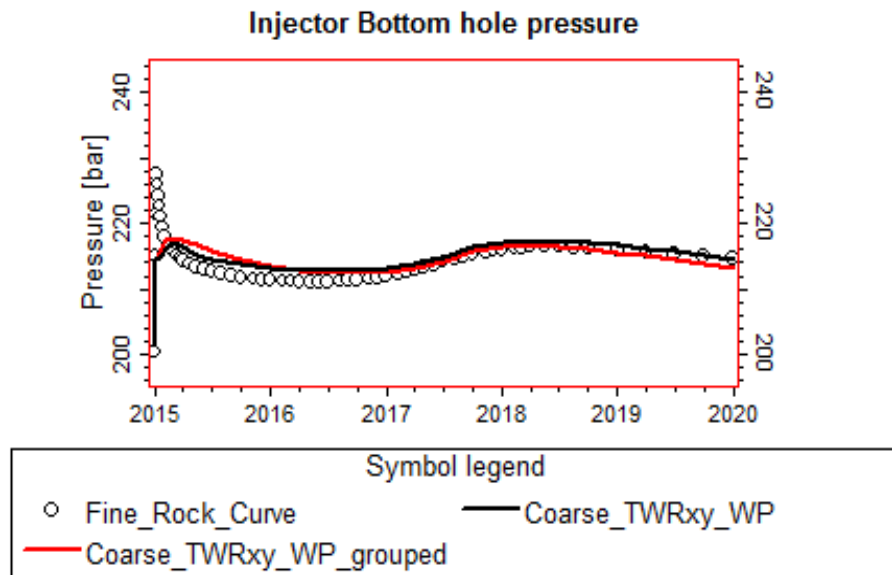


**Figure 4-48:** Comparison between results of the TWR pseudos (with and without grouping) in terms of injector bottom hole pressure.

#### **4.5. Summary and Conclusions**

The TWR pseudo functions as well as the well pseudos, generated using the methods described in Chapter 3, were tested using a synthetic 2D cross-sections model for the following cases:

- Permeability with log-normal distribution,
- Permeability coarsening upwards,
- Permeability fining upwards, and
- Thief zone in the middle of the model.

In all cases the TWR pseudos and the well pseudos succeeded in matching the coarse model results to the fine model results in terms of water breakthrough time, water flow rate and injector bottom hole pressure.

The TWR pseudos were further tested using a synthetic 3D model with permeability distributed using stochastic methods. The results were satisfactory and show that the fine model could be replaced by the coarse model with TWR and well pseudos. Also, this test showed (same as the test with thief zone in the middle) the importance of using directional pseudos in order to capture the fluid flow behaviour in all flow directions.

Grouping of the well pseudos was tested using the proposed method in Chapter 3 (i.e. using curve fitting of Chierici functional models (1984) to the TWR pseudos). The coarse models with grouped pseudos gave very similar results to the models that assigned one pseudo per each coarse cell.

**Chapter 5 : Application of the TWR method to  
the SPE 10 model 2**

## 5.1. Introduction

In this chapter, the methods proposed in Chapter 3 (i.e. the TWR method, well pseudos and the pseudos grouping method) were all tested using the SPE 10<sup>th</sup> Comparative Solution study model 2 (Christie and Blunt, 2001). Two separate tests were considered. The first test included the top 4 layers of the Tarbert formation; while the second test included the layer 59 (part of the Upper Ness formation). The objective of these tests is to check the method's performance when applied to a very heterogeneous reservoir. The upscaling approach applied here started with upscaling the absolute permeability of the fine models using flow-based method with no-flow boundary conditions. Afterwards, the fine scale simulation was run, and then the TWR pseudos were generated in the x and y directions for each coarse cell. Consequently, the TWR pseudos were grouped in order to make their use feasible. Also, the well pseudos were generated for each well and the coarse connection factors were calculated using Ding (1995) method. Finally, the coarse scale simulation was run using the grouped pseudos and the well pseudos. Results of the fine and coarse models were compared at both field and well levels.

## 5.2. Model description

The SPE 10 model 2 (Christie and Blunt, 2001) is a heterogeneous fine model with dimensions of 1200 x 2200 x 170 ft. The model consists of two formations; the top 70 ft (35 layers) represents the Tarbert formation, while the bottom 100 ft (50 layers) represents the Upper Ness formation. The SPE 10 model 2 size is 60x220x85 (1.122x10<sup>6</sup> cells). See the porosity distribution in Figure 5-1 below.

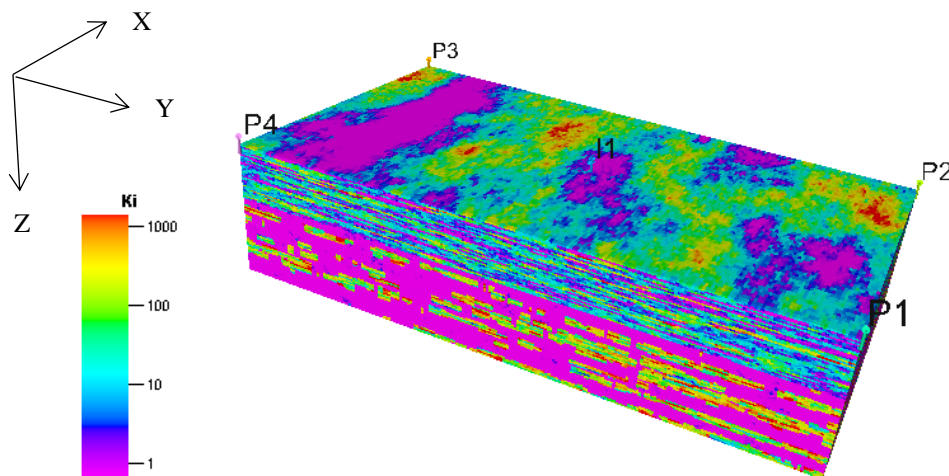


**Figure 5-1:** The permeability distribution of the SPE 10 model 2 (Christie and Blunt, 2001).

The fluid and rock properties used in the model are shown in Table 5-1 and the relative permeability curves (rock curves), used to run the fine scale simulation are illustrated in Figure 5-2 below.

Phases	Oil viscosity	Water viscosity	Initial reservoir pressure	Rock compressibility
Oil + water	3 cp	0.3 cp	6000 psi @ 12000 ft	$10^{-6}$ psi <sup>-1</sup>

**Table 5-1:** Fluid and rock properties associated to the SPE 10 model 2

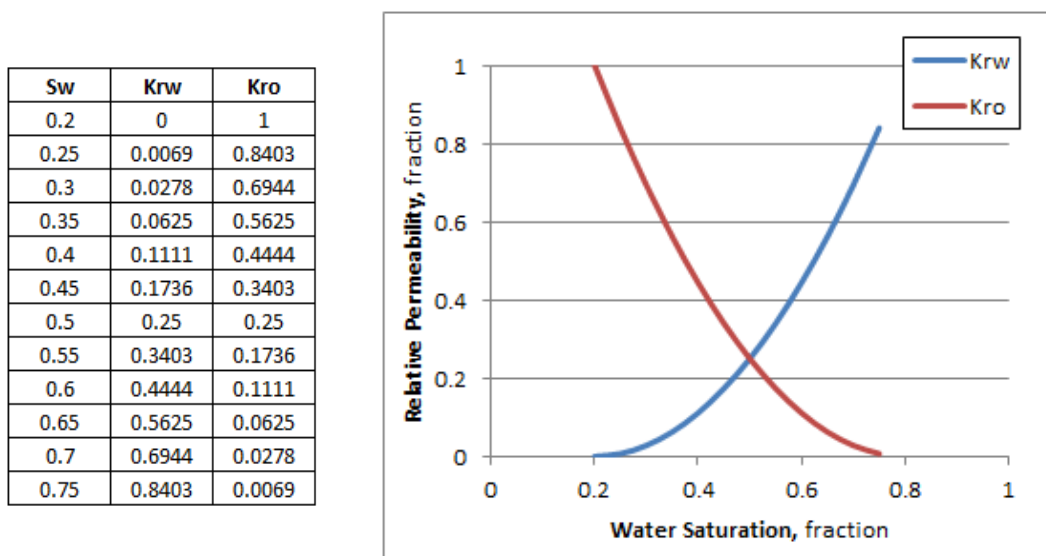


**Figure 5-2:** Relative permeability curves (rock curves) of the SPE 10 model 2

The development strategy of this model is a five-spot water flood, which includes four producers (P1, P2, P3 and P4) placed in the corners of the model and one water injector (I1), placed in the middle of the model, see the wells configuration illustrated in Table 5-2. All wells are vertical and are completed throughout the thickness of the model. The injector is controlled by injection rate of 500 bbl/day (max. injection bottom hole pressure allowed is 10 000 psi). The four producers are controlled by bottom hole pressure of 3000 psi. The simulation of the reservoir was run for five years of continuous water injection and oil production.

Well name	X-location (ft)	Y-location (ft)
Injection well (I1)	600	1100
Production well (P1)	0	0
Production well (P2)	1200	0
Production well (P3)	1200	2200
Production well (P4)	0	2200

**Table 5-2:** Wells configuration in the test models

### 5.3. The top 4 layers of the Tarbert formation

The fine model used in this test represents the top 8 ft of the Tarbert formation (i.e. only 4 layers). The fine model size in the x and y directions is kept the same as in the SPE 10 model 2 (i.e. 60x220 cells), while the model size in the z direction is 4 cells. This model was used to run fine scale simulations using the rock curves illustrated in Figure 5-2. The fine model was coarsened by a scale-up factor of 10 in both the x and y directions and scale-up factor of 4 in the z direction. Therefore, the coarse model size is 6x22x1. Table 5-3 below illustrates the fine and coarse models sizes used in the test.

Test models	Model dimensions	Model Size	No. of cells	No. of layers
Fine model	1200 x 2200 x 32 ft	60x220x4	52800	4
Coarse model	1200 x 2200 x 32 ft	6x22x1	132	1

**Table 5-3:** Fine and coarse models of the top 4 layers of the Tarbert formation.

The absolute permeability distribution in the x direction of both the fine and coarse models is shown in Figure 5-3. The permeability of the coarse model was upscaled using the flow based method with no-flow boundary conditions. Afterwards, the data required to generate the pseudo functions were exported from the black oil simulator (ECLIPSE 100, Schlumberger). These data are:

- (1) Water saturation and pore volume values in fine cells. These values were used to arithmetically average the water saturation in the coarse blocks using pore volume weighting.

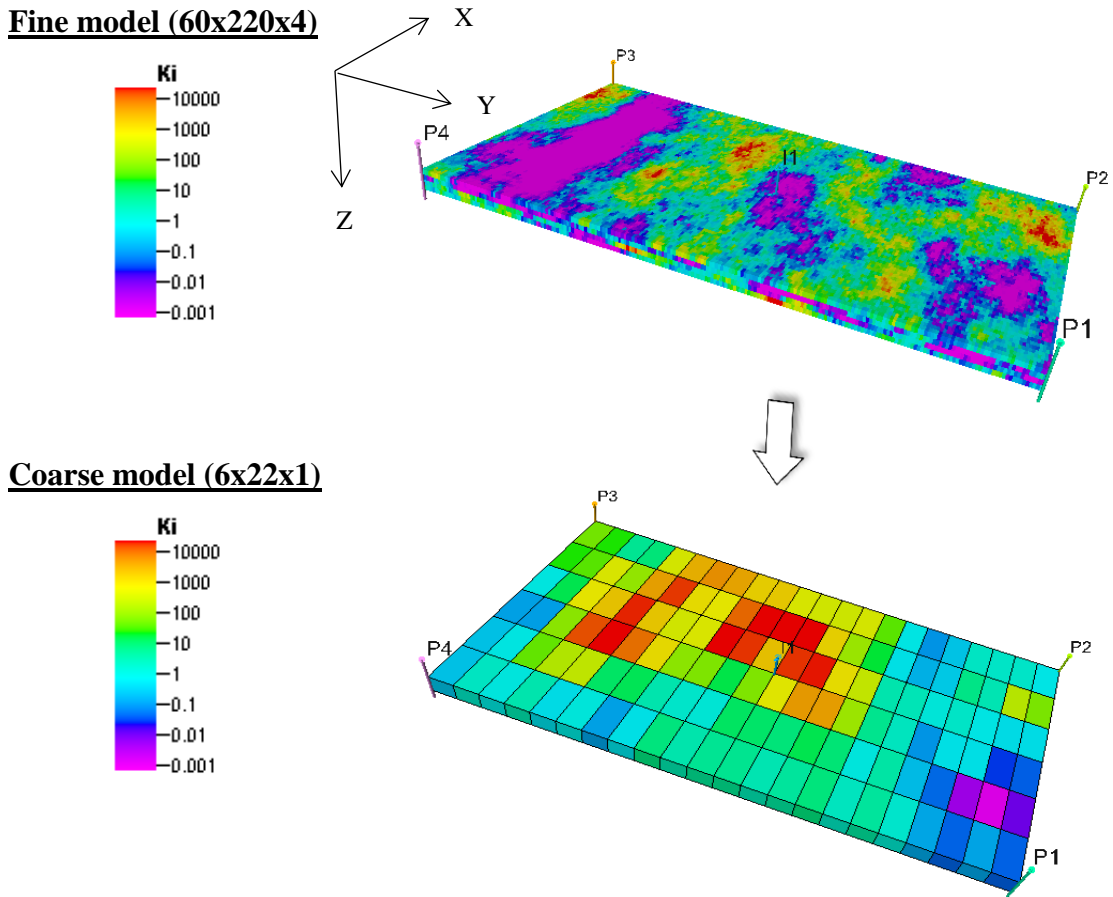


**Figure 5-3:** The permeability distributions (in the x direction) of the fine and coarse models, representing the top 4 layers of the Tarbert formation.

- (2) Water and oil relative permeability values in fine cells in addition to transmissibility in the x, y and z directions. These values were used to generate the TWR water and oil pseudo functions by arithmetically averaging relative permeability values at the interface between adjacent coarse blocks using transmissibility weighting (see the TWR method in Chapter 3).
- (3) Well connection factors and well locations in the fine cells. These values are used together with the water and oil relative permeability values to generate well pseudos for each well by arithmetically averaging the relative permeabilities in the fine well connections using well connection factor as weighting (see the well pseudos method in Chapter 3).

Directional TWR pseudos were generated for the coarse model in both the positive and negative, x and y flow directions. No pseudos were generated in the z



direction because the coarse model includes one layer only so that there is no flow in the z direction.

Figure 5-4 shows the TWR pseudos generated in the positive x and y directions. The dashed lines represent the rock curves, while the solid lines represent the oil and water pseudo relative permeabilities. It can be noticed that almost all of the water pseudos were shifted to the left of the water rock curve in order to make the water flow faster. On the contrary, most of the oil pseudos were shifted to the left of the oil rock curve in order to slow down the oil flow. The number of pseudos plotted in Figure 5-4 is 110 in the x direction and 126 in the y direction. Also, additional pseudos were generated in the negative flow directions (132 in the negative x direction and 132 in the negative y direction). This shows the importance of grouping the pseudos in order to make their assignment to the coarse grid more feasible.

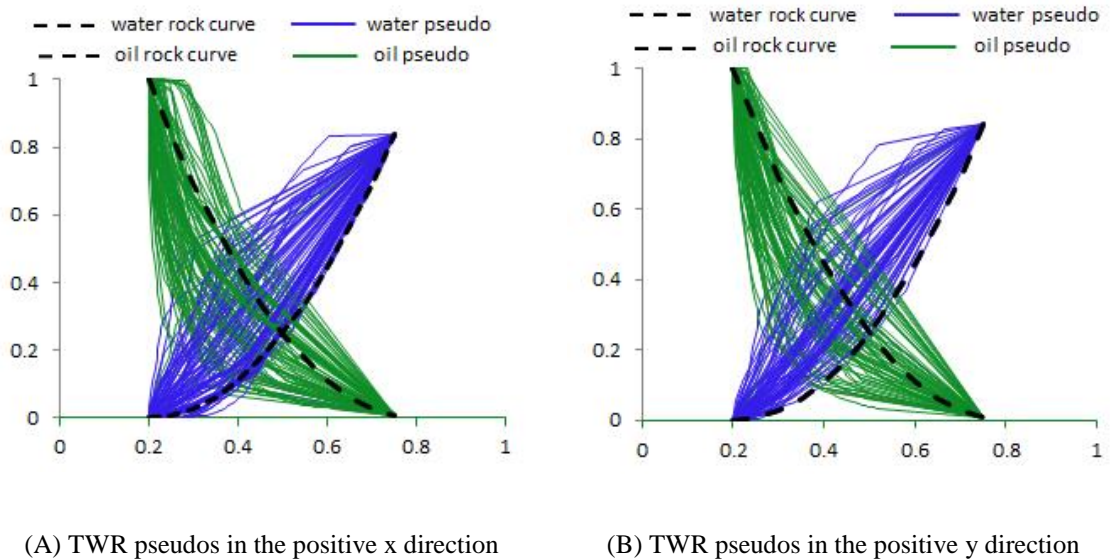
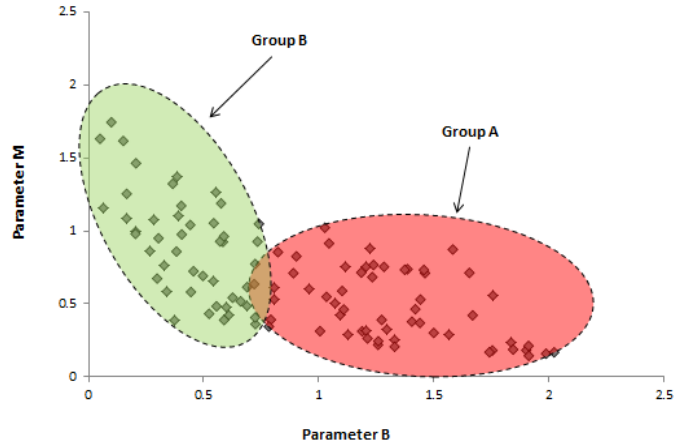


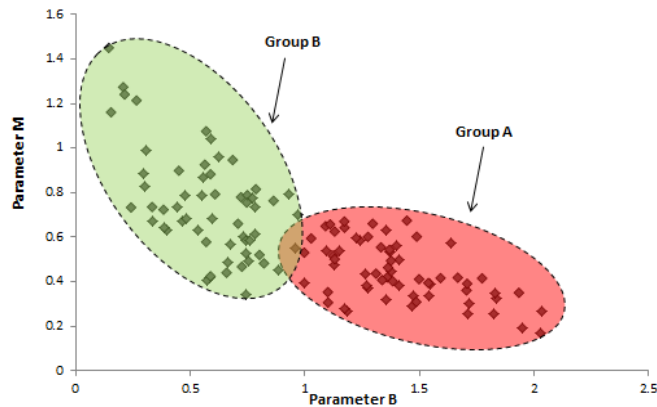
**Figure 5-4:** TWR pseudos generated for the coarse model in the positive x and y directions.

The TWR pseudos were grouped using the method described in Chapter 3 (i.e. curve fitting of the Chierici functional models (1984) to the TWR pseudos), see Figure 5-5. Grouping of the pseudos showed that, for each flow direction, 2 pseudo functions could be assigned to 2 regions in the coarse model instead of assigning one pseudo to each coarse cell. This would reduce the total number of pseudos from 500 to only 8 pseudos. Although clustering of pseudos was not obvious in this test, due to large contrast of permeability, it was noticed when plotting the Chierici (1984) parameters that the TWR pseudos are related to the transmissibility of the coarse grid blocks for

which they have been generated. Therefore, pseudos grouping was performed according to the transmissibility values by putting the pseudos of higher transmissibility region in one group (green) and putting the pseudos of lower transmissibility region in a different group (red), see Figure 5-5.



(a) TWR pseudos grouping in the positive x direction.

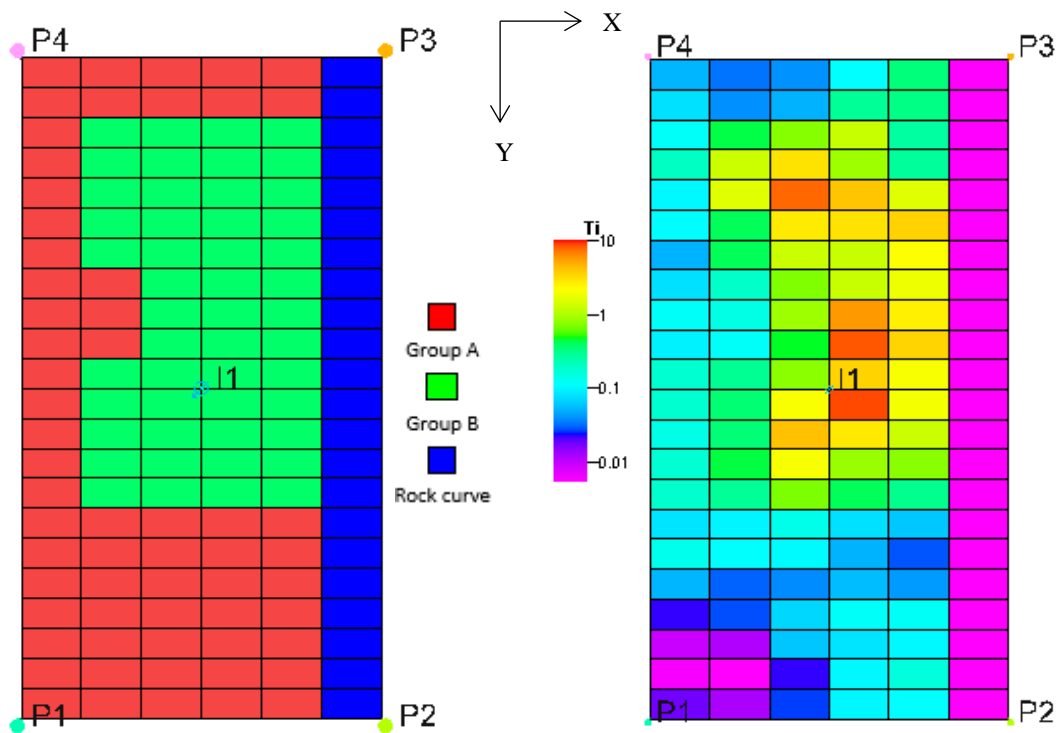


(b) TWR pseudos grouping in the positive y direction.

**Figure 5-5:** TWR pseudos grouping in the positive x and y directions.

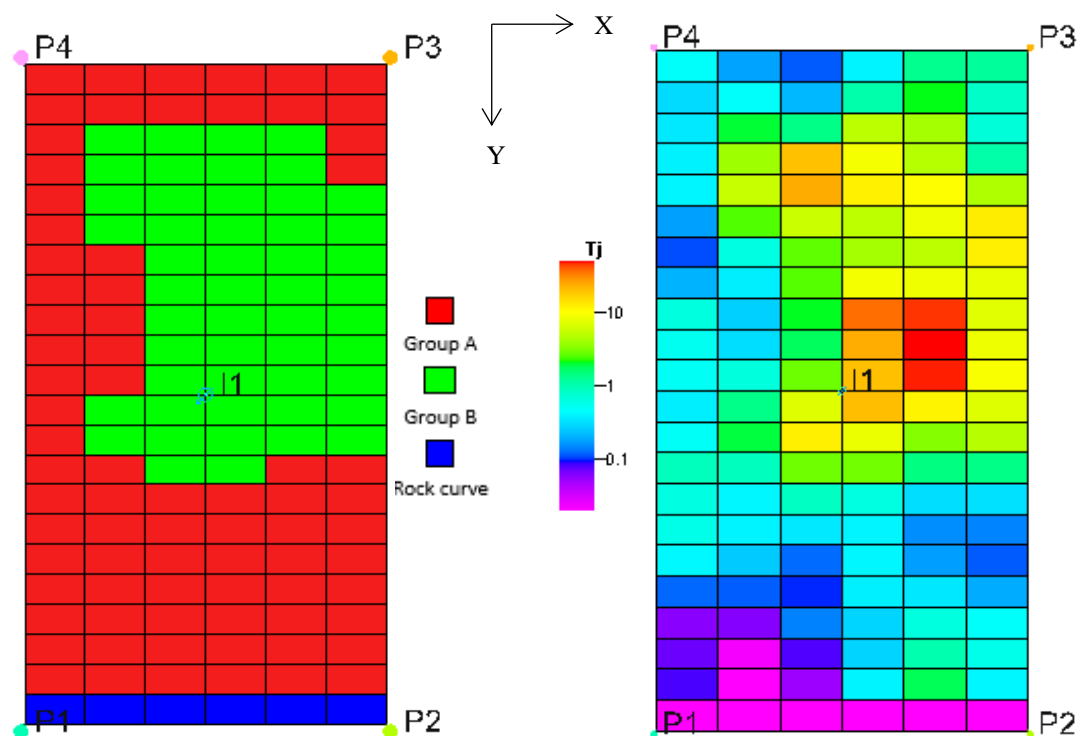
Regions to which the pseudo functions were assigned in the positive x and y directions are shown in Figures 5-6 (a). Blocks with zero transmissibility at the model edge were assigned rock curves (the blue colour). Figure 5-6 (b) shows the transmissibility in the x and y directions. Comparing the pseudos regions to the corresponding coarse blocks transmissibilities, shows that regions with similar transmissibility were assigned the same pseudo. This pseudos-transmissibility link is due to the log-normal distribution of the permeability, which makes some regions have very high permeability (and in turn transmissibility) than others. As a result, the pseudos will have different shapes in the high and low flow regions in order to control the water shock front speed, and in turn to control the water breakthrough time. For example, in

the high flow regions the pseudos shape would be shifted more to the right in order to slow down the water flow and vice versa.



(a) TWR pseudo regions in the x direction

(b) Transmissibility in the x direction



(c) TWR pseudo regions in the y direction

(d) Transmissibility in the y direction

**Figure 5-6:** TWR pseudos regions in the positive x and y directions (a) and (c), and the transmissibility in the x and y directions (b) and (d).

However, applying the same approach (i.e. assigning similar pseudos to regions with similar transmissibility) for individual grid blocks with similar transmissibility but in different positions in the model might not be feasible. This is because different positions in the model could mean different boundary conditions (Barker and Thibeau, 1997).

Before running the coarse scale simulation, the following steps were used to calculate the well pseudos and to calculate the coarse grid connection factors. The well pseudos were generated using the method described in Chapter 3, while the coarse grid well connection was calculated using the Ding (1995) method, described in Chapter 2. Also, since the absolute permeability was upscaled assuming linear boundary conditions, the transmissibility between the wells blocks and its neighbours were modified using the Ding (1995) method. The objective of the calculations mentioned above is to adjust the individual well results.

To summarize, the coarse scale simulation was run using the following:

- Flow-based upscaled permeability,
- Grouped TWR pseudos in the positive and negative x and y directions,
- Well pseudos, and
- Coarse well connection factor and modified transmissibilities between the wells connections and its neighbours.

Comparison between results of the fine and coarse models in terms of field water production rate, injector bottom hole pressure, and producers water production rate are shown in Figures 5-8 through 5-10 respectively. It can be noticed that the coarse model gave very close water breakthrough time to that of the fine model. Also, the field water production rate was well captured. Figure 5-7 shows a comparison between the water saturation profile of the fine model (layer no.4 only) and the coarse model (with TWR pseudos, not grouped) after 6 months of the water flood. The TWR pseudos provided high control over the water saturation in the coarse model. In Figure 5-9, the injector bottom hole pressure was maintained in the coarse model. Also, the well results, shown in Figure 5-10, indicate that the well pseudos in addition to Ding (1995) method adjusted the well results.

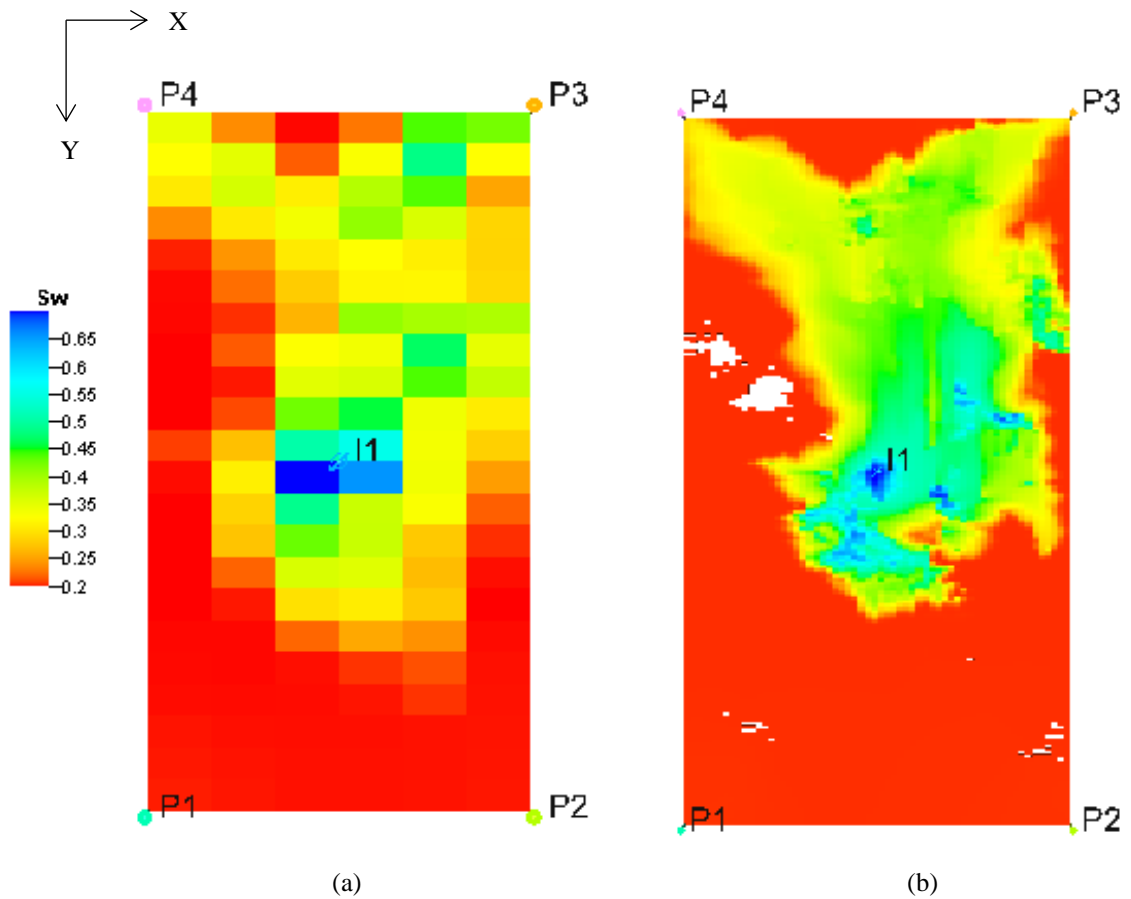


**Figure 5-7:** Comparison between the water saturation profile after 6 months of the fine model (layer no.4) with rock curves (b) and the coarse model with TWR pseudos, not grouped (a).

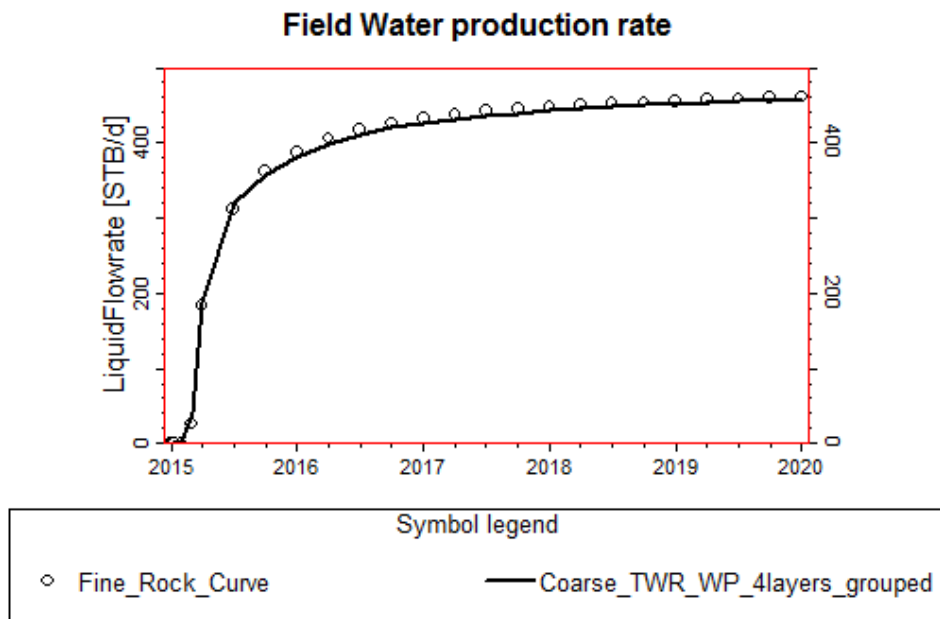


**Figure 5-8:** Comparison between the fine model (with rock curves) and the coarse model (with TWR pseudos + well pseudos) in terms of field water production rate.

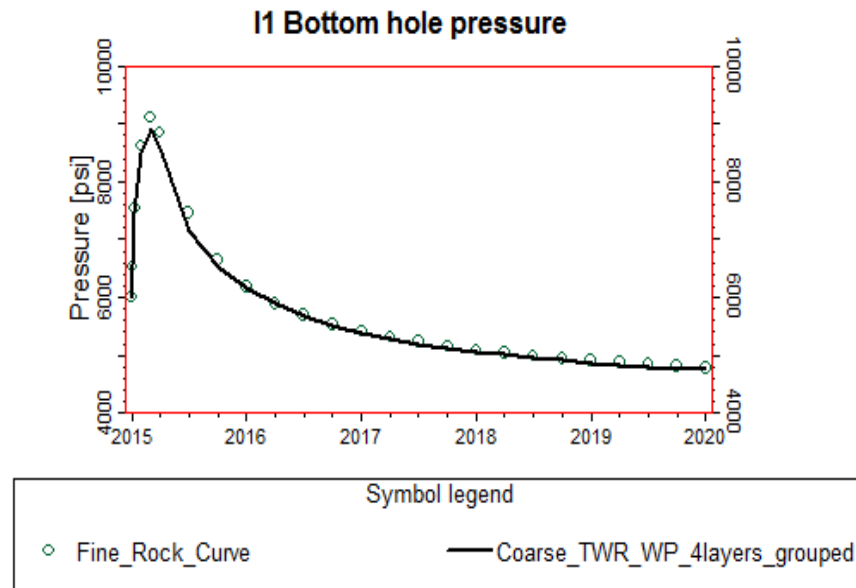


**Figure 5-9:** Comparison between the fine model and the coarse model results in terms of injector bottom hole pressure.

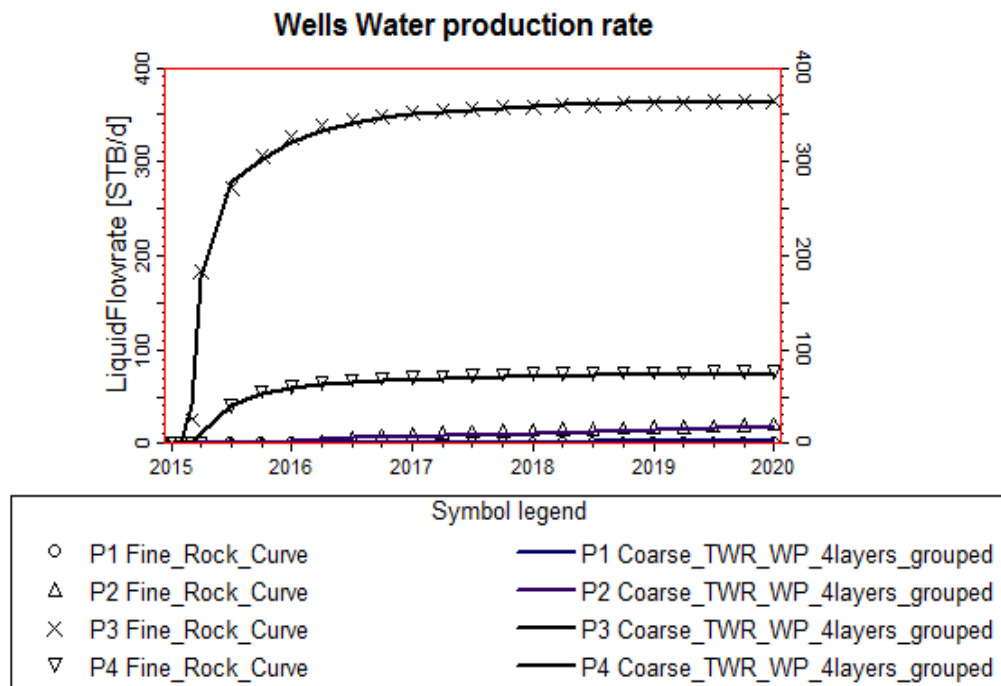


**Figure 5-10:** Comparison between the fine model and the coarse model results in terms of water production rate of the producers.

### 5.4. The Layer 59 (the upper Ness formation)

The layer 59 is part of the Upper Ness formation and it represents a typical fluvial channel system. The fine model size in this test is 60x220 in the x and y directions respectively. The coarse model size is 6x22 (i.e. scale-up factor is 10). Table 5-1 below illustrates the fine and coarse models sizes used in the test.

Test models	Model dimensions	Model Size	No. of cells	No. of layers
Fine model	1200 x 2200 x 2 ft	60x220x1	13200	1
Coarse model	1200 x 2200 x 2 ft	6x22x1	132	1

**Table 5-4:** Fine and coarse models of the layer 59 (the Upper Ness formation).

The absolute permeability distribution in the x direction of the fine model is shown in Figure 5-11. The permeability of the coarse model was upscaled using the flow based method with no-flow boundary conditions.

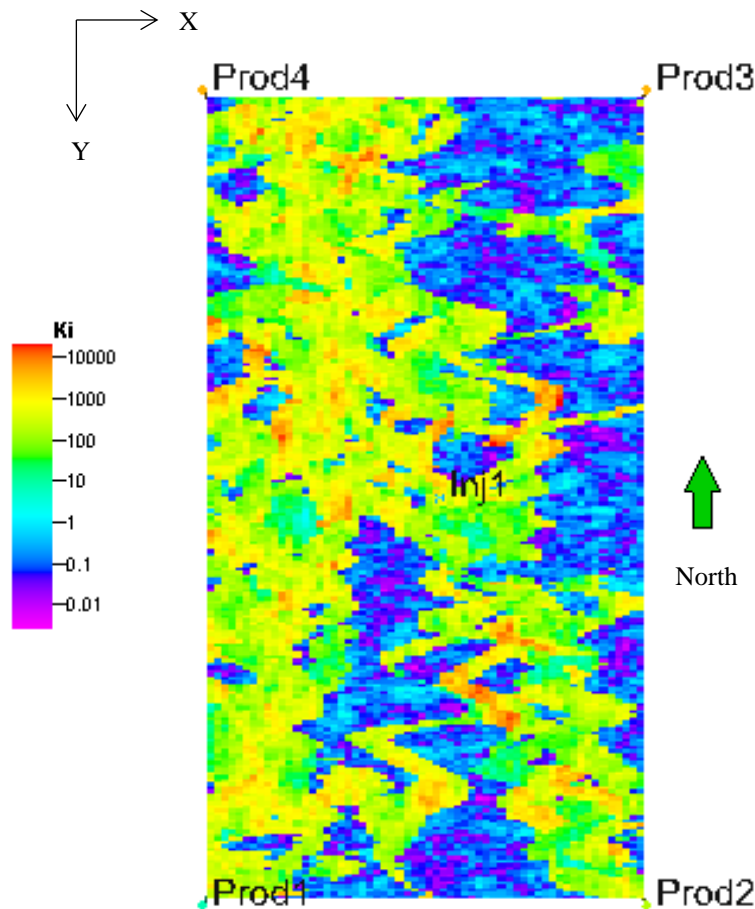


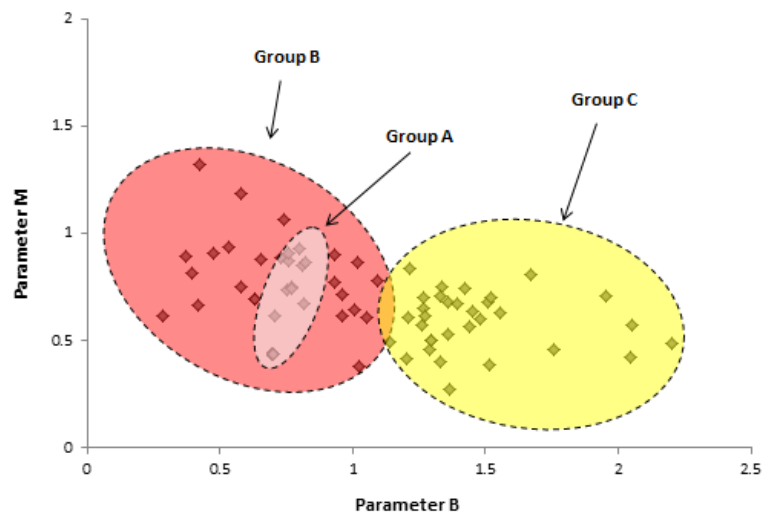
**Figure 5-11:** The permeability distributions (in the x direction) of the fine model representing the layer 59.

The procedure followed in this test is similar to that followed for the top 4 layers of the Tarbert formation in the previous section. After upscaling the absolute permeability, directional TWR pseudos were generated, and then grouped. Finally, the well pseudos were generated followed by calculation of the coarse grid well connection factor and the connection transmissibilities using Ding (1995) method.

The pseudos grouping process, see Figure 5-12, resulted in 3 groups of pseudos for each flow direction. This means that total of 12 pseudos have been used instead of 500 pseudos (in case of assigning 4 pseudos per each coarse cell for all flow directions).

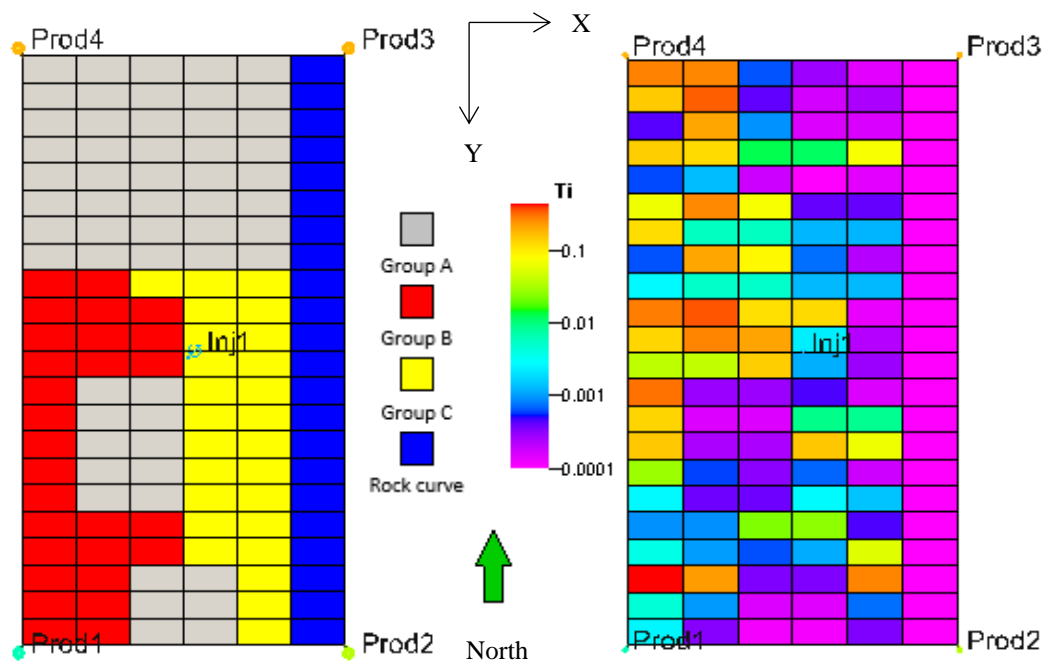
Figure 5-13 shows the pseudos regions in the coarse model in comparison to the transmissibility in the x and y direction. As previously mentioned, the TWR pseudos regions are related to the transmissibility ranges. Consequently, the channel system of layer 59 (i.e. the high transmissibility region) was assigned different pseudos than the pseudos that were assigned to the rest of the model (where the transmissibility is lower). Indeed the channel itself was assigned two different pseudos due to different ranges of transmissibility in the southern east branch than that in the southern west.

Figure 5-14 show that the TWR pseudos could control the water saturation in the coarse model to be as close as that in the fine model.



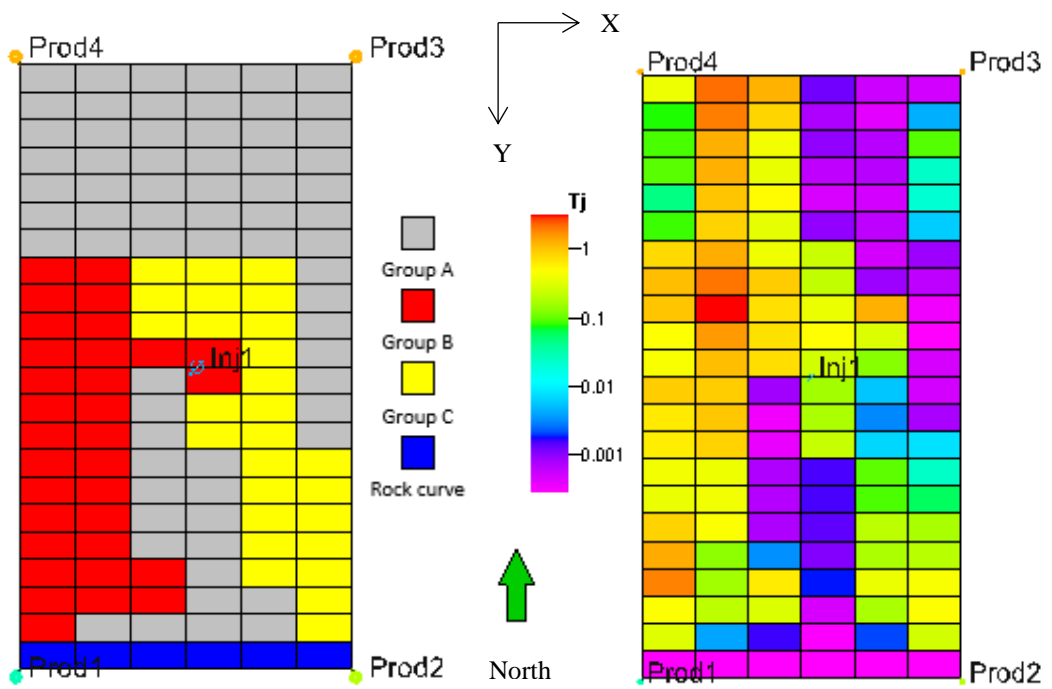
**Figure 5-12:** TWR pseudos grouping in the y direction.





(a) TWR pseudo regions in the x direction

(b) Transmissibility in the x direction



(c) TWR pseudo regions in the y direction

(d) Transmissibility in the y direction

**Figure 5-13:** TWR pseudos regions in the x directions (a), transmissibility in the x directions (b), TWR pseudos regions in the y directions (c), and transmissibility in the y directions (d).

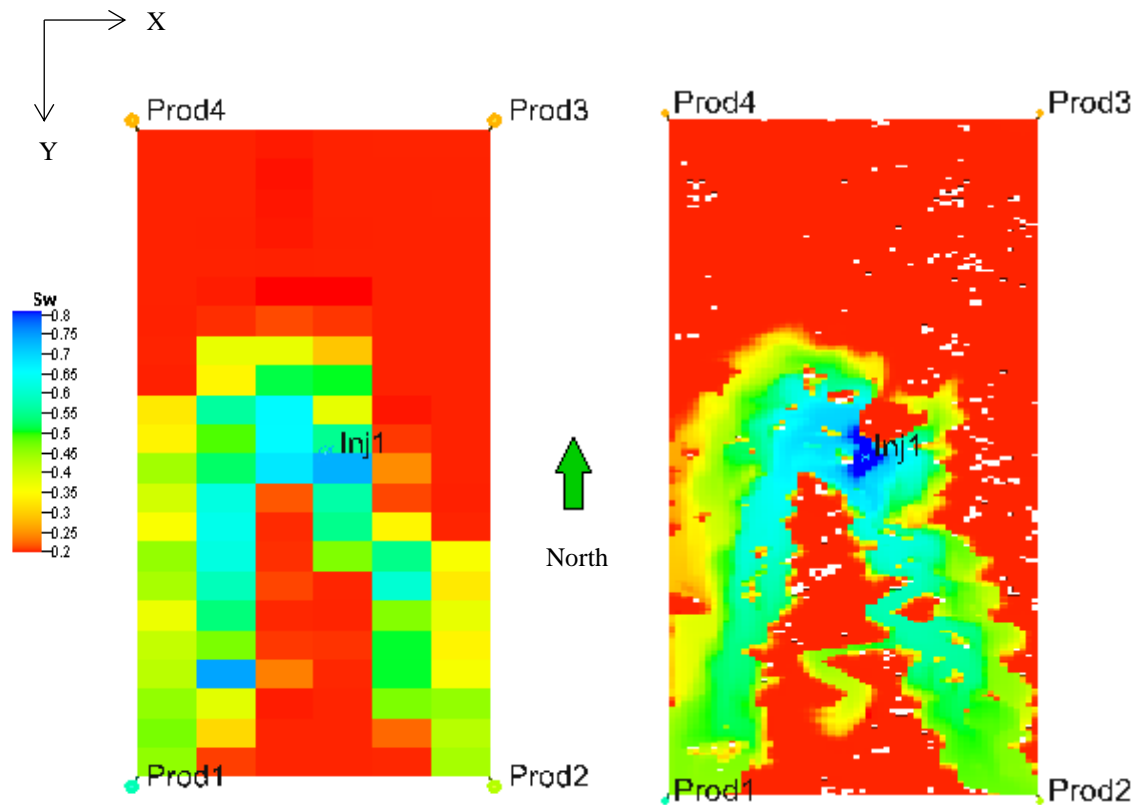


**Figure 5-14:** Comparison between the water saturation profile of fine model and the coarse model (with TWR pseudos, not grouped) after 3 years of water injection.

Comparison between results of the fine and coarse models are shown in Figures 5-15, 5-16 and 5-17 below. All figures show that the coarse model applying the methods proposed in this thesis reproduced the fine model results.

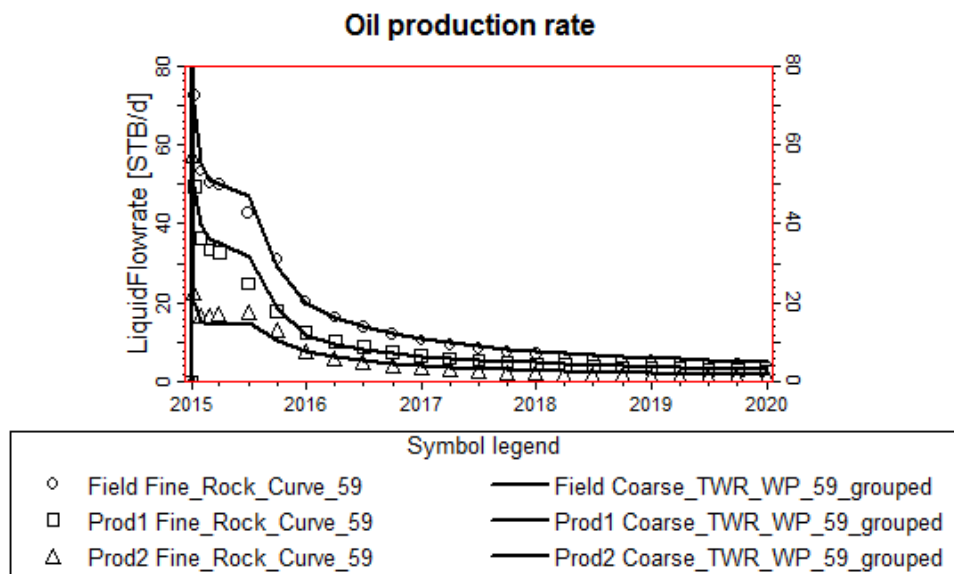


**Figure 5-15:** Comparison between the coarse and fine models in terms of oil production rate.

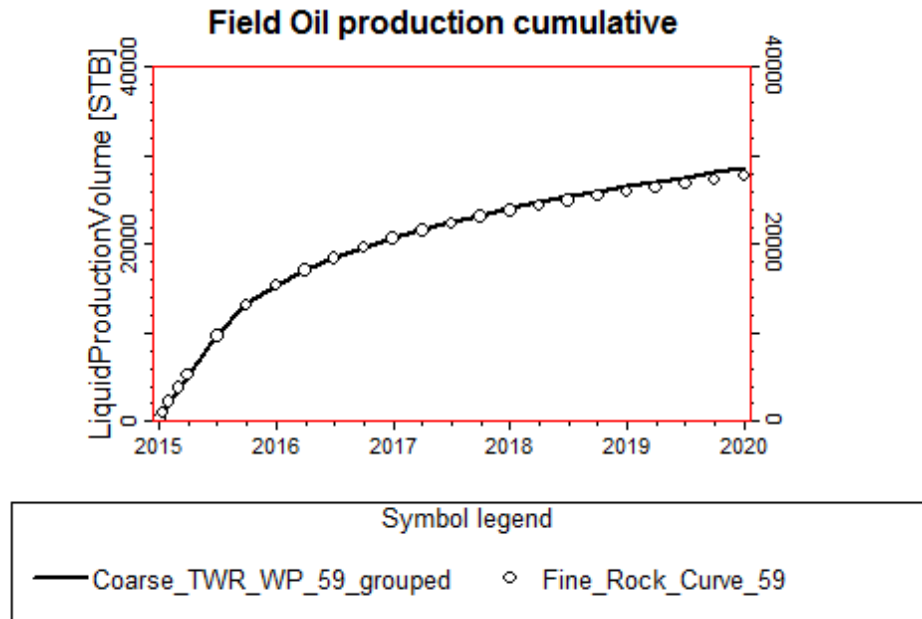


**Figure 5-16:** Comparison between the coarse and fine models in terms of cumulative oil production.

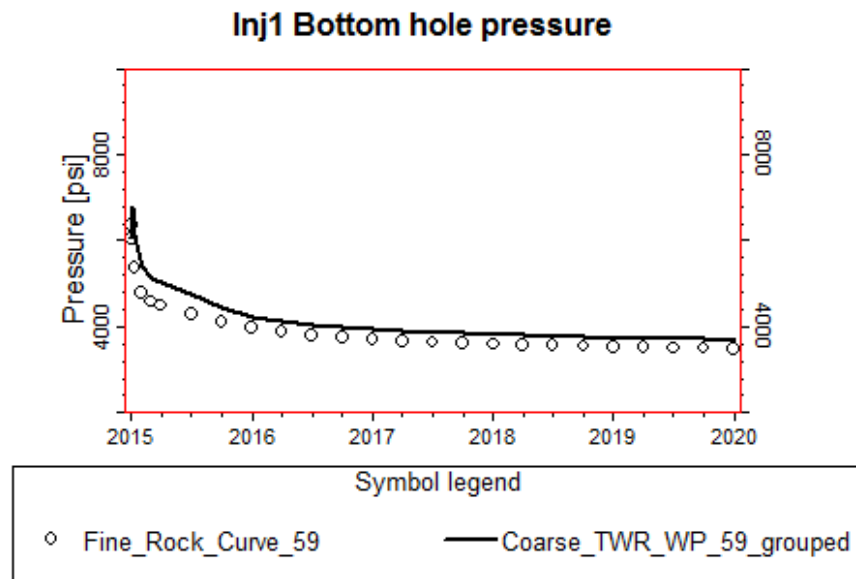


**Figure 5-17:** Comparison between the coarse and fine models in terms of injector bottom hole pressure.

## **5.5. Summary and Conclusions**

The TWR and well pseudos generation methods as well as the pseudos grouping method were all tested using the SPE 10<sup>th</sup> model 2 (Christie and Blunt, 2001). The tests included representatives of the Tarbert formation (top 4 layers) and the Upper Ness formation (layer 59). The results showed that application of the methods mentioned above for a coarse model, enabled reproduction of heterogeneous fine model results.

An important conclusion from this test is that, even in heterogeneous models, the pseudos, generated by the TWR method, are related to the transmissibility of the coarse gridblocks for which they have been generated.

## **Chapter 6 : Conclusions and Future Guidelines**

## **6.1 Summary and Conclusions**

The following was concluded based on the work introduced in this thesis:

- (1) There are many upscaling methods that have been introduced in the literature. The single phase upscaling methods aim to upscale absolute permeability (or transmissibility) by solving pressure equations. But, selecting inappropriate boundary conditions may greatly affect the results. The two phase upscaling methods are used to upscale relative permeability curves in order to capture the sub-grid heterogeneity and compensate for physical and numerical dispersions. However, two phase methods are less popular than single phase methods due to practicality and time cost issues.
- (2) Each upscaling method has got advantages, disadvantages and limitations. Some of the methods may work in some cases and fail in others. Many of the upscaling methods have been reviewed in this thesis in order to understand their points of strengths and weaknesses. This helped in forming a background on the upscaling techniques, and in turn in developing a new upscaling method.
- (3) A new two phase upscaling method called Transmissibility Weighted Relative Permeabilities (denoted as TWR) was introduced in this thesis. The method can be used to upscale relative permeability curves in heterogeneous reservoirs by arithmetically averaging relative permeability values at the interface between adjacent coarse cells using transmissibility weighting.
- (4) The TWR method was tested using 2D models for different conditions such as log-normally distributed permeability, high permeability streak (thief zone) in the middle, permeability coarsening upwards, and permeability fining upwards and. The method was also tested using a 3D model with log-normally distributed permeability. In all cases, the pseudo functions generated by the TWR method were able to adjust the coarse model results in order to be as close as possible to the fine model results.
- (5) A new method to generate well pseudos has been introduced in this thesis. The method uses well connection factors as weighting to arithmetically average the relative permeability curves in the well connections. The well pseudos are

generated for each coarse cell penetrated by wells rather than generating one well pseudo per well. This should give better control on the well flow rate from each coarse cell by preserving the well position in the coarse grid. The well pseudos were tested in combination with the TWR method using the models mentioned in point 4 above. The wells results were satisfactory.

- (6) For even better well results, especially in the heterogeneous reservoirs, Ding (1995) method was applied. The method was used to calculate the coarse grid well connection factor in addition to calculate the transmissibilities between the coarse connections and its neighbours.
- (7) A new method to group the TWR pseudo functions was proposed in order to make using the pseudos more feasible in practice. The method applies non-linear regression to match the Chierici (1984) functional models to the generated pseudos. The target was to reduce the number of the generated pseudos to a manageable number by grouping pseudos with similar Chierici (1984) parameters together. Pseudos that represent each group are assigned to a region rather than to one grid block, as the usual approach is. The pseudos that was grouped using the proposed method were tested using 2D and 3D models and provided very similar results to the models without pseudos grouping.
- (8) When assigning the grouped pseudos to the coarse grid, it was found that pseudos groups are related to the transmissibility values of the coarse blocks for which they have been generated. For example, a region with high transmissibility could be assigned a pseudo and region with low transmissibility is assigned a different pseudo.
- (9) The TWR method, the well pseudos and the grouping method were all tested using the SPE 10<sup>th</sup> Comparative Solution model 2 (Christie and Blunt, 2001). The tests included the top 4 layers of the Tarbert formation in addition to layer 59 (the upper Ness formation). This test showed that, when applied to a coarse model, the methods proposed in this thesis could be used to reproduce the results of heterogeneous fine models.

(10) The TWR method proposed in this thesis was found to have the following advantages:

- TWR pseudos avoids pressure averaging and in turn avoids the issues related to it such as:
  - a) Finding the proper method how to average the pressure.
  - b) Generation of negative pseudo functions when the flow direction is opposite to the direction in which average pressure gradient was calculated.
  - c) Infinite pseudos might be generated in case the average pressure gradient is zero while flow between the cells, for which this average gradient was calculated, is nonzero.
- The generated TWR pseudos could be grouped and assigned to the corresponding regions instead of assigning one pseudo to each coarse cell.
- Using transmissibility weighting to generate the pseudos helps in maintaining the pressure gradient in the coarse model.

(11) Like any method, the methods proposed in this thesis have some disadvantages such as:

- TWR pseudos are valid for the case for which they have been generated. This means that the change for example in well operating conditions, well locations and development strategy would require re-generation of the pseudos. However, due to the simple calculations involved in the method and possibility of applying the pseudos by grouping them, makes this task manageable.
- Although the flexibility provided by Chierici (1984) functional models by having two parameters for each relative permeability curve (two for oil and two for water), matching the pseudo curves might be difficult in some cases due to the shape of the pseudo.



## **6.2 Future Guidelines**

- (1) In this thesis, the TWR pseudos were generated assuming Cartesian grids, which mean that transmissibility calculation was dependent only on permeability values. It would be useful to check the method for corner point grids.
- (2) Since this work focuses on upscaling of relative permeability curves, capillary pressure was assumed to be taken care of when upscaling from lamina-scale to the geological model. However, it would be beneficial to check the method performance when capillary forces take place.
- (3) The grouping of pseudos using the method introduced in this thesis is based on curve fitting of Chierici (1984) functional models to one pseudo function at once, and then performing manual clustering of the pseudos. When applying this method to large models with thousands of pseudo functions, performing calculations without using a software to do the curve fitting and cluster analysis may make the grouping process difficult.

## REFERENCES

- Azoug, Y., & Tiab, D. (2003, January 1). *The Performance of Pseudofunctions in the Upscaling Process*. Society of Petroleum Engineers. doi:10.2118/80910-MS.
- Barker, J. W., & Thibeau, S. (1997, May 1). *A Critical Review of the Use of Pseudorelative Permeabilities for Upscaling*. Society of Petroleum Engineers. doi:10.2118/35491-PA.
- Brooks, R.H. and Corey, A.T. 1964. *Hydraulic Properties of Porous Media*. Hydrology Papers, No. 3, Colorado State U., Fort Collins, Colorado.
- Cao, H., & Aziz, K. (1999, January 1). *Evaluation of Pseudo Functions*. Society of Petroleum Engineers. doi:10.2118/54589-MS
- Chen, Y., & Durlofsky, L. J. (2007, January 1). *An Ensemble Level Upscaling Approach for Efficient Estimation of Fine-Scale Production Statistics Using Coarse-Scale Simulations*. Society of Petroleum Engineers. doi:10.2118/106086-MS
- Chen, T., Gerritsen, M. G., Durlofsky, L. J., & Lambers, J. V. (2009, January 1). *Adaptive local-global VCMP methods for coarse-scale reservoir modeling*. Society of Petroleum Engineers. doi:10.2118/118994-MS
- Chen, T., Gerritsen, M. G., Durlofsky, L. J. 2006. *Adaptive local-global upscaling for general flow scenarios in heterogeneous formations*. *Transport in Porous Media*, 62 (2): 157-185.
- Chen, Y., Durlofsky, L. J., Gerritsen M. and Wen, X. H., 2003. "A Coupled Local-global Upscaling Approach for Simulating Flow in Highly Heterogeneous Formations", *Advances in Water Resources*, 26 (10), 1041 – 1060.
- Chierici, G.L. 1984. *Novel Relations for Drainage and Imbibition Relative Permeabilities*. *SPE J.* 24 (3): 275-276. <http://dx.doi.org/10.2118/10165-PA>
- Christie, M. A. (1996, November 1). *Upscaling for Reservoir Simulation*. Society of Petroleum Engineers. doi:10.2118/37324-JPT
- Christie MA, Clifford PJ. *A fast procedure for upscaling in compositional simulation*, *Soc Pet Eng J* 1998;3 3 :272\_278.

Christie MA, Wallstrom TC, Durlofsky LJ, Sharp DH, Zou Q. *Effective medium boundary conditions in upscaling*. In 7th European Conference on the Mathematics of Oil Recovery, Baveno, Italy, 2000.

Christie, M. A., & Blunt, M. J. (2001, January 1). *Tenth SPE Comparative Solution Project: A Comparison of Upscaling Techniques*. Society of Petroleum Engineers. doi:10.2118/66599-MS

Christie, M. A., Mansfield, M., King, P. R., Barker, J. W., & Culverwell, I. D. (1995, January 1). *A Renormalisation-Based Upscaling Technique for WAG Floods in Heterogeneous Reservoirs*. Society of Petroleum Engineers. doi:10.2118/29127-MS

Coll, C., Muggeridge, A. H., & Jing, X. D. (2001, September 1). *Regional Upscaling: A New Method To Upscale Waterflooding in Heterogeneous Reservoirs for a Range of Capillary and Gravity Effects*. Society of Petroleum Engineers. doi:10.2118/74139-PA.

Corey, A.T. 1954. *The interrelation between gas and oil relative permeabilities*. Producers Monthly 19 (November): 38–41.

Dake. L.P .• *Fundamentals of Reservoir Engineering*. Elsevier Scientific Publishing Co. New York (1978) 343.

Darman, N.H., & Pickup, G.E. (1999, January 1). *The Development of Pseudo Functions for Gravity-Dominated Immiscible Gas Displacements*. Society of Petroleum Engineers. doi:10.2118/51941-MS.

Darman, N.H., Pickup, G.E. and Sorbie, K.S.: “*The Calculation of Pseudofunctions Using Potential Averaging Methods*” SPE66377, the SPE Reservoir Simulation Symposium held in Houston, Texas, 11-14 February 2001.

Deutsch, C.V., 1989. “*Calculating Effective Absolute Permeability in Sandstone/Sahel Sequences*”, SPE Formation Evaluation, 4:343-348.

Ding, Y.: “*Scaling Up in the Vicinity of Wells in Heterogeneous Field*,” paper SPE 29137 presented at the 1995 SPE Symposium on Reservoir Simulation, San Antonio, Texas, 12–15 February.

Ding, Y. (2003) *Permeability Upscaling on Corner-Point Geometry in the Near-Well Region*. SPE 81431, Presented at the 13th Middle East Oil Show & Conf., Bahrain, 9-12 June

Dupouy, P., Barker, J.W., and Valois, J.-P. 1998. *Grouping pseudo relative permeability curves*. In *Situ* 22: 1 -33.

Durlofsky, L. J., 1991. “*Numerical Calculation of Equivalent Grid Block Permeability Tensors for Heterogeneous Porous Media*”, *Water Resources Research*, 27, 699 – 708.

Durlofsky, L. J., R.A. Behrens, R.C. Jones, and A. Bernath (1996, September). *Scale Up of Heterogenous Three Dimensional Reservoir Descriptions*. *SPE Journal*, 313-326.

Durlofsky, L. J., Jones, R.C. & Milliken, W.J. 1997. *A nonuniform coarsening approach for the scale-up of displacement processes in heterogeneous porous media*. *Advances in Water Resources*, Volume 20, Pages 335-347.

Durlofsky, L. J., Milliken, W. J., & Bernath, A. (2000). *Scale Up in the Near-Well Region*. *SPE Journal*, 5 (1), 110-117.

Durlofsky, L. J. 2003. *Upscaling of geocellular models for reservoir flow simulation: a review of recent progress*. *International Forum on Reservoir Simulation*, Buhl/Baden-Baden Germany, June 23-27.

Dupouy, P., Barker, J. W. and Valios, J., “*Grouping Pseudo Relative Permeability Curves*,” *In Situ*, 22 (1), 1-33 (1998).

ECLIPSE 100 Technical Description, Schlumberger Geoquest, version 99A, 1999.

Efendiev, Y.R.: *The Multiscale Finite Element Method (MsFEM) and Its Applications*, Ph.D. Thesis, California Institute of Technology, 1999

Efendiev, Y., Durlofsky, L.J., and Lee, S.H. (2000, August), “*modelling of subgrid effects in coarse-scale simulations of transport in heterogeneous porous media*”, *Water Resources Research*, Vol.36, No.8, 2031-2041.

Ekrann, S., & Mykkeltveit, J. (1995, January 1). *Dynamic Pseudos: How Accurate Outside Their Parent Case?* Society of Petroleum Engineers. doi:10.2118/29138-MS.

Emanuel, A. S., & Cook, G. W. (1974, February 1). *Pseudo-Relative Permeability for Well Modeling*. Society of Petroleum Engineers. doi:10.2118/4731-PA.

Farmer, C.L. 2002. *Upscaling: a review*. *International Journal for Numerical Methods in Fluids*, 40:63–78, 2002.

Gomez-Hernandez JJ, Journel AG. *Stochastic characterization of grid-block permeabilities: from point values to block tensors*. In 2nd European Conference on the Mathematics of Oil Recovery, Arles, France, 1990.

Guzman, R. E., Giordano, D., Fayers, F. J., Godi, A., & Aziz, K. (1999, March 1). *Evaluation of Dynamic Pseudofunctions for Reservoir Simulation* (includes associated papers 38444 and 54638 ). Society of Petroleum Engineers. doi:10.2118/54692-PA.

Hales, H. B. (1983, January 1). *Parameterization of Match-Derived Pseudo-Relative Permeabilities*. Society of Petroleum Engineers. doi:10.2118/11494-MS.

Hearn, C. L. (1971, July 1). *Simulation of Stratified Waterflooding by Pseudo Relative Permeability Curves*. Society of Petroleum Engineers. doi:10.2118/2929-PA.

Hewett, T. A., & Archer, R. A. (1997, January 1). *Scale-Averaged Effective Flow Properties for Coarse-Grid Reservoir Simulation*. Society of Petroleum Engineers. doi:10.2118/37988-MS

Hewett, T. A., and Yamada T.: “*Theory for Semi-Analytical Calculation of Oil Recovery and Effective Relative Permeabilities Using Streamtubes*,” Report 8, Stanford Center for Reservoir Forecasting (SCRF), Stanford University, Stanford, May 1995.

Holden, L. and Nielsen, B. F., 2000. *Global upscaling of permeability in heterogeneous reservoirs: the Output Least Squares (OLS) method*. Transport in Porous Media, 40:115–143, 2000.

Ingsoy, P., Gauchet, R., & Lake, L. W. (1994, February 1). *Pseudofunctions and Extended Dietz Theory for Gravity-Segregated Displacement in Stratified Reservoirs*. Society of Petroleum Engineers. doi:10.2118/23601-PA.

Intera Information Technologies LTD, 1994, “PSEUDO Reference Manual”, 94A release.

Jacks, H. H., Smith, O. J. E., & Mattax, C. C. (1973, June 1). *The Modeling of a Three-Dimensional Reservoir with a Two-Dimensional Reservoir Simulator-The Use of Dynamic Pseudo Functions*. Society of Petroleum Engineers. doi:10.2118/4071-PA.

Kazemi, A., Shaikhina, D. S., Pickup, G. E., & Corbett, P. W. M. (2012, January 1). *Comparison of Upscaling Methods in a Heterogeneous Carbonate Model*. Society of Petroleum Engineers. doi:10.2118/154499-MS

- Jonoud, S., & Jackson, M. D. (2006, January 1). *Validity of steady-state upscaling techniques*. Society of Petroleum Engineers. doi:10.2118/100293-MS
- Journel, A. G., Deutsch, C., & Desbarats, A. J. (1986, January 1). *Power Averaging for Block Effective Permeability*. Society of Petroleum Engineers. doi:10.2118/15128-MS
- Kasap, E., & Lake, L. W. (1990, June 1). *Calculating the Effective Permeability Tensor of a Gridblock*. Society of Petroleum Engineers. doi:10.2118/18434-PA
- King, P.R., 1989. "The Use of Renormalisation for Calculating Effective Permeability", *Transport in Porous Media*, 4:37-58.
- King, P. R., Muggeridge, A. H., & Price W.G., *Renormalization Calculations of Immiscible Flow*, *Transport in Porous Media* 12, 1993, pp 237-260.
- King, M. J., & Mansfield, M. (1997, January 1). *Flow Simulation of Geologic Models*. Society of Petroleum Engineers. doi:10.2118/38877-MS
- Kossack, C. A., Aasen, J. O., & Opdal, S. T. (1990, September 1). *Scaling Up Heterogeneities With Pseudofunctions*. Society of Petroleum Engineers. doi:10.2118/18436-PA.
- Kyte, J. R., & Berry, D. W. (1975, August 1). *New Pseudo Functions To Control Numerical Dispersion*. Society of Petroleum Engineers. doi:10.2118/5105-PA
- Li, D., Cullick, A. S., and Lake, L.: "Global Scaleup of Reservoir Model Permeability With Local Grid Refinement," *J. Pet. Sci. & Engr.* (Dec.1995) I.
- Li, D., Cullick, A. S., & Lake, L. W. (1996, August 1). *Scale-Up Of Reservoir Model Relative Permeability Using A Global Method*. Society of Petroleum Engineers. doi:10.2118/29872-PA
- Lohne, A., Virnovsky, G., & Durlofsky, L. J. (2004, January 1). *Two-Stage Upscaling of Two Phase Flow: From Core to Simulation Scale*. Society of Petroleum Engineers. doi:10.2118/89422-MS
- Matheron, G., 1967. "Elements pour une Theorie des Milieux Poreux". *asspm aros*.
- Mascarenhas, O.: "Accurate Coarse Scale Simulation of Horizontal Wells," MS thesis, Stanford U., Stanford, California ~1999.

Muggeridge, A.H. and Hongtong, P. (2014, September 8-11). *An Upscaling Methodology for EOR*. ECMOR XIV – 14th European Conference on the Mathematics of Oil Recovery, Catania, Sicily, Italy, 8-11 September 2014.

Muggeridge, A.H., Cuypers, M., Bacquet, C. and Baker, J.W. (2002). *Scale-up of Well Performance for Reservoir Flow Simulation*. *Petroleum Geoscience*, 8, 2, 133-139.

Nielsen BF, Tveito A. *An upscaling method for one-phase flow in heterogeneous reservoirs. A weighted output least squares (WOLS) approach*. *Computational Geosciences* 1998; 2(2):93 –123.

Peaceman, D.W.: “*Interpretation of Well-Block Pressures in Numerical Reservoir Simulation*,” SPEJ ~June 1978! 183; Trans., AIME,265.

Peaceman, D. W. (1983, June 1). *Interpretation of Well-Block Pressures in Numerical Reservoir Simulation With Nonsquare Grid Blocks and Anisotropic Permeability*. Society of Petroleum Engineers. doi:10.2118/10528-PA

Pickup, G.E. et al.: “*A Method for Calculating Permeability Tensors Using Perturbed Boundary Conditions*,” Proc., Third European Conference on the Mathematics of Oil Recovery, M.A. Christie et al. (eds.), Delft U. Press, Delft, The Netherlands (1992) 225.

Pickup, G., Ringrose, P. S., & Sharif, A. (2000, June 1). *Steady-State Upscaling: From Lamina-Scale to Full-Field Model*. Society of Petroleum Engineers. doi:10.2118/62811-PA.

Pickup, G. E., & Sorbie, K. S. (1996, December 1). *The Scaleup of Two Phase Flow in Porous Media Using Phase Permeability Tensors*. Society of Petroleum Engineers. doi:10.2118/28586-PA

Renard, Ph. and de Marsily, G. 1997. *Calculating effective permeability: a review*. *Advances in Water Resources*, 20:253–278.

Reservoir Simulation course, Heriot Watt University.

Saad, N., Cullick, A. S., & Honarpour, M. M. (1995, January 1). *Effective Relative Permeability in Scale-Up and Simulation*. Society of Petroleum Engineers. doi:10.2118/29592-MS

Salazar, M. O., & Villa Piamonte, J. R. (2007, January 1). *Permeability Upscaling Techniques for Reservoir Simulation*. Society of Petroleum Engineers. doi:10.2118/106679-MS

Simon, A. D., & Koederitz, L. F. (1982, January 1). *An Improved Method for the Determination of Pseudo-Relative Permeability Data for Stratified Systems*. Society of Petroleum Engineers. doi:10.2118/10975-MS

Shook, M., Li, D., and Lake, L.: "Scaling Immiscible Flow Through Permeable Media by Inspectional Analysis," *In Situ* (1992) 16, 311.

Smith, E.H.: "The Influence of Small-Scale Heterogeneity on Average Relative Permeability," *Reservoir Characterization II*, Academic Press, London (1991) 52–76.

Soedarmo, E. (1994, January 1). *Length-Dependent Pseudofunction: An Improved Upscaling Method in Black Oil Simulation*. Society of Petroleum Engineers. doi:10.2118/28754-MS

Soeriawinata, T., Kasap, E., and Kelkar, M.: "Permeability Upscaling for Near-wellbore Heterogeneities," *SPEFE* ~December 1997! 255.

Taggart, I. J., Soedarmo, E., & Paterson, L. (1995, January 1). *Limitations in The Use of Pseudofunctions For Up-scaling Reservoir Simulation Models*. Society of Petroleum Engineers. doi:10.2118/29126-MS

Stephen, K. D., & Pickup, G. E. (1999, January 1). *Steady State Solutions of Immiscible Two Phase Flow in Strongly Heterogeneous Media: Implications for Upscaling*. Society of Petroleum Engineers. doi:10.2118/51912-MS

Stephen, K. D., Pickup, G. E., & Sorbie K. S. 2001. *The Local Analysis of Changing Force Balances in Immiscible Incompressible Two Phase Flow*. *Transport in Porous Media*, Volume 45, Issue 1, pp 63-88.

Stern, D. & Dawson, A.G. 1999. *A Technique for Generating Reservoir Simulation Grids to Preserve Geologic Heterogeneity*. Paper SPE 51942, presented at the SPE Reservoir Simulation Symposium, Houston, Texas, 14-17 February.

Stone, H. L. (1991, January 1). *Rigorous Black Oil Pseudo Functions*. Society of Petroleum Engineers. doi:10.2118/21207-MS.



Stone, M., Lyons, S. L., Wu, X.-H., & Parashkevov, R. (2007, January 1). *Challenges and Solutions in Global-Flow-Based Scaleup of Permeability: Isolated Flow Bodies*. Society of Petroleum Engineers. doi:10.2118/106084-MS

Tan, T. B. (1995, January 1). *Estimating Two and Three Dimensional Pseudo-Relative Permeabilities With Non-Linear Regression*. Society of Petroleum Engineers. doi:10.2118/29129-MS

Thibeau, S., Barker, J. W., & Souillard, P. (1995, January 1). *Dynamical Upscaling Techniques Applied to Compositional Flows*. Society of Petroleum Engineers. doi:10.2118/29128-MS

Thomas, L. K., & Coats, K. H. (1992, January 1). *Stones kro Methods And Modifications*. Society of Petroleum Engineers.

Wallstrom, T. C., Hou, S., Christie, M.A., Durlofsky, L. J., Sharp, D. H. and Zou, Q., 2002a. “*Effective Flux Boundary Conditions for Upscaling Porous Media Equations*”, *Transport in Porous Media*, 46 (2-3), 139 - 152.

Wallstrom, T. C., Hou, S., Christie, M.A., Durlofsky, L. J., Sharp, D. H. and Zou, Q., 2002b. “*Application of Effective Flux Boundary Conditions to Two-Phase Upscaling in Porous Media*”, *Transport in Porous Media*, 46 (2-3), 155 - 178.

Warren JE, Price HS. *Flow in heterogeneous Porous Media*. Society of Petroleum Engineers Journal, September 1961, 153–169.

Wen, X. H. and Gomez-Hernandez, J. J. 1996. *Upscaling hydraulic conductivities in heterogeneous media: an overview*. *Journal of Hydrology*, 183:ix–xxxii.

Wen, X.-H., Durlofsky, L. J., Lee, S. H., & Edwards, M. G. (2000, January 1). *Full Tensor Upscaling of Geologically Complex Reservoir Descriptions*. Society of Petroleum Engineers. doi:10.2118/62928-MS

White CD, Horne RN. *Computing absolute transmissibility in the presence of fine scale heterogeneity*. SPE 16011. In 9th SPE Symposium on Reservoir Simulation, San Antonio, USA, 1987.

Woods, E. G., & Khurana, A. K. (1977, August 1). *Pseudofunctions for Water Coning in a Three-Dimensional Reservoir Simulator*. Society of Petroleum Engineers. doi:10.2118/5525-PA

Wu, X.-H., Stone, M., Parashkevov, R., Stern, D., & Lyons, S. L. (2007, January 1). *Reservoir Modeling with Global Scale-up*. Society of Petroleum Engineers. doi:10.2118/105237-MS

Yang, P. H., & Watson, A. T. (1991, May 1). *A Bayesian Methodology for Estimating Relative Permeability Curves*. Society of Petroleum Engineers. doi:10.2118/18531-PA

Zapata, V. J., & Lake, L. W. (1981, January 1). *A Theoretical Analysis of Viscous Crossflow*. Society of Petroleum Engineers. doi:10.2118/10111-MS

Zhang, P., Pickup, G. E., and Christie, M. A., 2005. "A New Upscaling Approach for Highly Heterogeneous Reservoirs", SPE93339, presented at the 2005 SPE Reservoir Simulation Symposium held in Houston, Texas U.S.A., 31 January 2005 – 2 February 2005.

Zhou D., Fayers F.J., and Orr F.M.: "Scaling of Multiphase Flow in Simple Heterogeneous Porous Media", SPE 27833, the ASME Winter Meeting, New Orleans, Nov. 28-Dec. 3, 1993.